TECHNICAL REPORT STANDARD PAGE

1. Report No.	2. Government Accession No.	3. Recipient's Catalog No.
FHWA/LA-87/202		

4. Title and Subtitle

Heat-Straightening Effects on the Behavior of Full-Scale Simulated Bridge Girders

5. Report Date

6. Performing Organization Code

7. Author(s)

R. Richard Avent
George M. Fadous

8. Performing Organization Report No.

9. Performing Organization Name and Address

Department of Civil Engineering
Louisiana State University
Baton Rouge, LA 70803

10. Work Unit No.

11. Contract or Grant No.

LA. HPR Study No. 853ST

12. Sponsoring Agency Name and Address

Louisiana Transportation Research Center
P.O. Box 94245
Baton Rouge, LA 70804

13. Type of Report and Period Covered

1st Interim Report, Phase 2
Aug. 1986 - Aug. 1987

14. Sponsoring Agency Code

15. Supplementary Notes

Conducted in Cooperation with the U.S. Department of Transportation, Federal Highway Administration

16. Abstract

For over 50 years, the process of heat straightening has been used by experienced craftsmen to repair damaged steel members. However, engineers have yet to completely understand the process from an analytical point of view. In order to help reduce this gap, a field study of heat straightening effects on the actual behavior of damaged, full-scale simulated bridge girders was conducted. Each girder, supporting a concrete slab, was placed in a test frame to model actual conditions of a simply supported bridge member. Damage was induced by either statically or dynamically applying a horizontal force to the bottom flange. Heat straightening procedures were used to completely repair the member.

Various aspects of the process were evaluated during repair. The amount of applied external restraining force was varied between different heating cycles in order to study its effect on the amount of plastic deformation removed during each cycle. Different patterns of heat were applied to the damaged girder and comparisons were made to understand their effectiveness to straighten bent members. Several cycles of damage followed by repair were done to study the effects of repetitive damage.

Comparisons were made between the results of this experimental work and available information on the effect of heat on the yield stress. The results were also compared to those obtained using existing empirical equations.

Finally, a recommended procedure to heat-straighten damaged composite girders was developed.

17. Key Words	18. Distribution Statement
Steel Bridges, Damage, Repair, Heat-Straightening, Griders	Unrestricted. This document is available to the public through the National Technical Information Service, Springfield, VA 22161

19. Security Classif. (of this report)	20. Security Classif. (of this page)	21. No. of Pages	22. Price
Unclassified	Unclassified	142	

Form DOT F 1700.7 (8-69)

HEAT-STRAIGHTENING EFFECTS ON THE BEHAVIOR OF FULL-SCALE SIMULATED BRIDGE GIRDERS

VOLUME 4: FIRST INTERIM REPORT OF PHASE 2

by

R. RICHARD AVENT
PROFESSOR OF CIVIL ENGINEERING

and

GEORGE FADOUS
GRADUATE STUDENT

DEPARTMENT OF CIVIL ENGINEERING
LOUISIANA STATE UNIVERSITY
BATON ROUGE, LA 70803

STATE PROJECT NO. 736-10-46
FEDERAL AID PROJECT NO. HPR-0010(008)
LSU PROJECT NO. 127-15-4141

CONDUCTED FOR

LOUISIANA DEPARTMENT OF TRANSPORTATION AND DEVELOPMENT
LOUISIANA TRANSPORTATION RESEARCH CENTER
in Cooperation with
U.S. Department of Transportation
FEDERAL HIGHWAY ADMINISTRATION

AUGUST, 1987

ACKNOWLEDGMENTS

As with any research project, the cooperation of the sponsoring agencies are essential. The authors wish to thank the Louisiana Transportation Research Center, the Federal Highway Administration, and the Louisiana Department of Transportation and Development for their support of the project. Special thanks are extended to Mr. Ara Arman, Director of LTRC, and Mr. Masood Rasoulian, LTRC technical coordinator, for the helpful technical and managerial direction given to the project.

The authors would like to thank employees of the Maintenance Division of the Louisiana Department of Transportation and Development who assisted in the construction of the HEAT facility: Mr. Joseph T. Smith, structures and facilities maintenance engineer; Mr. Gil M. Gautreau, bridge inventory and inspection engineer; Mr. Frank Castjohn, bridge maintenance supervisor--statewide; and the construction crew: Mr. Marvin Cain, Mr. Jerry Cavanaugh, Mr. Terry Brunston, and Mr. Danny Morris.

ABSTRACT

For over 50 years, the process of heat straightening has been used by experienced craftsmen to repair damaged steel members. However, engineers have yet to completely understand the process from an analytical point of view. In order to help reduce this gap, a field study of heat straightening effects on the actual behavior of damaged, full-scale simulated bridge girders was conducted. Each girder, supporting a concrete slab, was placed in a test frame to model actual conditions of a simply supported bridge member. Damage was induced by either statically or dynamically applying a horizontal force to the bottom flange. Heat straightening procedures were used to completely repair the member.

Various aspects of the process were evaluated during repair. The amount of applied external restraining force was varied between different heating cycles in order to study its effect on the amount of plastic deformation removed during each cycle. Different patterns of heat were applied to the damaged girder and comparisons were made to understand their effectiveness to straighten bent members. Several cycles of damage followed by repair were done to study the effects of repetitive damage.

Comparisons were made between the results of this experimental work and available information on the effect of heat on the yield stress. The results were also compared to those obtained using existing empirical equations.

Finally, a recommended procedure to heat-straighten damaged composite girders was developed.

IMPLEMENTATION STATEMENT

The results of this report illustrate the practicality of using heat straightening in bridge repair. The methodology described is applicable to the repair of damaged steel girders on overpasses and elements on bridge trusses. Since research is continuing, full implementation is not yet appropriate. However, a technical paper is being planned for submission to a structural engineering journal. Publication of this material will ensure a wide dissemination of these research findings.

METRIC CONVERSION FACTORS

One pound force per square inch (psi)	= 6.89 kilopacals (kPa)
One inch (in.)	= 25.4 millimeters (mm)
One pound force (lb.)	= 4.45 newtons (N)

TABLE OF CONTENTS

LIST OF TABLES

LIST OF FIGURES

106

107

110

121

123

1. INTRODUCTION

General Background

Damage caused by vehicle impact, mishandling, or fire is a perennial problem associated with structural steel bridge members. For almost half a century, heat straightening techniques have been applied to bends and distortions in order to restore the original shape of steel elements. A few craftsmen, who have years of experience with heat straightening, perform the technique in the field with varying degrees of success. Some of these experts have mastered heat straightening, but the process is still considered more of an art than a science.

The ability to repair bent structural steel members in place, often without even the need for temporary shoring, has generated interest in heat straightening from the engineering profession. In recent years engineers have begun to study the effects of heat application on steel. However, much of the research data available is obscure, with contradicting remarks being found in different publications. As a result, engineers faced with the dilemma of choosing the appropriate and most efficient method to repair a damaged steel structure have little organized and reliable data or information upon which to base their decisions. These engineers must rely primarily on their own judgment and the advice of experienced technicians.

In order to provide a more comprehensive and authoritative data base, the Louisiana Transportation Research Center (LTRC) and the Louisiana Department of Transportation and Development (LDOTD), in cooperation with the Federal Highway Administration (FHWA), have initiated a research project on heat straightening of damaged steel bridges. The overall goal of the project is to develop a guide that will enable an engineer to design a repair scheme for damaged steel members in a rational manner. The first phase of the project was an extensive laboratory investigation of the fundamental behavior of heat-straightened steel. This phase is nearing completion, and results to date are reported in two companion volumes (4, 5) to this report. In addition to the laboratory study, a major focus of the project is a field evaluation of the heat-straightening process as applied to actual bridge conditions. The purpose of this report is to describe the

results of a field study for the evaluation of heat-straightening effects on the behavior of damaged, full-scale simulated bridge girders.

The process of heat straightening is a very elementary concept to understand. It consists of heating the bent steel member at appropriate locations in specific patterns. The adjacent, unheated material in the member (and/or external restraints) provides the necessary restraint to impede the longitudinal thermal expansion. During the cooling process, the unrestrained thermal contraction will induce curvature. If this curvature opposes the damage curvature, the member will tend to straighten.

Although there exist many types of heat configurations, such as the spot, line, strip, and edge heat, the vee heat is the basic pattern used to straighten bends in steel members. As can be seen in Figure 1, a typical vee heat starts with a very small spot heat, applied at the apex of the vee-shaped area using an oxy-acetylene torch. When the desired temperature is reached, the torch is moved progressively in a serpentine motion toward the base of the vee. The cool material ahead of the heated section resists and decreases the normal thermal expansion of the material in the longitudinal direction. As a result, the heated material will expand through the thickness. At the completion of the heat, the entire cross section is at a high and relatively uniform temperature. As the steel cools, the material contracts with less longitudinal restraint. The resulting thermal contraction is greater than the thermal expansion, producing curvature in the member.

By controlling the restraint conditions, the temperature variation, the size and location of heats, and the number of heating cycles, permanent modification to the dimensions of structural steel members can be achieved.

Purpose and Objectives

The primary purpose of this report is to describe the field investigation of the behavior of damaged structural steel bridge girders during the heat-straightening process. The specific objectives of the investigation are:

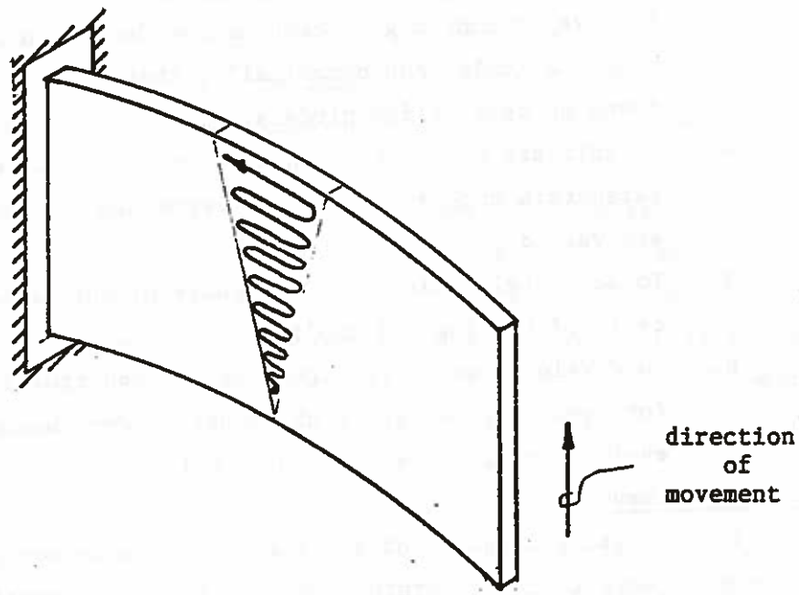

Figure 1. Typical Vee Heat Application in Plates

1. To design and construct a Heat-straightening Evaluation And Testing (HEAT) facility that will enable the simulation of actual field conditions for bridge girders.
2. To select a series of steel girder and concrete slab deck combinations that will simulate field conditions and cover a wide range of practical applications.
3. To develop inducing procedures for damage to test girders, both statically and dynamically, that will resemble damage found on bent bridge girders.
4. To initiate systematic repairs for each damaged beam in which parameters such as heating patterns and constraining forces are varied.
5. To accurately measure the response of the test beams to each cycle of heating and cooling.
6. To develop a set of engineering and construction guidelines for repairing damaged slab-girder bridges based on an evaluation of the experimental data.

Literature Review

In conducting a survey of the literature, a number of conflicting statements were found concerning the effect of heat straightening for the repair of damaged steel structures. This diverse information has contributed extensively to the reluctance of some engineers to accept the heat-straightening technique as an effective and reliable repair method. A summary of many of the facts and fables concerning heat straightening are given in a companion report (5). Outlined here is the pertinent literature related to field applications of heat straightening.

The literature review is divided into five general categories: (1) field studies associated with measuring the response of structural steel members during the heat-straightening process; (2) practical applications in the field; (3) laboratory studies of the behavior of members during heat straightening; (4) analytical studies for predicting the behavior of members during heat straightening; and (5) laboratory studies of the mechanical properties of heat-straightened steel members.

Field Studies. Moberg (20) is the only known investigator to conduct a field study of heat-straightening repair for a damaged bridge girder. Careful daily measurements were recorded for the progressive

straightening of the damaged girder on the Bothell bridge in Washington state. The lower flange of the girder was hit by an over-height vehicle.

In his thesis, Moberg outlined a set of general principles, tasks and procedures that can be used in assessing and repairing damage on steel bridge girders using heat straightening. He explained the fundamentals associated with the use of different types of heat patterns. Each pattern can be applied to specific situations to modify a damaged member's shape by curving or straightening the element as desired.

In setting guidelines for the assessment of damage, Moberg stressed the importance of public safety. Close access to the damaged area must be achieved and the integrity of the structure ascertained. A direct application of these principles was utilized on the Bothell Bridge. A traffic control plan was designed while a custom-built, truck-mounted scaffold was used to gain access to the damaged area. The damage assessment revealed that one W 33 x 118 beam was hit at the vertical midpoint of its web. The bottom flange was displaced 4.01 inches, while the top flange was displaced 0.1 inches. The top flange was rotated, leaving one edge 0.25 inches away from the concrete deck slab. The bottom flange had rotated about 0.92 inch over its 1-foot width. The web had yielded by bending about its weak axis and along a vertical line through the point of impact. The lower flange had been previously repaired and covered by a splice plate 3/8 in. x 12 in. x 12 ft. The length of the beam between piers was 45 feet, and it was hit about 9.1 feet from one interior pier. Diaphragms were located at the third points.

The damage assessment also revealed that another beam had deflected elastically 3/4 inch. That beam was displaced by the forces transferred to it through the diaphragm, which buckled due to the excessive axial forces caused by the impact.

In order to straighten the damage on the Bothell Bridge, the heat-straightening repair technique was used. To remove the web indentation, an 18,000-pound force was applied to the crest of the dent and circumferential line heats were applied. An additional force of 9,000 pounds was applied directly to the bottom flange. Assuming that

half of the force which was applied to the web was transferred to the bottom flange, a net total force of 18,000 pounds was transversely applied to the bottom flange so that the ratio of the actual moment in the flange and the attached cover plate to its yield moment was approximately 0.83. One-half-depth, 30-degree vee heats were used to straighten the lower flange of the damaged beam. Because the joint thickness of the flange and the cover plate was greater than one-half inch, two torches were used and both the top and bottom surfaces of the flange were heated simultaneously.

The damaged beam was divided into three separate areas. Area 1 included the damaged portion of the beam where the impact occurred. Areas 2 and 3 encompassed the reverse bend on either side of Area 1. About 94 vee heats were applied along an 18-foot span of the beam. These heats caused an over-straightening in the regions on both sides of the impact point. To correct this over-straightening, 20 more vee heats were applied to the opposite side of the flange to counteract the improperly placed heats.

In the repair of the Bothell Bridge, Moberg tried to correlate his experimental measurements to an analytical model. To make comparisons between measured and predicted bends, he used the Holt equation (15) to predict the amount of curvature caused by one 1200°F, half-depth, 30-degree vee heat. He divided the beam into one-foot increments and determined the slope of each small increment from field measurements. The change in slope between two consecutive increments was then divided by the change in slope predicted by the Holt equation. The ratio yielded the number of vee heats required at each increment.

Since displacements at each of the one-foot increments were not taken every day, the linear tangent method was used for measuring the beam response during repair. In this method, the linear tangents between curves were identified, and displacements were measured only at the end points of these tangents. By computing changes in slope between tangents and knowing the number of vee heats utilized, a comparison could be made with Holt's equation. The linear tangent method was used to examine the results of each day's heating patterns.

Because of time constraints, the measurements of deflections caused by heat straightening were taken only at the end of each day and not

after every heat application. Moberg used only one heating pattern and did not vary the applied jacking force. He also applied vee heats to elastic zones of the damaged girder, which caused an over-straightening. He concluded that heat straightening should only be performed within the length of the member that displays a curvature on the concave side, as well as on the convex side.

Moberg's work is the only documented field study providing detailed measurements during the heat-straightening process. One of the goals of the current project is to conduct a much broader study into the behavior of in-place damaged steel girders during the heat-straightening process. Measurements of the response of the damaged girders after each heating/cooling cycle were recorded for comparison purposes. Various constraining forces and heating patterns were applied to study their effect on the behavior of each member. Thus, Moberg's work formed a starting data base for the current study.

Practical Applications. In 1938, Joseph E. Holt, one of the leading pioneers in the field of heat straightening, wrote what appears to be the first paper (15) describing the use of the heat-straightening procedure for dimensional modification. The same paper was republished in 1955 in a revised and updated version (14). This article listed in detail the methods of applying heat to straighten flat bars, angles, channels, and wide-flange beams. It was mentioned that the use of external forces could speed up the straightening process. The author also pointed out that it is very beneficial to repeat the heat process if the amount of curvature is large.

Richard E. Holt presented two papers (16, 17) describing the behavior of heated steel subjected to single-axis, perfect confinement. He also mentioned the importance of perfect biaxial confinement in producing larger thermal stresses for the same temperature change. Various graphs relating strain to temperature were given. He discussed the basics of vee heats, pointing out the importance of not retracing the heating path because the cooling material behind the torch is adding confinement to the next section to be heated. He recommended that the external restraint be applied before and not during the heating process and that the temperature be limited to 1200°F.

Engineering News Record (10), an article by Ernest Newman in Military Engineer (21), and Welding Engineer (12, 23) all documented one of the largest and most successful heat-straightening repair jobs at McCord Air Force Base near Tacoma, Washington. On January 15, 1957, fire damaged two adjacent hangars each composed of eleven three-hinged trussed arches with a span of 275 feet and a height of 90 feet. The most serious fire damage occurred in areas where the temperature reached as high as 1200°F to 1900°F. These high temperatures occurred in four distinct areas where very flammable materials were stored.

A total of 1486 members of the 7327-member structure were damaged. Those members formed about 500 tons of the 1900-ton structural steel framework. From the 1486 distorted members, 1440 members were heat-straightened and only 46 members were replaced. A detailed description of the heat-straightening repair process was described. Joseph Holt supervised the repair operation.

Engineering News Record (19) described the approach used to heat-straighten fire damaged columns. The columns were straightened using vee heats.

Shanafelt and Horn (28) developed a practical user's manual that established guidelines for evaluation and repair of damaged steel bridge members. Even though other repair methods are discussed, the emphasis of the report is on heat-straightening. The manual gives a detailed description of how to inspect the damage, assess the damage, select a repair method, and repair the damage. It is recommended that heat straightening not be applied to members with maximum nominal strains larger than 15 times the yield point strain. A detailed description of all the heat patterns is given. Several examples of damage repair are presented.

Each of these publications provides examples of how to apply heat straightening to actual damage. Few, if any measurements were taken, so the discussion is qualitative in nature. While some details vary, these papers provide a good description of current practice, which formed an initial framework for the present study.

Member Behavior. Brockenbrough presented a paper (7) describing an experimental investigation into the heat curving of plate girders using edge heats. Six edge heating passes were made using different

temperatures. The main objective of the study was to determine the residual stresses, strains, and curvatures. The sectioning method was used to determine residual stresses. The study of the final residual stresses indicated yielding in tension at the heated edge, moderate tension at the opposite flange edge, and compression predominating in the web.

Weerth (29) and Nicholls and Weerth (22) conducted an experimental investigation of heat-straightening steel plates. The angles of vee heats varied from 24 to 60 degrees in 6-degree increments, with depths of one half, three quarters, and full depth. In addition to producing the lowest residual stresses and maximum residual strains, full depth vee heats produced the largest curvature. However, they also resulted in an overall shortening of the member.

Horton (18) presented the results of an experimental study on 18 wide-flange beam sections. Several different heating sequences were performed on the wide-flange sections to produce either sweep or camber.

Roeder (24, 25) performed heat-straightening tests on 50 plate specimens and ten wide-flange sections. His study showed that plastic rotation increases with heating temperature, applied load, and vee angle. He also concluded that the residual stresses do not appreciably influence the behavior of plate members but may influence the behavior of wide-flange sections.

In 1986, Avent (3) presented a report describing an extensive study on the bending behavior of steel members subjected to heat straightening. Heating temperature, applied load, plate thickness, depth of vee, and angle of vee were varied. The progression of plate movement during the heating process was described. The experimental results showed that the plate thickness has negligible effect on plastic rotation. The amount of plastic rotation increases with temperature, applied load, vee depth, and vee angle. Heat straightening was performed successfully on three 24-inch long and three 72-inch long plates deformed plastically with a midpoint and a third point loading, respectively. No external restraining forces were used in the straightening process.

Experimental tests were performed on wide-flange sections to determine the effect of single vee heats. Studies of vee heats applied

to the flanges to produce sweep showed a regular increase that is directly proportional to the vee angle. Heat straightening was also performed on a W 6 x 9 wide flange beam that was bent plastically about one flange by applying a lateral concentrated load at the midpoint of that flange. No external jacking force was applied during the heat-straightening process.

While each of these papers provides useful experimental data, the scope was limited to simple elements. A key missing ingredient is the correlation between such elements and actual member behavior in a building or a bridge system. One of the goals of this report is to begin to bridge this gap by studying a simulated bridge girder system.

Analytical Studies. Brockenbrough (8) presented a theoretical study on the use of edge heats on wide-flange girders. The analysis was based on Duhamel's analogy. A specific girder was analyzed for several heat widths and different residual stress patterns.

Holt (16) presented a camber prediction equation based on the dimensions shown in Figure 2 with a full-depth vee. Assuming a linear variation of the strain, Sp, through the depth of the vee, neglecting out-of-plane buckling and using the concept of similar triangles:

$$\phi = \frac{h}{d} = \frac{[U/\cos(\alpha/2)]}{[w/\cos(\alpha/2)]} \qquad (1)$$

thus,

$$U = \frac{hw}{d} \qquad (2)$$

or, taking the plastic strain over the vee width

$$U = Sp\ w_v \qquad (3)$$

where,

U = upset
h = displacement of the member at distance d
w = width of the member
d = length from the bend where the displacement, h, is measured to the location of the vee heat
Sp = plastic strain caused by heating

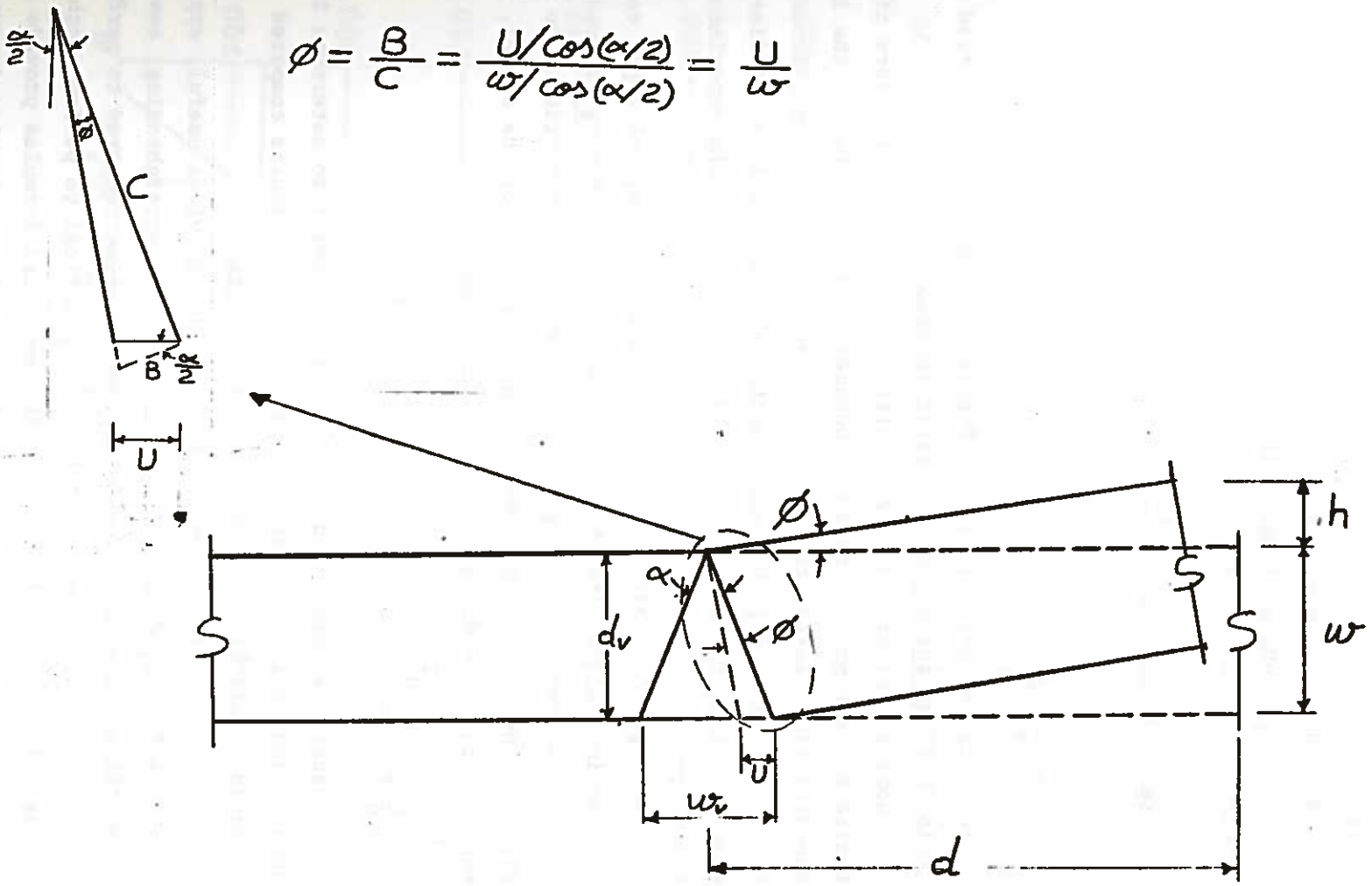

Figure 2. Vee heat geometry.

$$w_v = \text{width of the vee heat} = 2\, d_v \tan(\alpha/2) \quad (4)$$

where,

d_v = depth of vee heat

α = apex angle of vee heat

Combining Eqs. 2, 3 and 4

$$Sp\ [2\, d_v \tan(\alpha/2)] = \frac{hw}{d} \quad (5)$$

or,

$$\frac{h}{d} = \frac{2\ Sp}{w}\, d_v \tan(\alpha/2) \quad (6)$$

where Sp can be determined from Figure 3. Roeder (24) referred to the ratio "h/d" as the angle of plastic rotation, ϕ.

Horton (18) presented a theoretical analysis in the form of a finite element program based on Duhamel's analogy. Due to the lengthy computer time needed, the theoretical analysis was not performed on all the tests reported in his experimental study. For those studies which were reported, the results compared favorably with the experimental results.

Moberg (20) modified the Holt equation for partial depth vees based on experimental results obtained by Weerth (29). Moberg assumed that the displacement, h, at a given distance, d, is proportional to the ratio of the depth of the vee, d_v, and the width of the member, w. From equation 6, the modified Holt equation becomes:

$$\frac{h}{d} = \frac{2\ Sp\ d_v^2}{w^2} \tan(\alpha/2) \quad (7)$$

Roeder (24) presented a finite element model to determine the deformation caused by heat straightening. The results compared reasonably well with the experimental results.

While each of these analytical studies provides useful, approximate solutions for the deformations caused by heat straightening, several drawbacks are present. The large computer time required to perform a theoretical analysis makes it highly impractical to perform such an analysis in field applications. The empirical formulas provide a promising answer to the problem. However, these formulas do not take

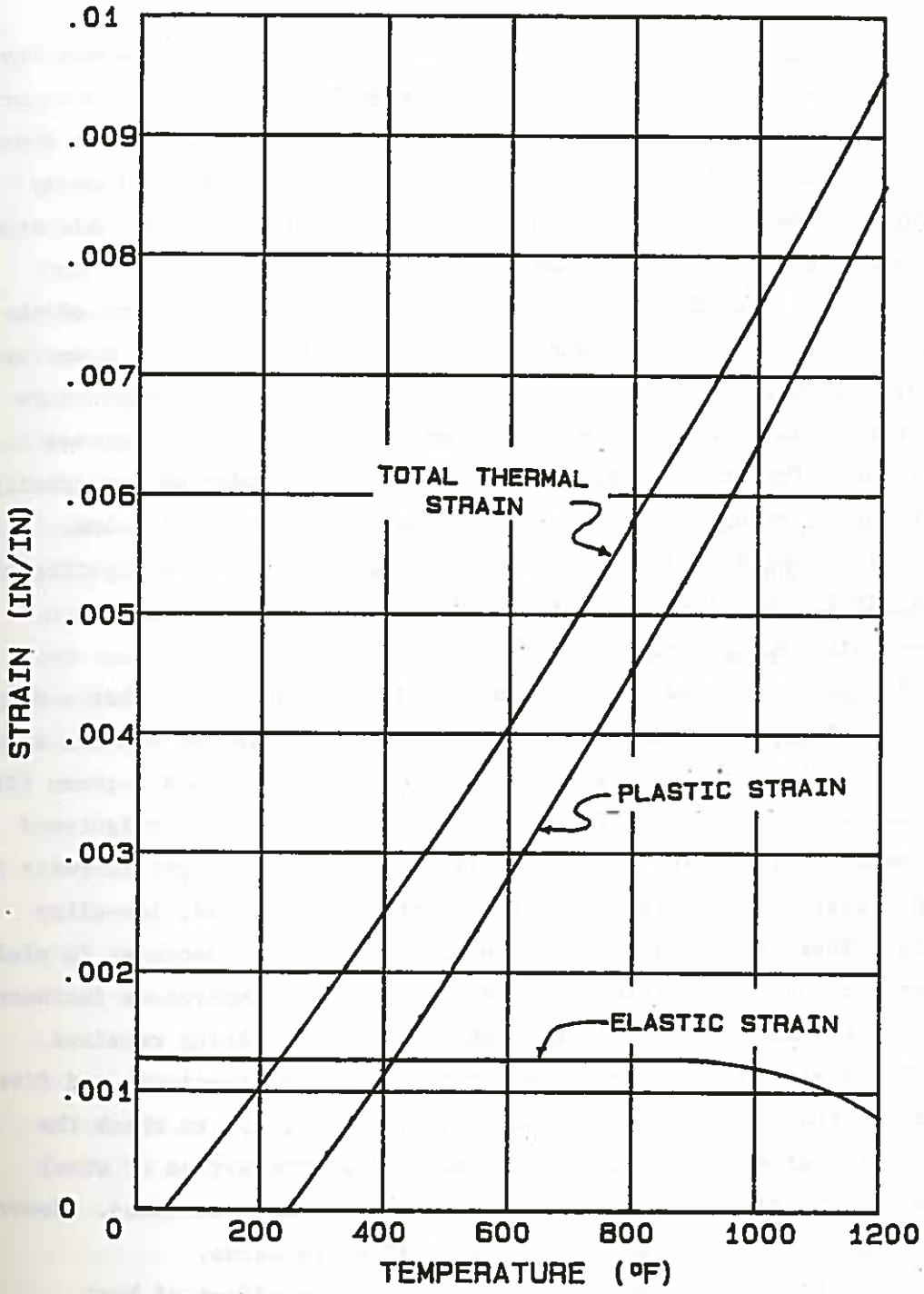

Figure 3. Strain vs. temperature for A-36 steel (16).

into account the effect of applied loads or restraining forces, which were reported to be very important variables by some researchers (3, 24, 25). In this report, a comparison of the results obtained by the authors to the results obtained using the existing analysis formulas will be provided.

Member Properties. Tests performed on heated steel members have shown that no significant changes in the mechanical properties occur after cooling has taken place, provided the heating temperature does not exceed approximately 1600°F. There is ample evidence that properly executed flame straightening does not significantly degrade mild steel or low alloy bridge steel members.

The coefficient of thermal expansion, which is a measure of the rate of strain per degree temperature, varies directly with temperature (6, 9, 22, 24). The modulus of elasticity decreases as temperature increases. As a result, the heated member experiences a decrease in stiffness. This may require the member to be unloaded or temporarily supported to reduce the stress in the member to a nominal value. But Horton (18) and Nicholls and Weerth (22) have reported no significant change in the modulus of elasticity after the completion of the heat-straightening process.

A study performed by Harrison (13) in 1950 has shown that a slight increase of 3 percent in yield stress occurred in tested members after heat straightening. Brockenbrough (7), Horton (18), and Rothman (26, 27) have all performed different tensile tests on heat-straightened specimens after cooling, and their results showed a slight increase in yield stress for all steels except for the heat-treated, low-alloy steels. These steels showed an average of 6 percent decrease in yield stress. Because the yield stress decreases when temperature increases, it might be necessary to brace or shore the member being repaired.

The analysis performed on seven tensile steel specimens and five rivets at the McCord Air Force Base (10, 12, 21, 23) to check the effect of heat straightening on the mechanical properties of steel showed a negligible change in the yield and ultimate stresses. However, the elongation was reduced by 25% below ASTM standards.

A substantial amount of data related to the effect of heat straightening on the ultimate stress, fatigue strength, percent

elongation, ductility, hardness and toughness has been recorded, and there is no evidence of detrimental effects on these properties for mild steels (13, 18, 29).

Scope of Investigation

The purpose of this study was to develop and quantify procedures which can be used to effectively repair damaged structural steel bridge girders by heat straightening. A Heat-straightening Evaluation And Testing (HEAT) facility was built to act as an actual bridge girder repair and rehabilitation simulation facility. A description of the detailed design and construction of the HEAT facility is presented in Chapter 2. Chapter 3 describes the experimental testing associated with damaged composite steel girders. The damage inducement process is described. Chapter 4 presents a detailed description of the repair procedure, including the application of different heating patterns on the tested girders and an evaluation of the girders' behavior. The effects of the various heating sequences on the girder specimens are compared. This comparative study provides a basis for evaluating the effectiveness of the heat-straightening repair techniques for different steel members. In addition, the results obtained in this investigation are compared with those obtained by the use of existing empirical analysis formulas. Finally, the effect of the applied constraining forces on the inelastic behavior of the girders is described.

2. DESIGN AND CONSTRUCTION OF THE HEAT FACILITY

Justification

The original plan for this project called for the in-place repair of an actual, damaged bridge girder using heat straightening. However, the decision to design and construct the HEAT facility (11) was made after careful consideration of the following: (1) traffic control and convenience; (2) control of damage; (3) opportunity of parameter variation; and (4) the need for a training facility.

Traffic Control and Convenience. The purpose of experimentally repairing an in-place bridge girder is to obtain detailed documentation of the effect of the heat-straightening process. The existence of elements such as a bridge deck, composite construction, restraining supports, and diaphragms are possible sources of variation. To obtain such controlled data, careful and accurate measurements of the response of heat-straightened girders would have to be made following each heating cycle. With this consideration in mind and adding the constraints of the weather and the part-time investigator status of the authors, it was estimated that two months would be needed to complete the repair process for one girder.

Traffic control was immediately viewed as a problem, since lane(s) in which the repairs are being carried out would have to be partially or completely blocked from traffic. This restricted traffic flow for such a long period of time would be a harsh inconvenience to area motorists. Thus the idea of a separate, full-scale simulated bridge girder facility to be placed near the Louisiana State University campus was considered.

Moberg (20) addressed the subject of traffic control. Because the highway on which Moberg was working carried a large volume of commuter traffic, a traffic control plan was designed. Even with this traffic control plan in use, a serious breach of safety provisions occurred. Pedestrians and spectators ventured into the work area and the work was interrupted. The proposed simulated bridge facility will allow research activities to be carried out without any unnecessary restriction on traffic. The progressive behavior of the damaged girder can be measured and analyzed after each heat.

Having the HEAT facility located near the LSU campus would also be more convenient to the researchers, as well as allow for a more

2. DESIGN AND CONSTRUCTION OF THE HEAT FACILITY

Justification

The original plan for this project called for the in-place repair of an actual, damaged bridge girder using heat straightening. However, the decision to design and construct the HEAT facility (11) was made after careful consideration of the following: (1) traffic control and convenience; (2) control of damage; (3) opportunity of parameter variation; and (4) the need for a training facility.

Traffic Control and Convenience. The purpose of experimentally repairing an in-place bridge girder is to obtain detailed documentation of the effect of the heat-straightening process. The existence of elements such as a bridge deck, composite construction, restraining supports, and diaphragms are possible sources of variation. To obtain such controlled data, careful and accurate measurements of the response of heat-straightened girders would have to be made following each heating cycle. With this consideration in mind and adding the constraints of the weather and the part-time investigator status of the authors, it was estimated that two months would be needed to complete the repair process for one girder.

Traffic control was immediately viewed as a problem, since lane(s) in which the repairs are being carried out would have to be partially or completely blocked from traffic. This restricted traffic flow for such a long period of time would be a harsh inconvenience to area motorists. Thus the idea of a separate, full-scale simulated bridge girder facility to be placed near the Louisiana State University campus was considered.

Moberg (20) addressed the subject of traffic control. Because the highway on which Moberg was working carried a large volume of commuter traffic, a traffic control plan was designed. Even with this traffic control plan in use, a serious breach of safety provisions occurred. Pedestrians and spectators ventured into the work area and the work was interrupted. The proposed simulated bridge facility will allow research activities to be carried out without any unnecessary restriction on traffic. The progressive behavior of the damaged girder can be measured and analyzed after each heat.

Having the HEAT facility located near the LSU campus would also be more convenient to the researchers, as well as allow for a more

productive use of their time. The heat-straightening process requires the use of several pieces of equipment. Therefore, with easy access to the HEAT facility, travel and set-up time would be saved.

Control of Damage. It is very important to have a facility where the application of damage to the steel girder can be completely controlled. The concept of the HEAT facility offers the advantage of allowing the researchers to control the damage induced to the girder specimen. The facility allows researchers to apply both static and impact loads anywhere along the length of the member. Midpoint, third point, or any other type of loading can be administered to the girder. The load can also be applied to the bottom flange, web, or top flange. Flanges can be bent and rotated to any degree desired. Such freedom in applying the damage will enable an enormous amount of data to be generated. This data will be very valuable in achieving the future goal of generating a computer program to analyze and design a heat-straightening repair procedure.

Another important aspect of damage control is that the structural behavior of the specimens can be evaluated. When structural systems involve a complexity of support constraints, coupled with composite or non-composite construction, structural properties of the specimen, such as plastic moment capacity and load-deflection behavior, cannot be easily calculated. With the HEAT facility, loads can be applied gradually while deflections at selected points can be monitored. This type of information for various cross sections would be necessary for planning the heat-straightening process.

Opportunity for Parameter Variation. As indicated earlier, a variety of support connections exist in bridge and overpass construction. The HEAT facility offers the user the freedom to select the size and shape of the girder desired. The facility is capable of imitating such field end conditions as hinged, fixed, or simply supported. Single-span or double-span girders can be used. It was also anticipated that a concrete slab could be placed on top of a girder specimen to simulate the dead load of a bridge deck. This would allow the slab-to-girder connection to be varied as either composite or non-composite. Parallel girders connected by diaphragms could also be used in the HEAT

facility. This type of set-up would identify possible problems in simultaneously straightening multiple girders.

The Need for a Training Facility. The final phase of the extensive research project on the use of heat-straightening techniques for repair of damaged steel structural elements in bridges calls for the development of a training program for both LDOTD engineers and maintenance personnel on how to design heat-straightening repair schemes and how to execute the repair in the field. However, problems can arise in conducting such repair training on an actual bridge or in the laboratory. Laboratory training sessions are very elementary and cannot involve complex variations in parameters found on actual bridge elements. In addition, actual field training sessions are practically impossible to conduct because of the reasons mentioned previously. The HEAT facility provides an excellent opportunity for training, thus eliminating the problems associated with training LDOTD engineers and maintenance personnel on an actual bridge or in the laboratory.

Based on its ability to handle full-scale simulated bridge girders, the HEAT facility could serve as a proficiency testing facility. After thorough training, LDOTD personnel and others could be certified to perform heat-straightening repair work on actual, damaged steel bridge elements.

Design

The problem in constructing the HEAT facility was to design a frame which would: (1) hold the steel girder specimen in place; (2) serve as a reaction for inducing damage; (3) allow the measurement of the progressive movement of the member under the influence of heat straightening; and (4) provide a means of restraint similar to that encountered in actual, full-scale bridge structures. The frame had to be reasonably simple in construction and sufficiently rigid to resist the large forces required to plastically deform the steel girder specimen. Several different types of frames were considered before finalizing the design.

Range of Parameters. The HEAT facility provides an excellent opportunity for simulating a wide range of parameters found on actual bridges. Possible parameter variations greatly influenced the decisions made as to the final size and shape of the facility.

First, it was necessary to select the length of the facility. The ability to use single span as well as double span members greatly influenced the decision. For this specific reason, the facility consisted of three separate plane frames, with 19.5-foot spacing between adjacent frames. That spacing was selected to accommodate the standard size of the concrete slab deck, which had an approximate length of 19 feet, thus requiring the overall length of the facility to be 39 feet.

The second and third parameters considered were the height and width of the HEAT facility. It was important to provide enough clearance in height and width so as to be convenient for working personnel. The height of the facility was designed to accommodate a 36-inch girder. In addition, special consideration was given to the average height of working personnel so that no scaffolding would be required and there would be enough clearance below the bottom flange of a typical test girder. The width was designed to provide enough working space between the specimen girder and the two parallel placed girders on the HEAT frame. In addition, a width of 10 feet would allow two parallel girders to be placed on the frame and connected by diaphragms.

A fourth parameter was the capability of the HEAT facility to carry many sizes and shapes of structural steel girders. For this reason, the frame was designed to handle different sizes of wide flanges, channels, angles, or built-up sections. The depth of the girder specimen is restricted to 36 inches, while its width can vary up to 9 feet. If members with a smaller depth than 36 inches are used as a test girder, a special support has to be provided between the girder and the frame.

Another parameter to consider was the ability to change the location of diaphragms. Diaphragms could be placed at the ends of the girder and at the third points or midpoint of 39-foot-long specimens. The diaphragms also served the purpose of restricting the rotation of the concrete deck slab without carrying any of its load. Thus, even when the girder is damaged, it must carry the total weight of the concrete slab above.

Another important parameter is that the girder end conditions should be very flexible. The supports were constructed to handle any

ideal support condition. The end of the girder could be fixed in all or any of the three directions, hinged, or free.

Still another parameter was the ability to utilize two types of steel girder to concrete slab deck connections. These two types are composite and non-composite. Two 19-foot-long normal weight concrete slabs were used. Holes were punched at 2-foot intervals in the slab. To simulate the action of actual composite girders, 1-inch holes were also punched along the length of the steel girder specimen at 2-foot intervals on either side of the flange. Then the slab and girder were bolted together. For non-composite action, only two rows of holes were punched on either end of the girder, and bolts were used only at those locations. Figure 4 shows the arrangement of bolts for composite action, while Figure 5 shows the arrangement of bolts for non-composite action.

The final parameter to consider for designing the different members of the HEAT facility was the magnitude of the constraining forces. Because the jacking forces needed to deform a girder specimen must be applied horizontally to the girders of the HEAT frame, these girders were placed on their sides and were connected to the columns through their webs. Each girder is capable of carrying a 90-kip load applied to the midpoint of either span or two 50-kip loads applied to the third points of each span.

Final Design. The HEAT facility was designed to withstand the large jacking force required to deflect and deform a large girder specimen. At the same time, the facility needed to possess all the special features mentioned in this chapter. In addition, it was desired to construct the facility using scrap steel available from the Maintenance Division of the Louisiana Department Of Transportation and Development (LDOTD) to reduce the cost. The facility was also designed to allow easy installation and removal of specimens. Figures 6 and 7 show the final size and shape of the facility. All the steel was ASTM A-36. The facility was designed according to the AISC specifications (1). The columns were constructed from wide-flange sections that are capable of resisting all the forces transferred to them from the jacking frame through the two side girders. Those girders were placed on their side in order to carry the transverse force needed to deflect the girder

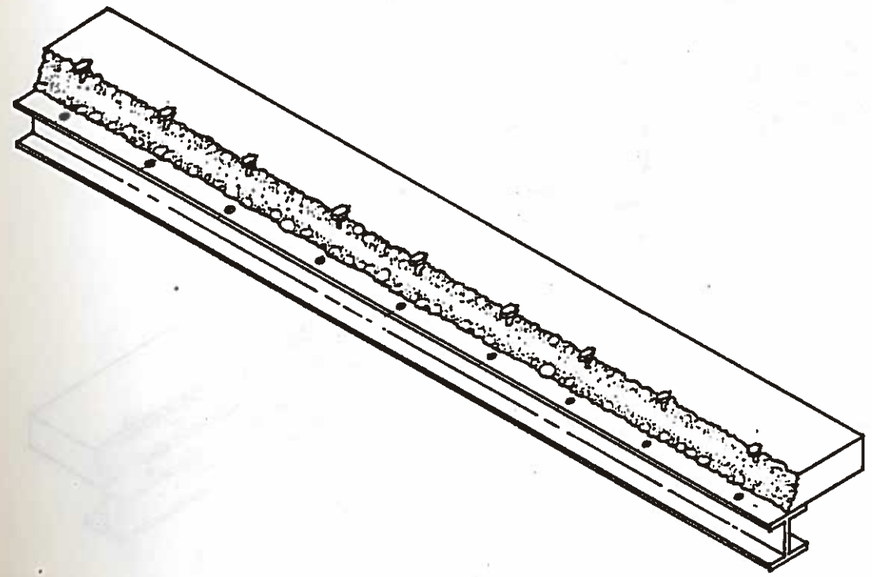

Figure 4. Slab-to-Girder Connection for Composite Action

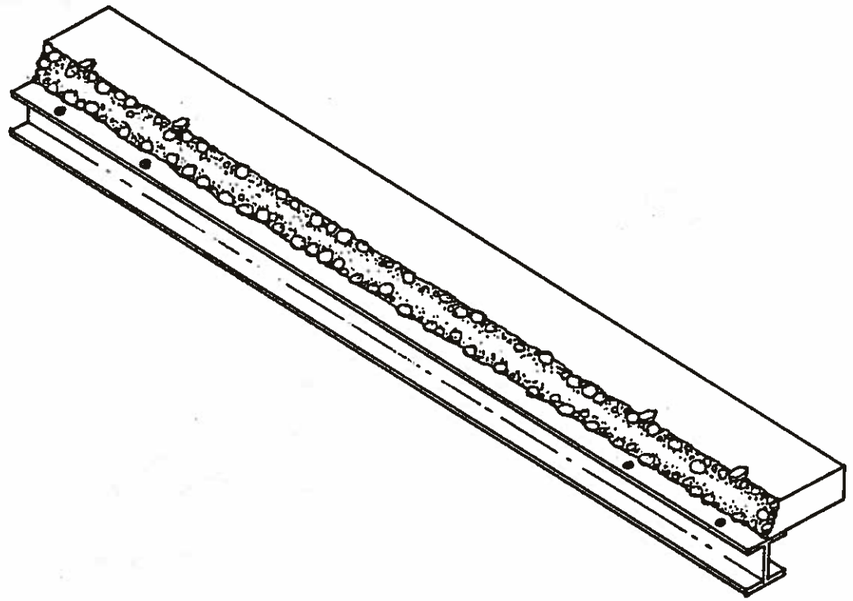

Figure 5. Slab-to-Girder Connection for Non-Composite action

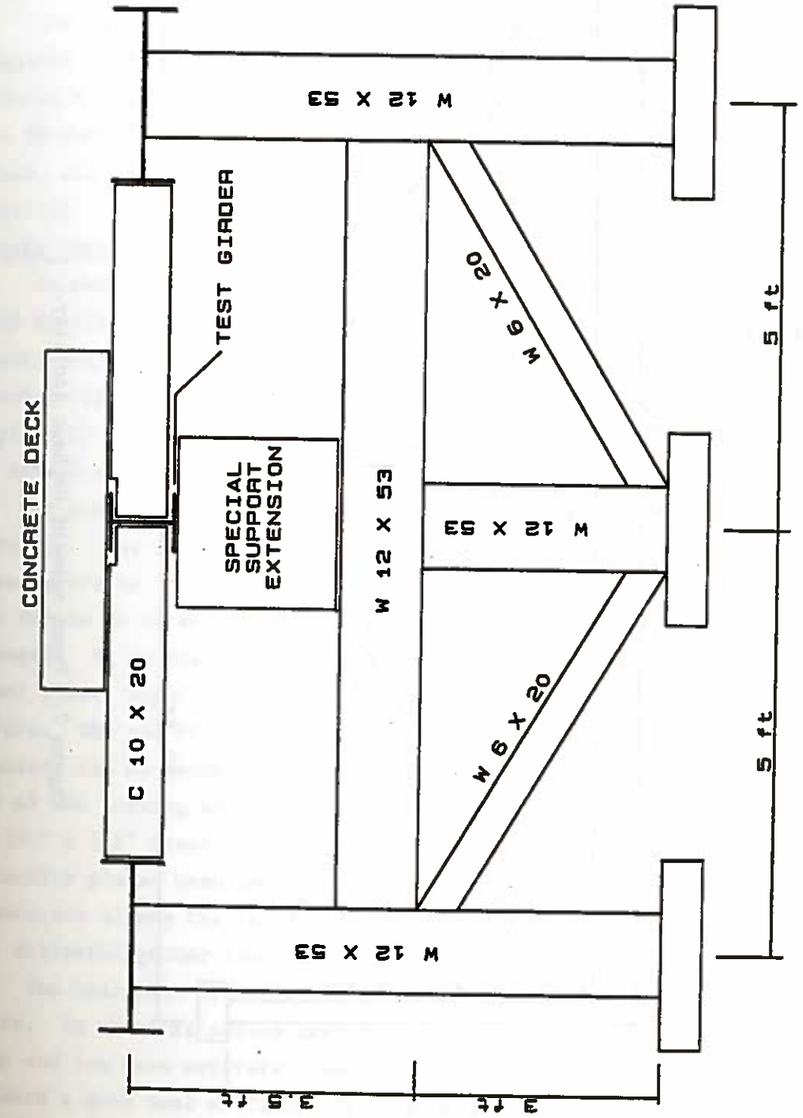

Figure 6. Side view of the HE

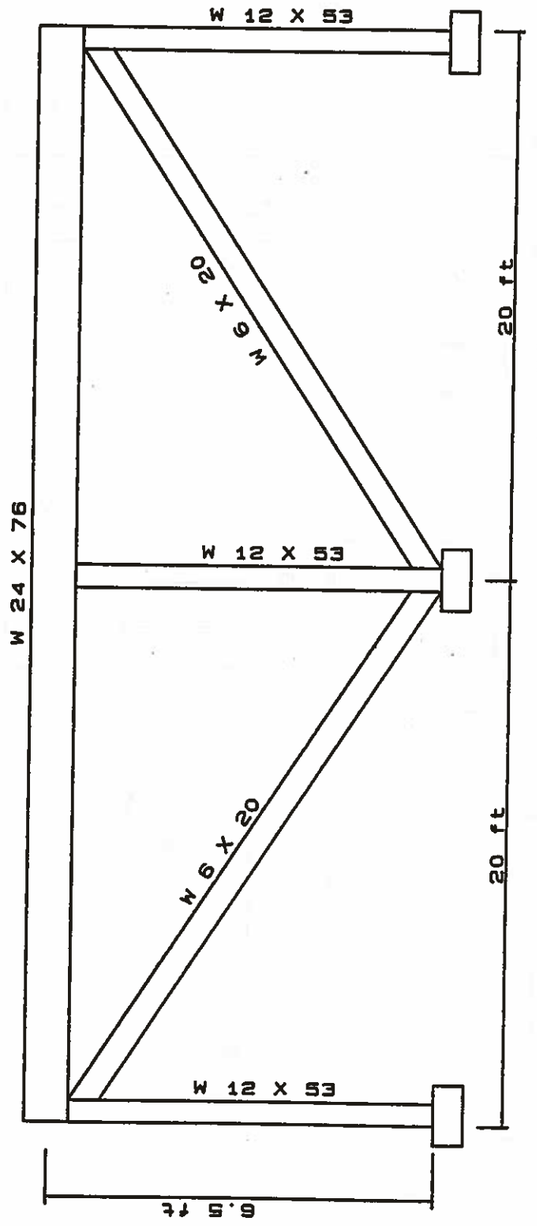

Figure 7. Front view of he heat facility.

specimen. The lower beam is a W 12 X 53 wide flange section and its primary role is to provide support for the test girder. If the test girder is less than 36 inches deep, another special support has to be placed between the girder and the beam.

The HEAT facility is made up of three separate frames connected together by the top side girders and the diagonal braces. Also seen in Figures 6 and 7 are the actual dimensions of the facility. Even though the 39-foot span is a little smaller than many of the actual bridge spans, all the features of actual bridges can be simulated in the facility.

Damage Inducement

As mentioned earlier, one of the most prominent features of the HEAT facility is the ability to control the damage inducement process. Static loading as well as dynamic loading can be applied to the girder specimen in order to plastically distort the member. Static loads are applied by the use of a hydraulic jack while dynamic loads are created by actual ram impact.

To statically deform members, a special jacking device was constructed. The same jacking device was also used to produce additional constraints on the member and expedite the heat-straightening process. The device is capable of transmitting a 30-ton force to the member to be damaged. It consists of a 4 1/2-inch diameter, double-extra strong steel pipe. Figure 8 provides a schematic drawing of the jacking device. The end of the jacking device, where the 8-inch long angle is located, can be hooked to the bottom flange of a test girder. The other end of the jacking device fits into the special slot on the 8 1/4" x 14 3/4" x 1/2" steel plate that can be clamped to the flange of the laterally placed beam on the HEAT frame. This type of round bar-to-slot connection allows the jacking device to rotate as the bottom flange of the deflected girder tends to rotate as it deflects.

The hydraulic system employed was from the ENERPAC line of products. In the test set-up used in this research project, the hydraulic pump and ram were separate items connected by a hose. This set-up allowed a good deal of flexibility in using the jack. The pump was of a model P-391 and was capable of delivering 10,000 psi of pressure. Each

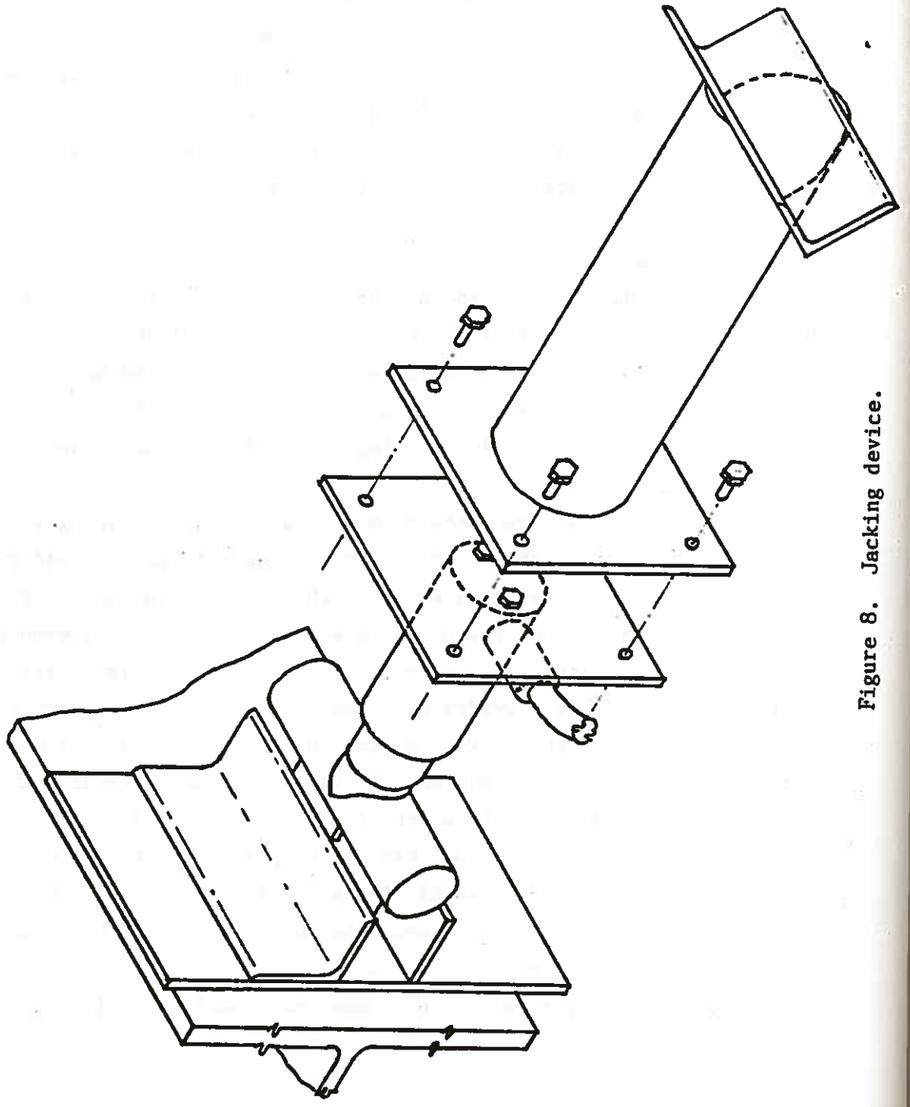

Figure 8. Jacking device.

pump was fitted with a gage (model GP-15S and adapter GA-2) which could read the oil pressure in 200 psi increments up to 15,000 psi.

A number of different hydraulic rams were used in which both the load capacity and length of extension varied. Included was a 10-ton ram with a 4-inch extension, a 15-ton ram with 6 inches of extension, a 25-ton ram with 14 inches of extension, and a 50-ton ram with 6 inches of extension (model numbers RC-104, RC-156, RC-2514, and RC-506T, respectively). The base of each cylinder was supplied with two thread holes for attaching a base plate, as well as internal thread on the extended end of the plunger.

Experimental Measurement

The main goal of this research project was to accurately measure the response of deflected steel girders after the heat-straightening process. To accomplish this goal, a precise and reliable measurement system had to be designed. A special U-shaped reference frame was built from 3/4-inch square steel tubes. The reference frame is shown in Figure 9. Eight measuring points were taken at each cross section, as shown in Figure 10. The arrows shown in the figure indicate positive directions. The reference frame could rest on two steel angle rails located on either side of the damaged girder. The rails ran along the whole length of the HEAT facility. This set-up allowed the reference frame to be moved and measurement readings to be taken along the whole length of the deformed girder specimen. Each of the two rails rested on four 6 x 13 channels that were spaced about 4 feet center to center. The ends of each rail were clamped to the diaphragms. This measuring frame system allowed the reference frame to be moved freely in the longitudinal direction, while restricting its movement in the horizontal and vertical directions. In this manner, different measuring locations along the length of the girder could be specified at different intervals for each test set-up. Because it is important to restrict the deflection of the rails and the channels, bolts were used to attach the rails to the channels and the latter to the flange of the side girder. Bolts were used so that the channels and rails could be removed separately when the heat-straightening repair of one girder is completed and another girder is to take its place.

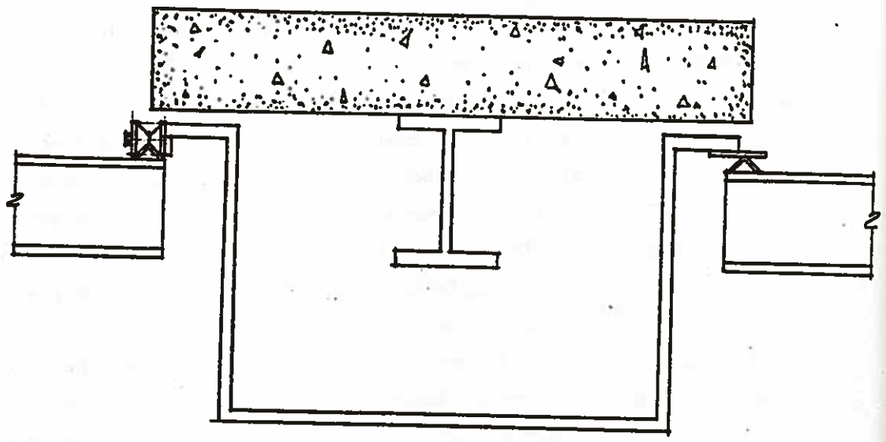

Figure 9. Measuring frame.

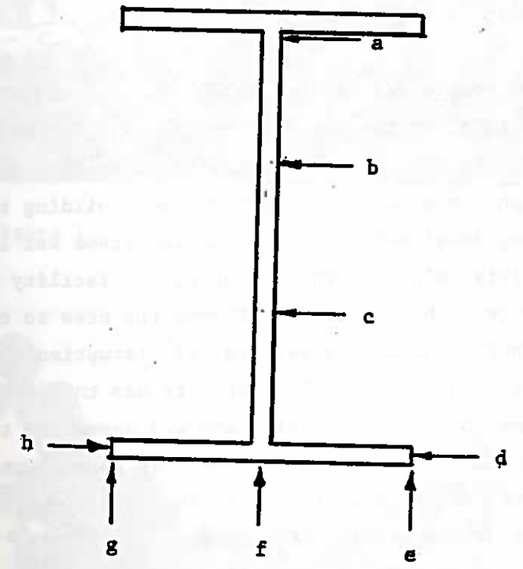

Figure 10. Cross Section Showing Typical Measurement Locations and Positive Directions

A 24-inch Mitotoyo 16R No. 182-162 stainless tempered ruler, graduated in one hundredth of an inch increments, was used to measure the distance between the reference frame and the measuring point on the damaged girder. However, readings were taken only to one fiftieth of an inch.

Another measuring device was needed to control the constraining force. For this reason, the jack was controlled by a separate hydraulic pump. A 15,000 psi capacity pressure dial gage was attached to the pump to accurately measure the force exerted by the jack on the girder. The dial gage was graduated in 200 psi increments, and approximate readings can be made with 50 psi accuracy.

Construction

Upon completion of the design phase of the HEAT facility, it was necessary to start the construction phase. The Maintenance Division of LDOTD agreed to construct the facility. For this reason, a special crew was assigned the task of assembling and building the HEAT facility. Since the scrap steel selected to build the frame was located at the Maintenance Division's construction shop, the facility was constructed at the shop site. This procedure allowed the crew to construct the HEAT facility without inducing a great deal of disruption to its other important work at hand. The HEAT facility was then transported in separate pieces to the campus site, and was assembled together there. Figures 11 and 12 show the construction crew assembling the facility at the campus site, and Figures 13 and 14 show the completed structure. The total cost of the construction phase was estimated to be $27,000.

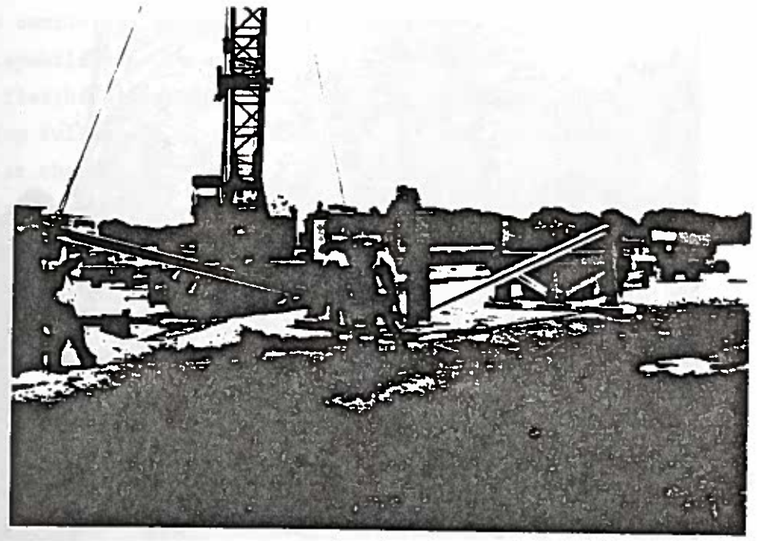

Figure 11. The HEAT Facility During the Construction Phase

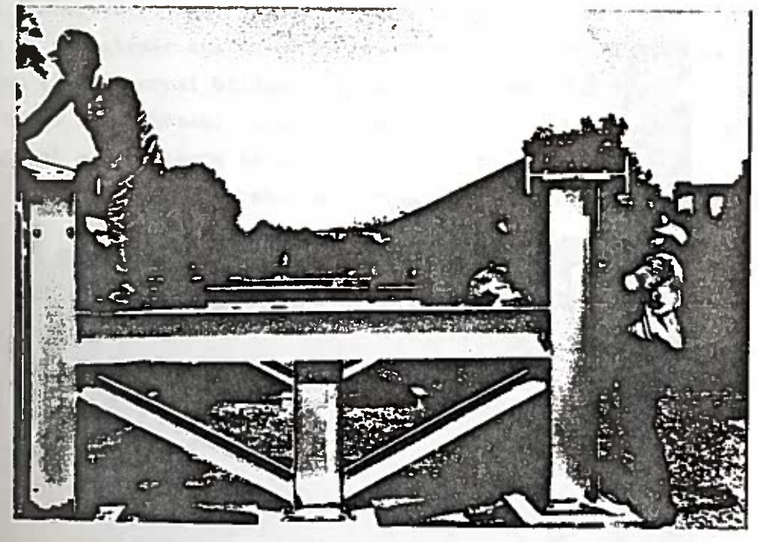

Figure 12. The HEAT Facility Toward the End of the Construction Phase

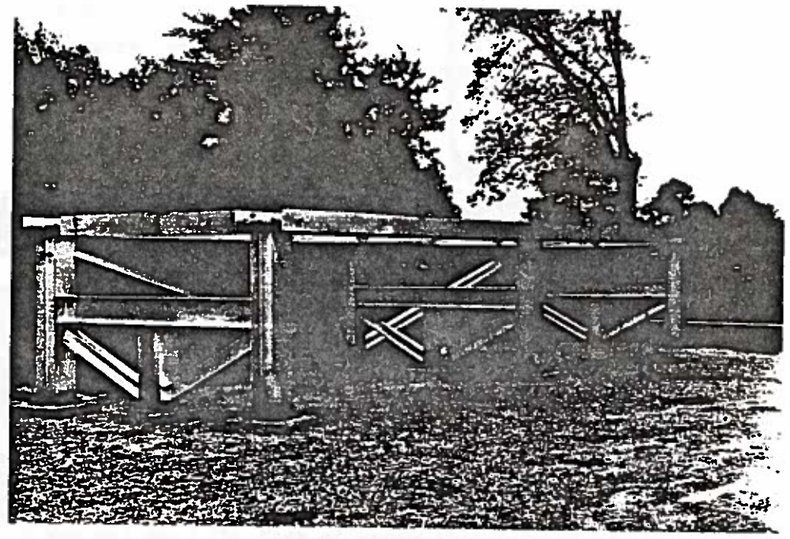

Figure 13. Completed HEAT Facility

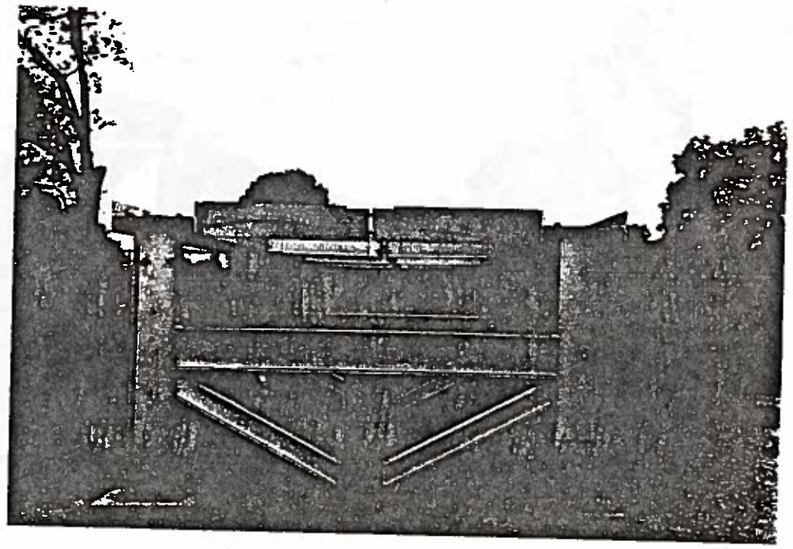

Figure 14. Complete HEAT Facility (Side View)

3. DESCRIPTION OF DAMAGED COMPOSITE STEEL GIRDERS

The completion of the HEAT facility has given the research team a unique capability to conduct heat-straightening research. The facility has the flexibility of handling a wide variety of structural shapes and simulating full-scale field bridge conditions. The initial field studies at the facility have involved slab-girder systems with simulated damage from over-height vehicles. This chapter describes the damage inducement and damage assessment for all three cases.

Selection of Test Specimens

In order to represent the wide range of girders found in actual bridges, the selection process involved considered variation in size, length, type and location of damage, support conditions, diaphragm locations, intensity of load, and type of girder-to-slab connection. Four wide-flange sections were selected initially. The sections, two W 10 x 39s and two W 24 x 76s, were chosen in order to compare the behavior of shallow sections to that of deep sections during heat straightening.

Two normal-weight concrete slab decks, 19 feet long, 4 feet wide, and 12 inches deep, were chosen as dead load. The slabs could be placed on top of the girder specimens to resemble the action of dead weight found on top of actual bridge members. Two types of girder to slab connections were chosen: composite and non-composite. Table 1 shows the initial set of tests to be conducted at the HEAT facility.

In this report, the results of the tests on the composite girders in Table 1 are presented. The other girders will be tested during the third year of the project.

Case SB-1: First Test on W 10 x 39 Composite Girder

Test Set-Up. The first experiment of this project involved the evolution of the behavior of a damaged W 10 x 39 wide-flange composite girder repaired by heat straightening (11). The HEAT facility, as described in Chapter 2, was used to simulate an actual bridge system.

The wide-flange girder consisted of A-36 steel and was 20 feet long. The girder was connected to the dead weight concrete slab by the use of 18 one-inch diameter bolts to simulate composite action. The bolts were placed on both sides of the flange and spaced at 2-foot

Table 1. Summary of completed and proposed heat-straightening tests at the HEAT facility.

Member Size	Length (ft)	Bridge Simulation Type	Diaphragm Locations	Test Designation	Damage Inducement Procedure* (each damage cycle listed separately)	Heating Cycles to Repair (completed tests only)
W10 x 39	20	Composite slab-girder	Ends only	SB-1	Mid-point static load on bottom flange	36
				SB-2	Mid-point static load on bottom flange	16
W24 x 76	20	Composite slab-girder	Ends only	SB-3	Mid-point impact load on bottom flange	28
				SB-4	Mid-point static load on bottom flange	
				SB-5	Mid-point static load on bottom flange	
W10 x 39	20	Non-composite slab-girder	Ends only	SB-6	Mid-point impact load on bottom flange	
				SB-7	Mid-point static load on bottom flange	
W24 x 76	20	Non-composite slab-girder	Ends only	SB-8	Mid-point impact load on bottom flange	
				SB-9	Mid-point static load on bottom flange	
W24 x 76	40	Composite slab-girder	Ends and third-points	SB-10	Mid-point impact load on bottom flange	
				SB-11	Mid-point static load on bottom flange	
W10 x 39	20	Axially loaded truss member	None	SB-12	Mid-point static load on web mid-point	
W10 x 39	20	Axially loaded truss member	None	SB-13	Mid-point static load on one flange	
Total Straightening Cycles				13		

*Load-deflection curves are obtained for all static loads applied to induce damage including final curve after last repair.

intervals along the entire length of the girder. After assembly, the composite girder was lifted by a crane and placed in the HEAT facility.

Because the test girder was only 9.92 inches deep, a special support extension was provided at both ends of the girder, consisting of a W 24 x 76 wide flange section 23.92 inches deep. An additional 2-inch thick steel plate was added so that the concrete slab deck was located about one half inch higher than the top flange of the diaphragm channels. The bottom flange of the support extension was bolted to the support beam on the HEAT frame using six 3/4-inch diameter bolts in 3 rows. The bolts were placed at the ends and at the middle of the support. This connection restricted the movement of the special support extension in all directions.

The diaphragms were placed only at the ends of the girder. These diaphragms provided resistance to lateral forces applied to the girder specimen and also restricted the rotation of the concrete slab deck. The diaphragms were centered slightly less than 19 feet apart so that they could provide support for the 19-foot-long concrete deck if it was to rotate.

The ends of the girder specimen were simply supported. One end of the girder, located on the exterior plane frame of the HEAT facility, was idealized and constructed as a roller support. A set of four 2 1/2-inch long slots were cut in both the 2-inch-thick plate and the top flange of the W 24 x 76 support extension. This type of end condition was designed to permit the free movement of the girder in the longitudinal direction. The other end of the girder, which was located on the interior plane frame, was idealized and constructed as a pin support. Only four 1 1/4-inch standard holes were cut in the support extension on this side. All cuts were made in the field using an oxy-acetylene cutting torch. The simple support condition was provided in order to allow the girder to displace longitudinally when damaged without inducing any unwanted tensile stresses that would be present if the longitudinal movement of the girder was restricted.

The concrete slab deck provided a permanent uniform dead load on the W 10 x 39 test girder. The dead load was about 600 pounds per linear foot acting over the 19.5-foot span of the simply supported girder specimen. The elastic moment capacity of the A-36 steel girder

was about 77 foot-kips. The maximum moment in the girder caused by the applied uniform dead load of the concrete slab was approximately 28.5 foot-kips. The ratio of the maximum actual moment in the girder to its elastic moment capacity was 0.37.

Damage Inducement Operation. The W 10 x 39 wide-flange girder was originally straight. The girder was damaged in-place so that heat-straightening techniques could be applied and their effects on the behavior of the full-scale simulated bridge girder studied. In order to damage the girder, the jacking device described in a previous section was used. The damage was induced by placing the jacking device near the midpoint location of the girder at a distance of 10.1 feet away from the left support. The front end of the jacking device, which has the 8-inch-long steel angle, was hooked to the bottom flange of the test girder. The other end, which had the 2-inch-round steel bar attached to the stroke of the jack, was fitted into a specially made slot (see Figure 8) on a steel plate that was attached to the side girder of the testing facility. Figure 15 shows the jacking device in place while the girder specimen was being deformed. The applied load was monitored by a 15,000 psi-capacity pressure dial gage, which was attached to the hydraulic pump that controls the jack. The load was applied gradually. The maximum pressure achieved was approximately 9,000 psi, which corresponds to an applied concentrated force of about 28,000 pounds exerted on the bottom flange of the test girder by the 3.14-square-inch plunger of the 15 ton hydraulic jack. Figure 16 shows a photograph of the jacking device in position while the damage inducement operation was in progress. The final deflected shape of the girder specimen as viewed from several directions is shown in Figures 17-19.

Damage Assessment Measurements. To accurately measure the deflected shape of the structure, the reference measuring frame previously described was used. Thirty-one sets of measuring points were selected along the entire length of the girder, taking into account the need to understand the response of the girder specimen to the application of the heat-straightening process. The spacing between these measuring points varied from 1 inch in the vicinity of the damage location to 36 inches next to the supports on both ends. Each set consisted of eight measuring points taken around the perimeter of the

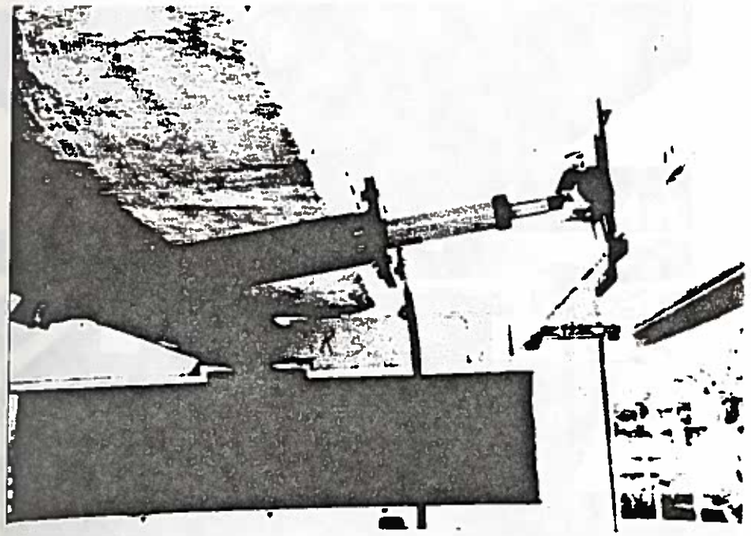

Figure 15. Jacking Device in Place During the Damage Inducement Process for Girder SB-1

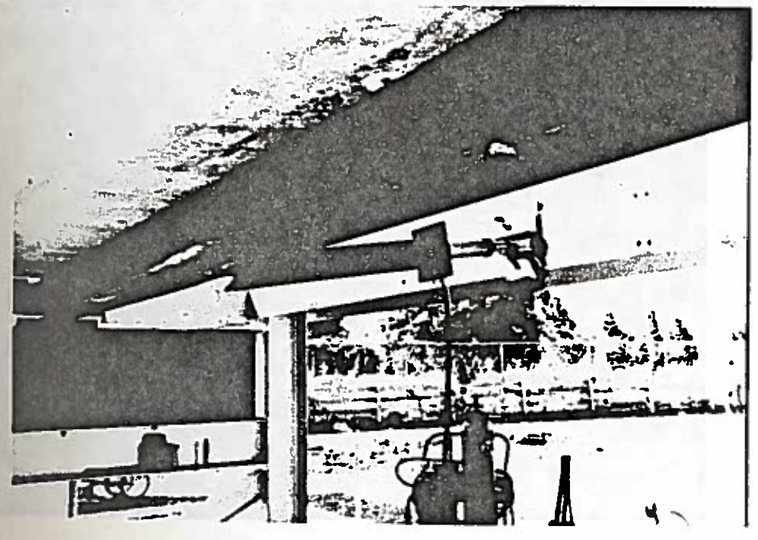

Figure 16. The Damage Inducement Operation in Process

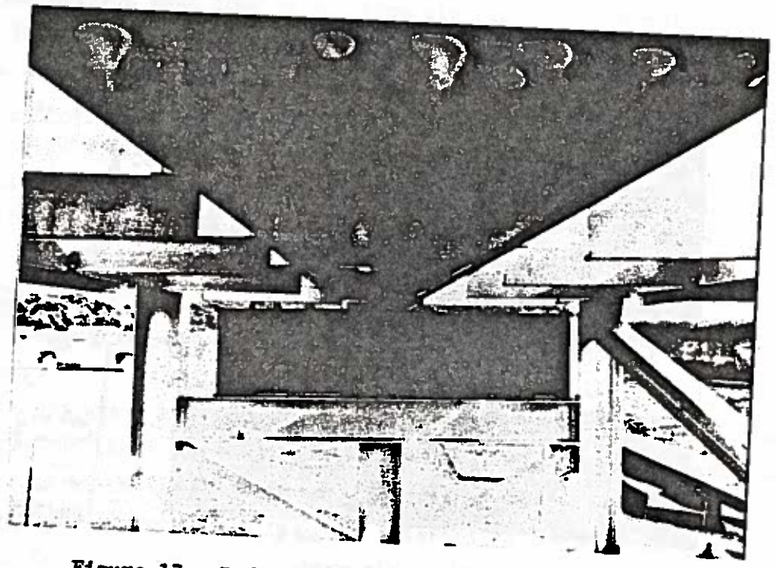

Figure 17. Deflected Shape of the Test Girder SB-1 Viewed from Underneath

Figure 18. Side View of the Deflected Shape of the Test Girder SB-1

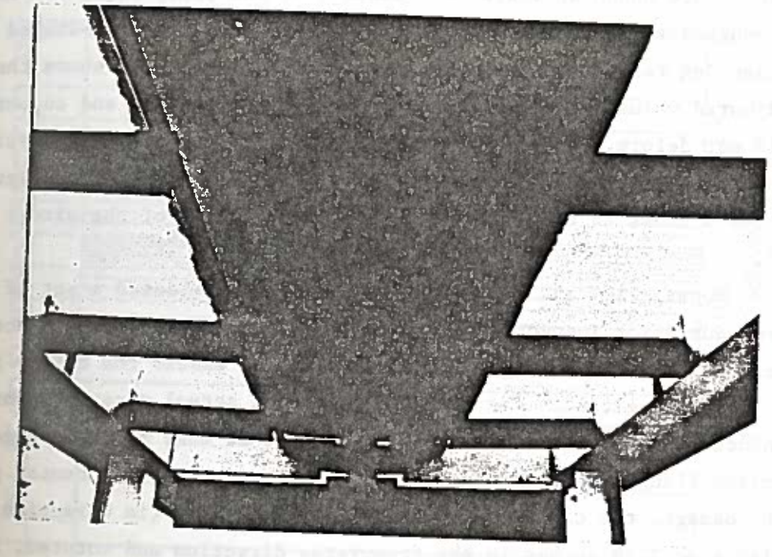

Figure 19. Another Side View of the Initial Damage in the Girder SB-1

cross section of the girder, as was shown in Figure 10. The center of the damage, which was located at 10.1 feet away from the left support, corresponded to the central set of measuring point set 16 on Figure 20. The other sets of measuring points were symmetrically placed on both sides of that point. Figure 20 provides a schematic illustration of the layout of the sets of measuring points and their locations along the test girder.

The damage assessment displacements were taken at all 31 sets of measuring points along the entire girder span of 19.5 feet. Initial measurements taken along the convex side (side "h") of the bottom flange are shown in Table 2. Column 3 of the table shows the raw measurements as taken in the field with respect to the U-shaped measuring reference frame. Column 4 of the same table shows the adjusted values of the deflection with respect to the end supports which did not deform. Figure 21 provides a plot of these adjusted values showing the actual deflected shape of the girder specimen. Figure 22 shows a cross section view of the deflected shape of the girder at point 16.

Moberg (20) and Shanafelt and Horn (28) presented a set of standard procedures for inspection and assessment of damage. Those procedures were followed in this project to inspect and assess the damage induced on the test girder. The measurement of the actual plastic deformations induced in the girder specimen revealed that most of the damage in the bottom flange was confined to a 21-inch length. At the center point of the damage, the concave side of the bottom flange (in direction "d") was displaced 3.18 inches in the transverse direction and rotated, leaving its edge 1.44 inches below its original position (direction "e"). At the same point, the lateral displacement of the convex side of the same flange (direction "h") was measured to be 2.75 inches, while its vertical movement was found to be 1.64 inches upward (direction "g"). This damage assessment revealed that the bottom flange had yielded as a long flat plate in bending about its strong axis. In addition, it yielded about its weak axis along two horizontal lines through points 12 and 20 and along the junction of the bottom flange and the web between these two points, producing a "dish-like" distortion. However, the back side of the flange at this location remained relatively perpendicular to

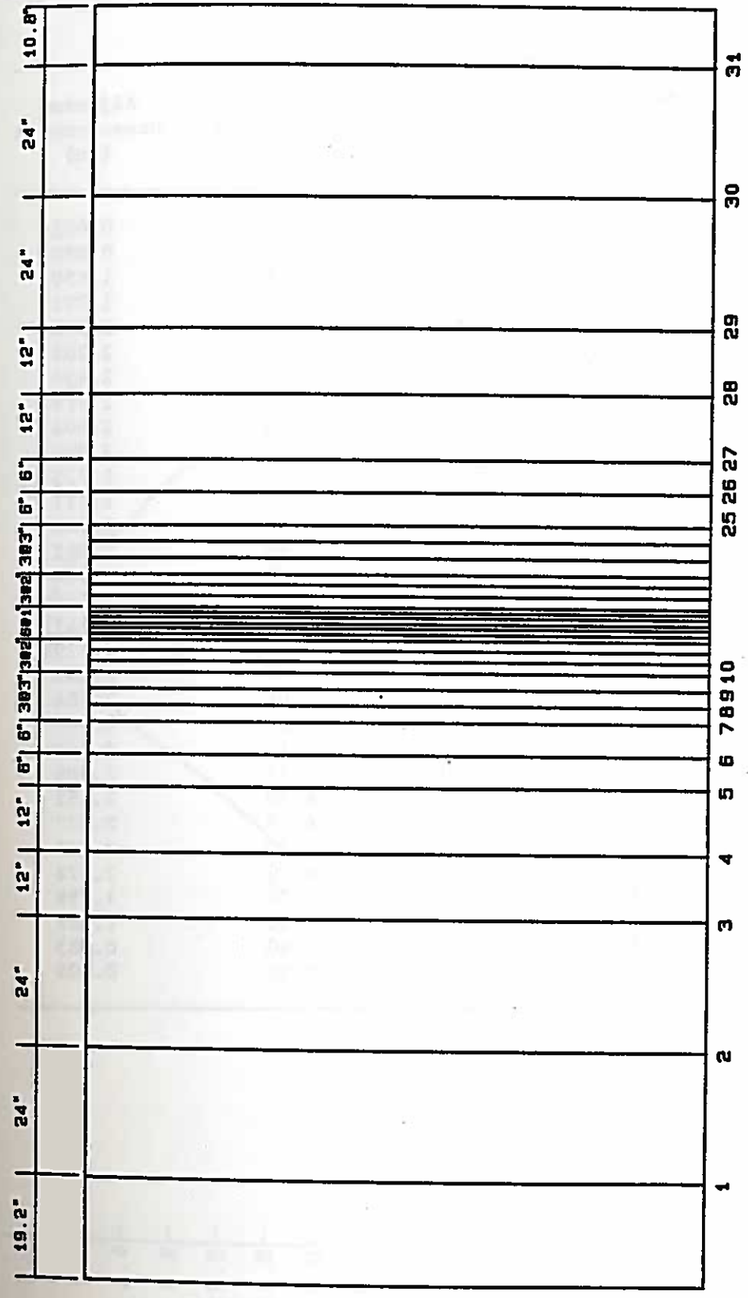

Figure 20. Measuring point layout for girder SB-1.

Table 2. Initial Deflection Measurements of the Damaged Steel Girder SB-1

Measuring Points	Distance (ft)	Raw Measurements (in)	Adjusted Measurements (in)
1	1.60	8.14	0.405
2	3.60	7.70	0.888
3	5.60	7.18	1.450
4	6.60	6.86	1.791
5	7.60	6.58	2.092
6	8.10	6.40	2.283
7	8.60	6.24	2.454
8	8.85	6.18	2.519
9	9.10	6.10	2.604
10	9.35	6.00	2.709
11	9.52	5.98	2.733
12	9.69	6.00	2.717
13	9.85	5.98	2.740
14	9.94	5.98	2.742
15	10.03	6.00	2.724
16	10.10	5.98	2.745
17	10.19	5.98	2.747
18	10.27	6.00	2.729
19	10.35	6.00	2.731
20	10.52	6.04	2.684
21	10.69	6.04	2.698
22	10.85	6.10	2.641
23	11.10	6.16	2.586
24	11.35	6.30	2.452
25	11.60	6.38	2.377
26	12.10	6.50	2.268
27	12.60	6.70	2.078
28	13.60	7.00	1.799
29	14.60	7.30	1.521
30	16.60	7.90	0.983
31	18.60	8.50	0.405

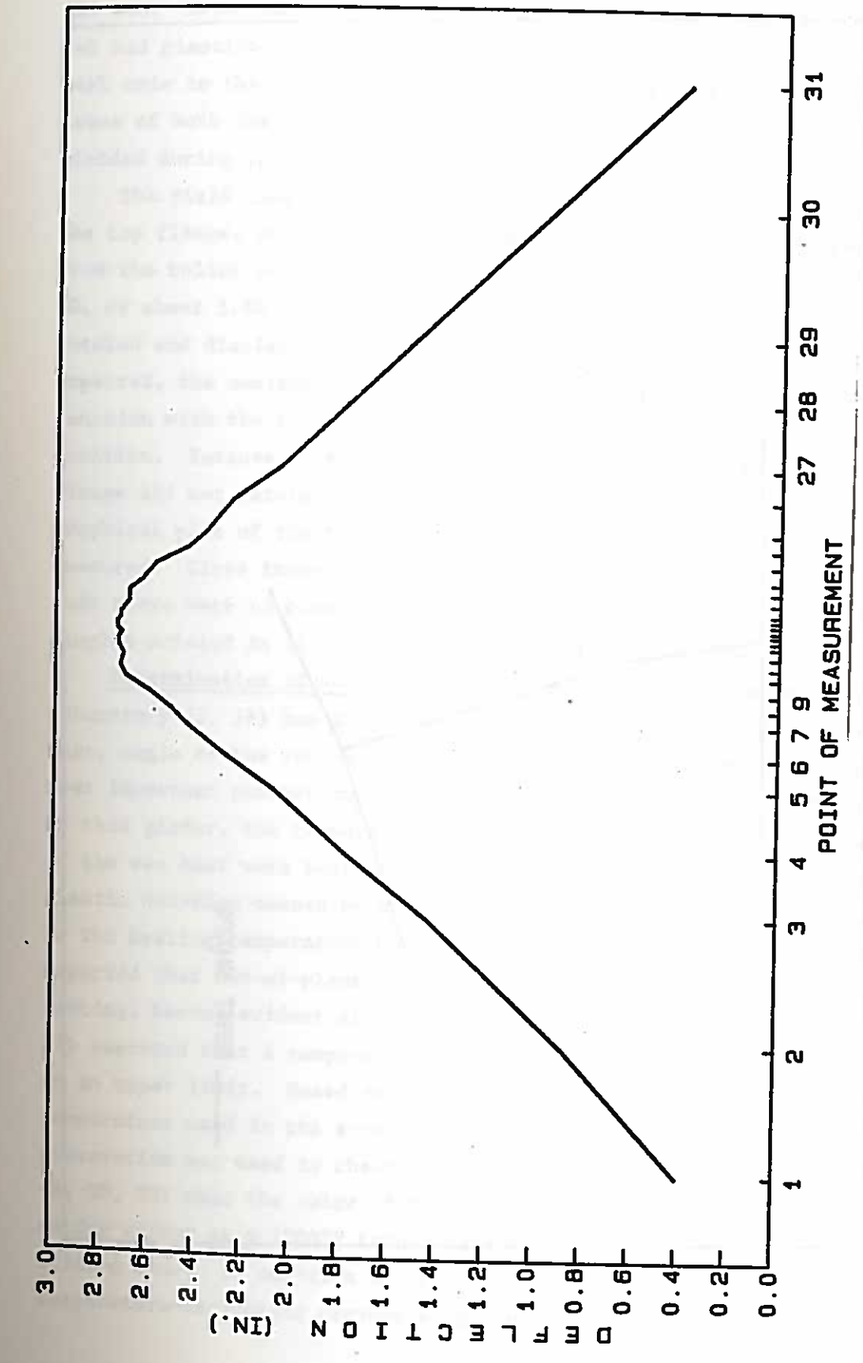

Figure 21. Initial damage assessment deflection measurements along point 'h' of girder SB-1.

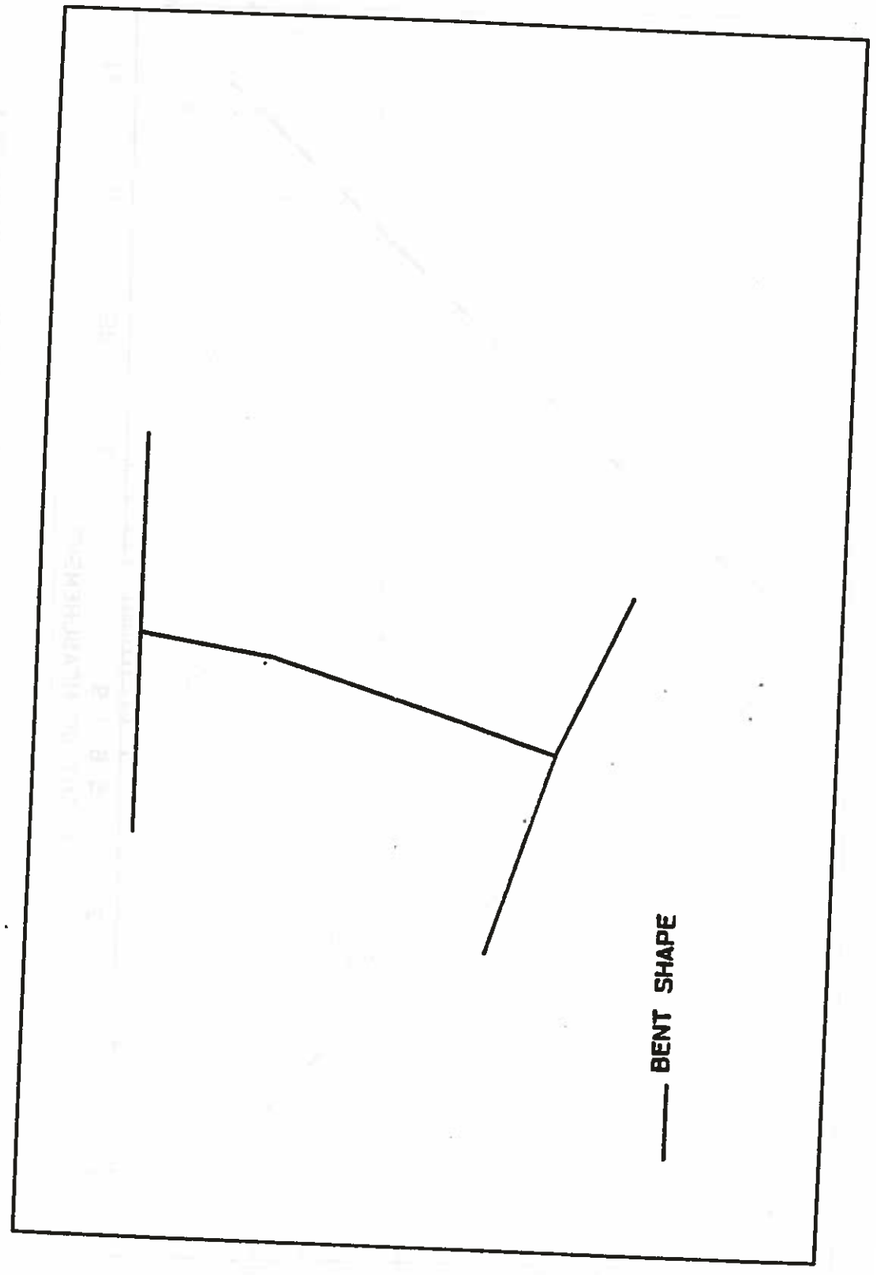

Figure 22. Deflected shape of the damaged girder SB-1 at pont 16.

the web. Measurements of deflections along the web revealed that the web had plastically deflected as a long, flat plate in bending about its weak axis in the longitudinal direction. Referring to Figure 23, dashed areas of both the flange and the web correspond to zones which had yielded during the damage inducement process.

The yield line in the web occurred approximately 2.25 inches below the top flange, starting midway between points 2 and 3, 4.60 feet away from the roller support, and extending to midway between points 29 and 30, or about 3.40 feet away from the hinged support. The web had rotated and displaced along each of points 3 through 29. As can be expected, the maximum web rotation occurred at point 16, leaving its junction with the bottom flange 2.75 inches away from its original position. Because of the composite behavior of the upper flange, the flange did not deform in any shape or fashion. Figure 23 also shows a graphical plot of the final deformed shape of the test girder as measured. Close inspection of the damaged area of the girder revealed that there were no cracks, tears, or kinks present. However, some local dimples existed in the bottom flange at the point of load contact.

Determination of Variables. Experimental work performed in the laboratory (3, 24) has shown that the temperature, depth of the vee heat, angle of the vee heat, and external constraints and forces are the most important parameters of heat straightening. Throughout the repair of this girder, the temperature, depth of the vee heat, and apex angle of the vee heat were kept constant. Roeder (24) has shown that the plastic rotation caused by heat straightening is directly proportional to the heating temperature up to approximately 1600°F. However, he reported that out-of-plane distortion and surface damage, such as pitting, become evident at this temperature. Most researchers (3, 20, 28) reported that a temperature in the range of 1200°F should be adopted as an upper limit. Based on these findings, the intended maximum temperature used in the straightening process was 1200°F. Visual color observation was used to check maximum temperature. It was reported (3, 20, 28) that the color of the steel near the torch tip should be satiny silver at a 1200°F temperature when viewed through a No. 4 welding lens. In addition to color observation, tempil stick temperature-indicating crayons were used to determine the temperature of

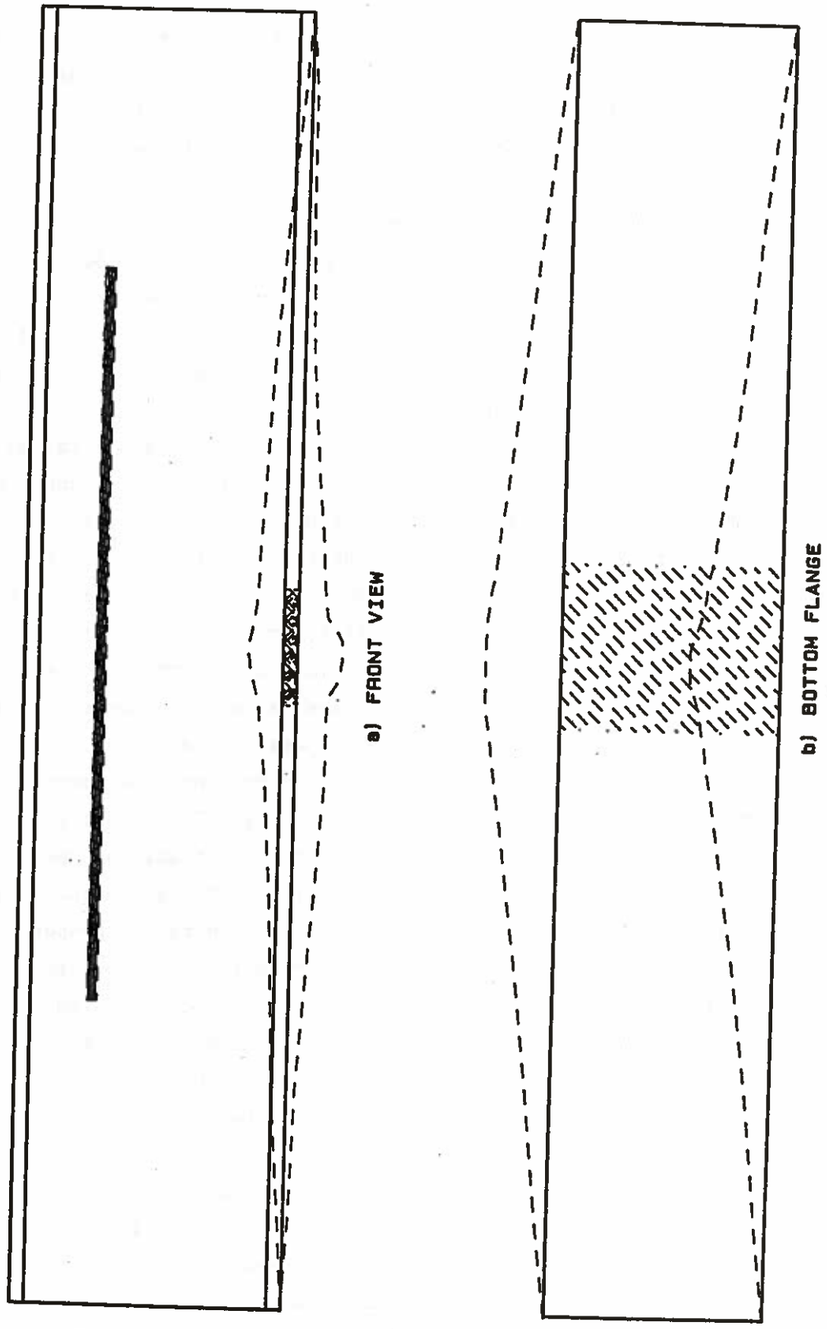

Figure 23. Identification of the yield zones in the damaged girder SB-1.

the heated steel immediately after the completion of each heat application. A single orifice oxy-acetylene torch with a Victor No. 7 torch tip was utilized in applying heats.

The effect of the depth of the vee heat in comparison to the depth of the plate was also reported by various investigators (3, 22, 24, 28, 29). The plastic rotation of the heated member increased with an increase in depth of the vee heat. However, it was reported (20, 22, 24, 28, 29) that full-depth vee heats resulted in an overall shortening of the member length. For this reason three-quarter-depth vee heats were used in the heat-straightening repair of the damaged girder.

The angle of the vee heat is of primary influence on the plastic rotation (3, 20, 22, 24, 28, 29). The larger the vee angle, the larger the amount of plastic rotation obtained. However, some of these investigators (3, 20, 28) reported that the tendency of the heated flange to buckle increases as the base of the vee heat gets wider. As a result, a vee heat angle of 30 degrees was selected for field application.

The only other important variables to consider were the auxiliary constraints and forces acting on the damaged girder during the heat-straightening process. Practitioners usually apply an external jacking force in the direction of the desired movement in order to accelerate the heat-straightening repair process. The external constraints impede the longitudinal thermal expansion during the heating phase, thus increasing the plastic strains and producing more plastic rotation during the cooling phase. Most practitioners have no equipment to monitor the amount of external force applied to the heated member, and they often rely solely on their own judgment.

Experimental tests (3, 24) on mild steel plate specimens have shown that the plastic rotation is proportional to the load ratio. The load ratio is defined as the ratio of the actual moment in the member at the vee location to the plastic moment capacity of the section. That proportionality is relatively linear. It was decided to apply an auxiliary constraining force to the member that would produce a load ratio of 50 percent of the bottom flange capacity (acting independently) at the location of the vee in the bottom flange. That ratio was defined by assuming that the entire applied force is carried solely by the

bottom flange. The term load ratio as hereafter used will correspond to this definition. As will be shown, the load ratio was varied during the course of the repair.

Description of Heating Sequences. For all heating sequences, 1200°F, three-quarter-depth, 30-degree vee heats were used to reduce the curvature on the bottom flange of the damaged girder. The edges of the vee were layed out on the lower surface of the bottom flange, and a single orifice torch was used to heat the steel inside the vee. Deflection measurements were taken after each heating cycle, and the point of maximum curvature was identified. The vee heat was then applied at that location during the next cycle. The jacking force was always applied 9 inches before the location of the vee heat if the maximum curvature was found to be at or after point 16. If the maximum curvature occurs at a location before point 16, the jacking force was applied 9 inches preceding that location. This procedure ensured that the application of the jacking force remained always in the middle portion of the girder and away from the heated area. The jacking force was applied to the bottom flange prior to the application of the heat-straightening process. As the member straightened during the cooling phase, the applied force decreased. No adjustment or additional forces were applied until the next heating cycle. Both the initial and final pressures exerted on the girder were recorded. Eight heating sequences were applied to the plastically deformed areas of the damaged girder in order to investigate the effect of different heating patterns on the behavior of the heat-straightened girder. The only variables were the load ratio and the location of heat applications.

Case SB-2: Second Test on W 10 x 39 Composite Girder

The second experiment of this project consisted of repairing the same W 10 x 39 wide-flange composite girder after re-damaging. For this reason, the girder was left in place and damaged by a gradual application of the jacking force, while careful measurements of the lateral deflection were taken.

The jacking force was applied 10.1 feet from the left support, as in the previous girder. The maximum load applied was about 32 kips.

Damage Assessment Measurements. The same measuring points used in the first repair operation on this girder were again used to assess the

damage. Again, the guidelines for inspection and assessment of damage presented by Moberg (20) and Shanafelt and Horn (28) were followed. Figure 24 shows the deflected shape of the newly damaged girder specimen. Table 3 shows the initial damage assessment deflections taken along the convex side of the bottom flange (along direction "h").

A study of the actual measurements of the plastic deformation revealed that the worst damage was confined to a 24-inch-long zone. The maximum lateral displacement, which was located at measuring point 16, was measured to be 2.68 inches on the concave side of the bottom flange (along direction "d") and 2.23 inches on the convex side (along direction "h"). At the same cross section, the bottom flange was rotated, leaving the concave edge (along direction "e") 1.45 inches below its original position, while the other edge (along direction "g") had deflected 1.45 inches upward. Dashed areas in Figure 25 show the yield zones of the girder specimen. All the yield areas produced during this damage inducement operation were similar to those described earlier for SB-1. However, the magnitude of the damage was slightly less. In addition, the yield line in the web occurred about 4 inches below the top flange, starting midway between points 2 and 3 and extending to midway between points 29 and 30. Again, a close-up inspection of the girder showed no signs of cracks, tears, or kinks.

Case SB-3: First Test on W 24 x 76 Composite Girder

The third experiment of this project involved the repair of a W 24 x 76 wide-flange composite girder by the heat-straightening technique. The girder was simply supported in a manner similar to the previous cases. Diaphragms were placed at the ends of the girder specimen. The elastic moment capacity of the W 24 x 76 A-36 steel girder was about 215 foot-kips. The uniform dead load applied by the concrete slab was 28.5 foot-kips. The ratio of the actual moment in the girder to its elastic moment was 0.13.

Damage Inducement Operation. In order to damage the W 24 x 76 composite girder specimen, a 3400-pound steel battering ram was swung from a crane's 40-foot boom. The ramming was designed to simulate actual accidental damage of highway overpass bridge girders by over-height trucks. Figure 26 shows a photograph of the actual damage inducement operation, while Figure 27 shows a view of the deflected shape of the girder.

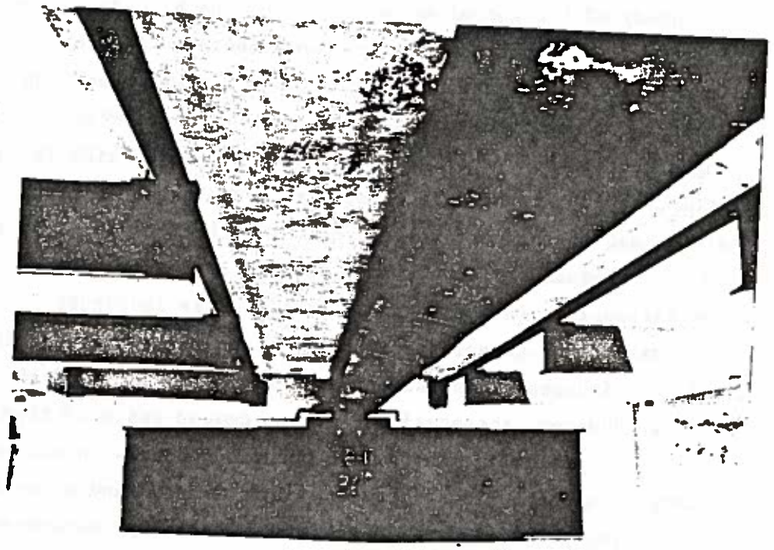

Figure 24. Deflected Shape of the Test Girder SB-2

Table 3. Initial Deflection Measurements of the Damaged Steel Girder SB-2

Measuring Points	Distance (ft)	Raw Measurements (in)	Adjusted Measurements (in)
1	1.60	8.16	0.205
2	3.60	7.80	0.602
3	5.60	7.34	1.100
4	6.60	7.06	1.399
5	7.60	6.78	1.698
6	8.10	6.64	1.847
7	8.60	6.50	1.996
8	8.85	6.42	2.081
9	9.10	6.36	2.146
10	9.35	6.32	2.191
11	9.52	6.32	2.194
12	9.69	6.32	2.197
13	9.85	6.32	2.200
14	9.94	6.32	2.202
15	10.03	6.32	2.203
16	10.10	6.30	2.225
17	10.19	6.32	2.206
18	10.27	6.34	2.188
19	10.35	6.32	2.209
20	10.52	6.36	2.173
21	10.69	6.36	2.176
22	10.85	6.38	2.159
23	11.10	6.44	2.104
24	11.35	6.52	2.028
25	11.60	6.60	1.953
26	12.10	6.74	1.822
27	12.60	6.90	1.672
28	13.60	7.20	1.391
29	14.60	7.48	1.129
30	16.60	7.96	0.687
31	18.60	8.48	0.205

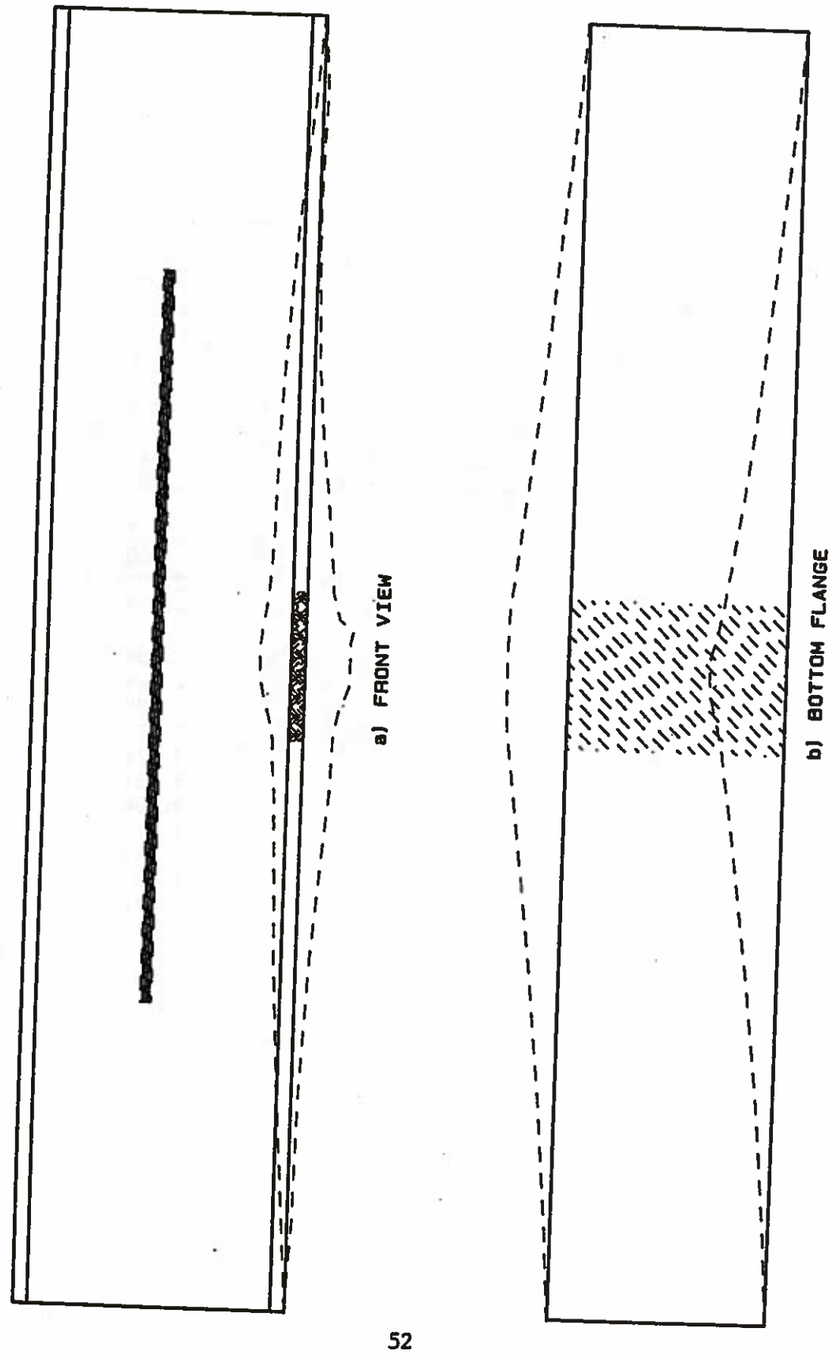

Figure 25. Identification of the yield zones in the damaged girder SB-2.

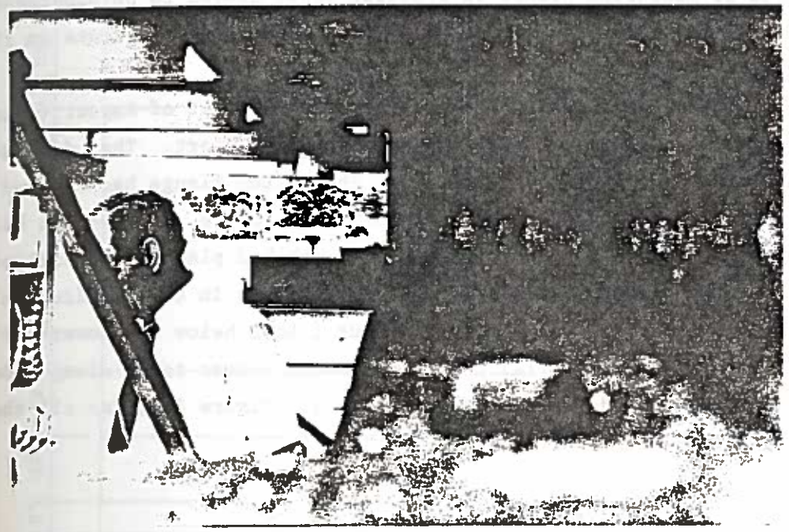

Figure 26. Damage Inducement Operation on Girder SB-3

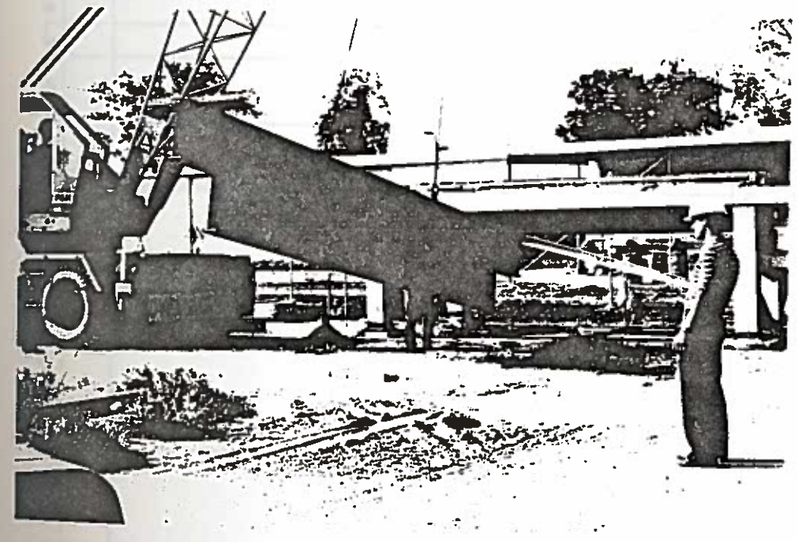

Figure 27. Deflected Shape of the Test Girder SB-3

Damage Assessment Measurements. The close spacing between the sets of measuring points on previous tests proved to be unnecessary. For this reason, the layout of the sets of measuring points on this girder was revised, as shown in Figure 28.

The largest deflection occurred at the point of impact (point 11) which is located 10.1 feet from the roller support. That deflection was measured to be about 4.33 inches. The bottom flange had rotated approximately 5 degrees over its 8.99-inch width. Deflection measurements along the web revealed that the web had plastically yielded as a long, flat plate, bending about its weak axis in the longitudinal direction. That yield line occurred about 1 inch below the lower surface of the top flange. Initial deflection measurements taken along side "h" of the damaged girder are shown in Table 4. Figure 29 shows all the yield areas in this girder specimen.

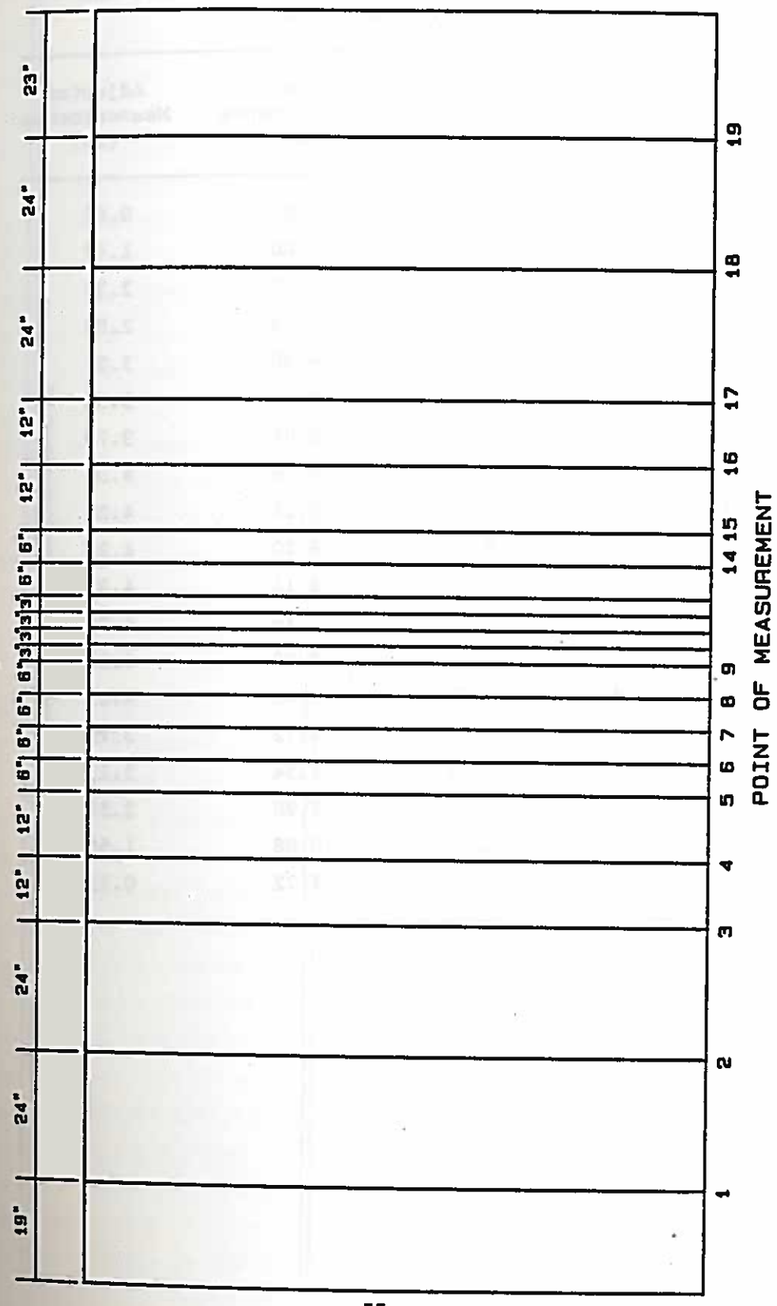

Figure 28. Measuring point layout for SB-3.

Table 4. Initial Deflection Measurements of the Damaged Steel Girder SB-3

Measuring Points	Distance (ft)	Raw Measurements (in)	Adjusted Measurements (in)
1	1.58	11.82	0.65
2	3.58	11.00	1.47
3	5.58	10.12	2.35
4	6.58	9.64	2.83
5	7.58	9.20	3.27
6	8.08	8.96	3.51
7	8.58	8.68	3.79
8	9.08	8.46	4.01
9	9.58	8.26	4.21
10	9.83	8.20	4.27
11	10.08	8.14	4.33
12	10.33	8.18	4.29
13	10.58	8.20	4.27
14	11.08	8.42	4.05
15	11.58	8.72	3.75
16	12.58	9.34	3.13
17	13.58	9.90	2.57
18	15.58	10.88	1.59
19	17.58	11.72	0.75

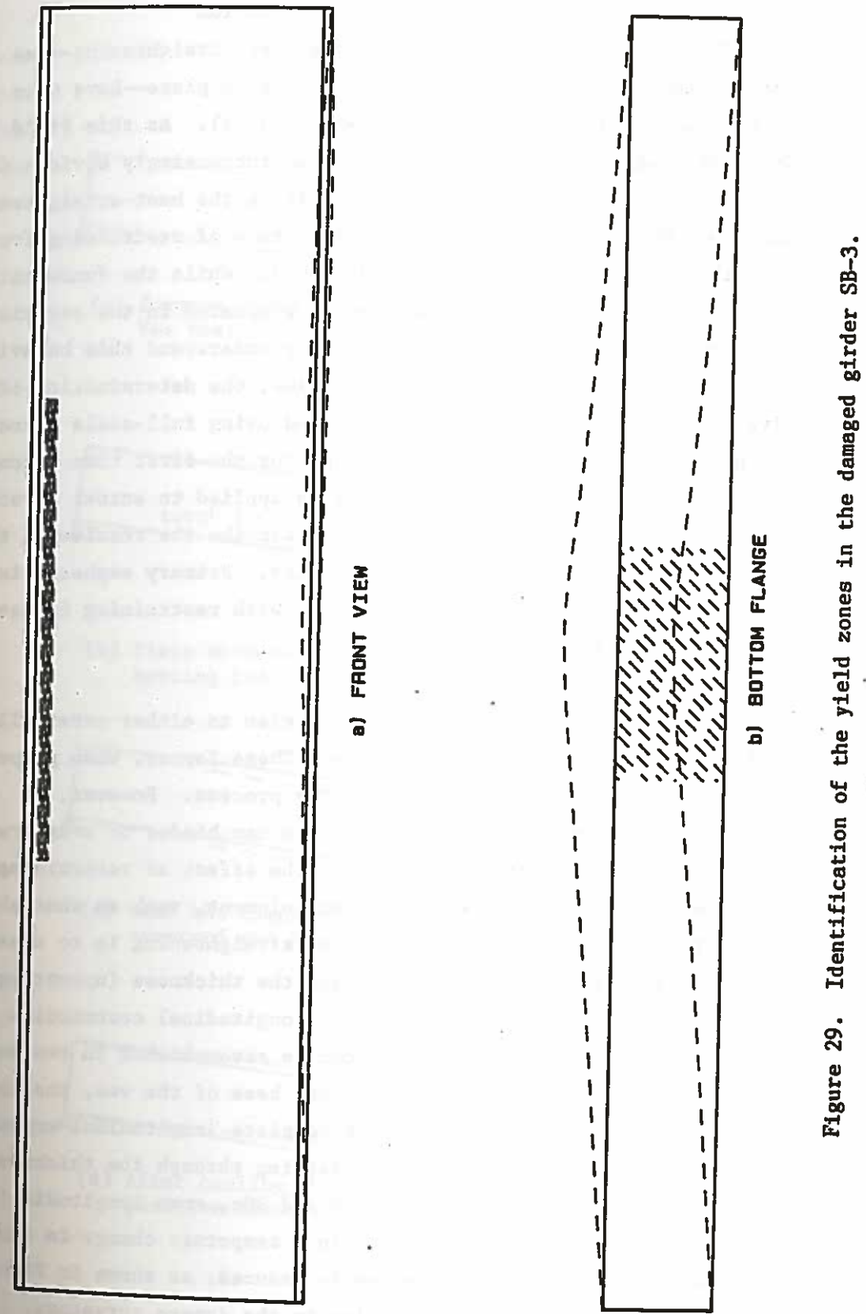

Figure 29. Identification of the yield zones in the damaged girder SB-3.

4. EVALUATION OF BEHAVIOR

Three primary parameters affecting heat straightening--vee angle, heating temperature, and depth ratio of vee to plate--have been studied in the laboratory and reported elsewhere (3, 4). As this field investigation has unfolded, it has become increasingly obvious that two additional parameters play a central role in the heat-straightening process. One factor relates to the influence of restraining forces and the other to the heating patterns utilized. While the fundamental effects of restraining forces are being evaluated in the associated laboratory studies, the only way to fully understand this behavior is to study actual structural systems. Likewise, the determination of effective heating patterns can best be studied using full-scale structures. The HEAT facility is unique in allowing for the first time a comprehensive evaluation of heat straightening as applied to actual structures.

The purpose of this chapter is to describe the results of the first three tests conducted in the HEAT facility. Primary emphasis is placed on the evaluation of behavior associated with restraining forces and heating patterns.

Role of Restraining Forces

The term "restraining forces" can refer to either externally applied forces or internal redundancy. These forces, when properly utilized, can expedite the straightening process. However, if improperly understood, restraining forces can hinder or even prevent straightening. In its simplest terms, the effect of restraining forces can be explained by considering a plate element, such as that shown in Figure 30. The basic mechanism of heat straightening is to create plastic flow, causing expansion through the thickness (upsetting) during the heating phase, followed by elastic longitudinal contraction during the cooling phase. This upsetting can be accomplished in two ways. First, as the heat progresses toward the base of the vee, the cool material ahead of the torch prevents complete longitudinal expansion of the heated material, thus forcing upsetting through the thickness. However, as illustrated in Figure 30b and 30c, some longitudinal expansion does occur, which results in a temporary change in damage. After cooling, the degree of damage is reduced, as shown in Figure 30d so that the net effect is a reduction in the damage curvature.

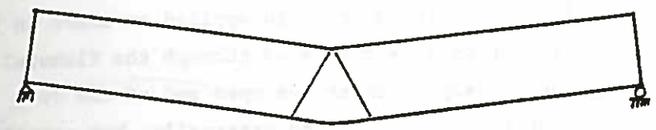

(a) Damaged Plate to be repaired with a single Vee heat

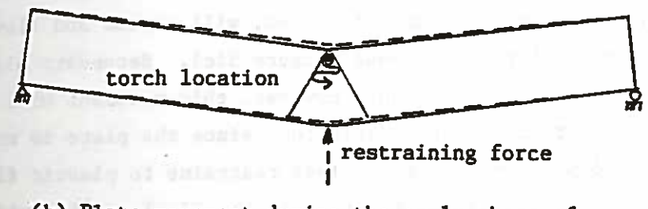

(b) Plate movement during the early phase of heating reduces the damage

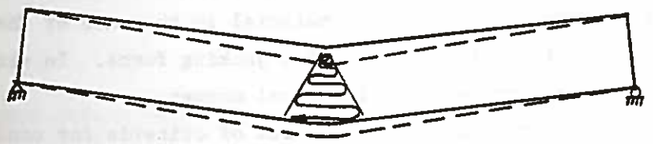

(c) Near the completion of heating the movement is reversed and the damage is increased

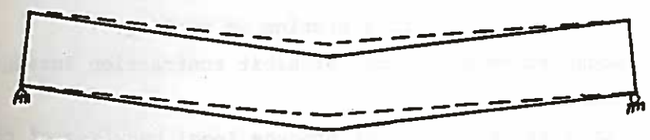

(d) After cooling the final movement is in the positive direction to remove curvature

Figure 30. Progression of movement for a plate during the heat-straightening process

A second method of producing the desired upsetting (usually used in conjunction with the vee heat) is to provide a restraining force. The role of the restraining force is to reduce or prevent beam movements which tend to favor longitudinal expansion during the heating phase. For example, if a restraining force is applied as shown in Figure 30b, the upsetting effect will be increased through the flexural constriction of free longitudinal expansion at the open end of the vee. A restraining force is usually applied externally, but sometimes the structure itself provides restraint through internal redundancy.

In essence, a restraining force acts in an identical manner to that of the vee heat concept itself. The material behavior can be viewed as illustrated in Figure 31. A small element from a plate, when constrained in the x-direction and heated, will expand and flow plastically primarily through the thickness (Figure 31c). Secondary plastic flow will occur in the y-direction. However, this movement will be small in comparison to that of the z-direction, since the plate is much thinner than its y dimension and offers less restraint to plastic flow. Upon cooling with contraction unrestrained, the final configuration of the element will be smaller in the x-direction and thicker in the z-direction. The material itself cannot distinguish the cause of the constraint: either cooler adjacent material in the case of the vee heat, or an external force in the case of a jacking force. In either case, the plastic flow occurs in an identical manner.

In light of this disucssion, a set of criteria for constraining forces can be developed. This criteria applies for internal as well as external constraints.

1. Constraints should be passive during the heating phase; i.e., they should be applied prior to heating and not increased by external means during heating or cooling.
2. Constraints should not prohibit contraction during the cooling phase.
3. Constraints should not produce local buckling of the compression element during the heating phase.
4. Constraints should not produce an unstable structure by either the formation of plastic hinges or member instability during the heating phase.

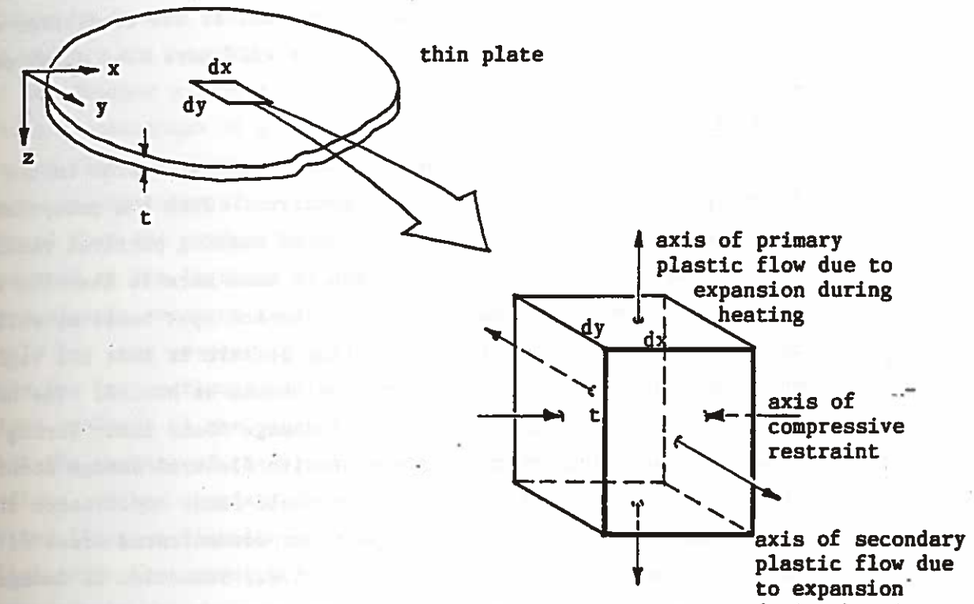

(a) Element from a thin plate

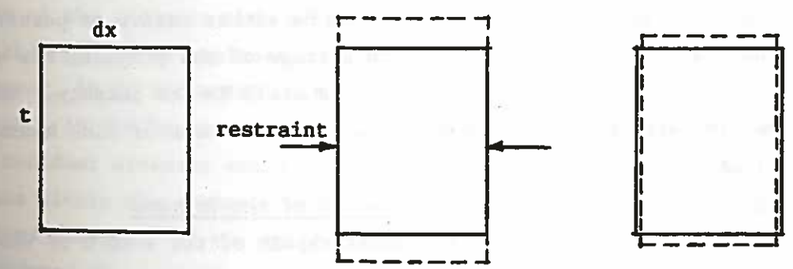

(b) original element

(c) Plastic flow during heating with full restraint in x direction

(d) Final Configuration of element after cooling

Figure 31. Characteristics of plastic flow and restraint during heat-straightening

From a practical viewpoint, this criteria means that: (1) the vee angle should be kept small enough that local buckling is avoided; (2) the jacking forces must be applied prior to heating and be self-relieving as contraction occurs; and (3) the maximum level of any external jacking forces must be based on a structural analysis which includes the reduced strength and stiffness due to the heating effects. At present only subjective guidelines can be given. However, at the completion of this project, quantitative analysis procedures will have been developed for engineering guidance.

Role of Heating Patterns

A related factor which has received little attention in the literature is the effect of heating patterns. With the exception of the vee heat itself, the proper application of heating patterns remains undeveloped. The term heating pattern is used here to describe the layout of not only the vee heats, but line and spot heats as well. The basic principle in selecting the heating pattern is that all regions which have suffered plastic deformation should be heated. Vee heats are used on plate elements having flexural damage about their strong axes. Line heats are used for plate elements with flexural damage about the weak axis that produces a well-defined yield line. Spot heats are used for localized, inelastic bulges or similar concentrated areas of damage. Vee heats are usually active in nature; i.e., reduction in damage is a direct result of contraction of the vees. Line heats are usually passive in that the line heat itself does not mitigate the damage. Rather, the line heat allows plastic flow to occur as a result of forces from other elements. A spot heat can be either active or passive, depending on the situation. At this stage of the project, the study of the most effective heating patterns is still in its infancy. However, some research results related to the effective use of line heats are available.

Case SB-1: Description and Evaluation of the Process

The approach used for the first repair of the W 10 x 39 was to try a number of combinations of heating patterns and restraining forces. A series of at least four cycles was conducted for each combination so that the pattern of behavior could be well-established. A total of 36 vee heats were applied to the bottom flange in order to straighten it.

Each vee heat consisted of three-quarter depth, 30-degree vees heated to about 1200°F. The first heating sequence chosen was one of the simplest: a single vee heat on the bottom flange at the point of maximum curvature, with a restraining force producing a load ratio of 56 percent. The load ratio is defined here as the moment due to the applied force divided by the plastic moment capacity of the bottom flange by itself. Only one single-orifice oxy-acetylene torch was used to perform the heating. One vee heat was applied to the bottom flange of the damaged girder at the location of maximum curvature. Figure 32 shows a photograph of a vee heat applied to the lower surface of the bottom flange. Seven cycles were heated with this pattern. Deflection measurements taken after the application of the first heating cycle showed that the maximum change in displacement was 0.1 inches, which occurred at the location of the vee heat (point 16). That corresponded to a plastic rotation angle of 0.00176 radians. The plastic rotation angle has been previously defined and corresponds to the rotation of only the bottom flange of the girder where the vee heat is applied. A close analysis of the next six heating cycles (numbers 2 to 7) showed that the average of the plastic rotation angle obtained was 0.00043 radians, with a standard deviation of 0.00016. A graphical plot of the bottom flange deflection obtained after the completion of each of the first seven heat-straightening cycles is shown in Figure 33. The measurements are summarized in Tables 5 and 6.

In this sequence, as well as most of the others, it was observed that a significantly larger amount of movement occurred after the first heat of the sequence than after most other heats during the sequence. At this point, no explanation has been found for this phenomenon. However, it is suspected that residual stresses may be the primary cause. At the beginning of a new heating sequence, a significant change in residual stresses would be likely to occur. However, successive heats within the sequence would not result in significant residual stress changes. If the initial residual stress pattern acted to reinforce the restraint effectiveness, then movement would be increased. However, if the new pattern of residual stresses after the first heat did not reinforce the restraining force as much, then the movement would be smaller. More study is needed into this behavior, including the

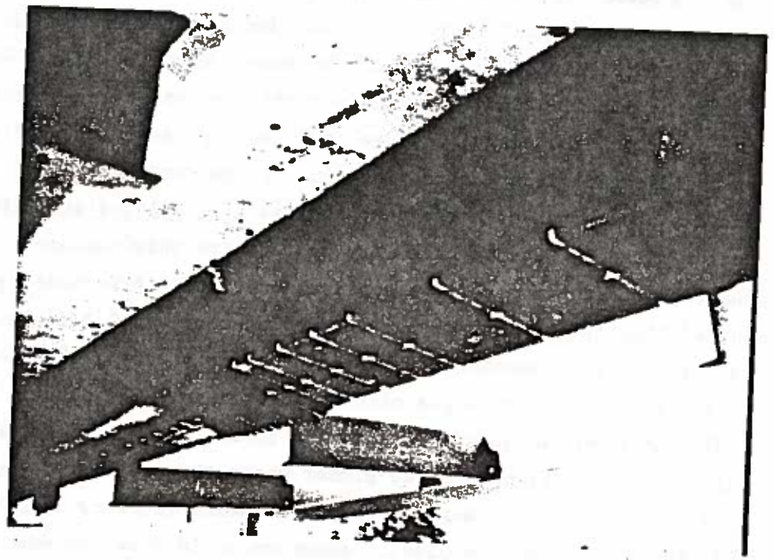

Figure 32. Vee Heat Located on the Lower Surface of the Damaged Bottom Flange of Girder SB-1

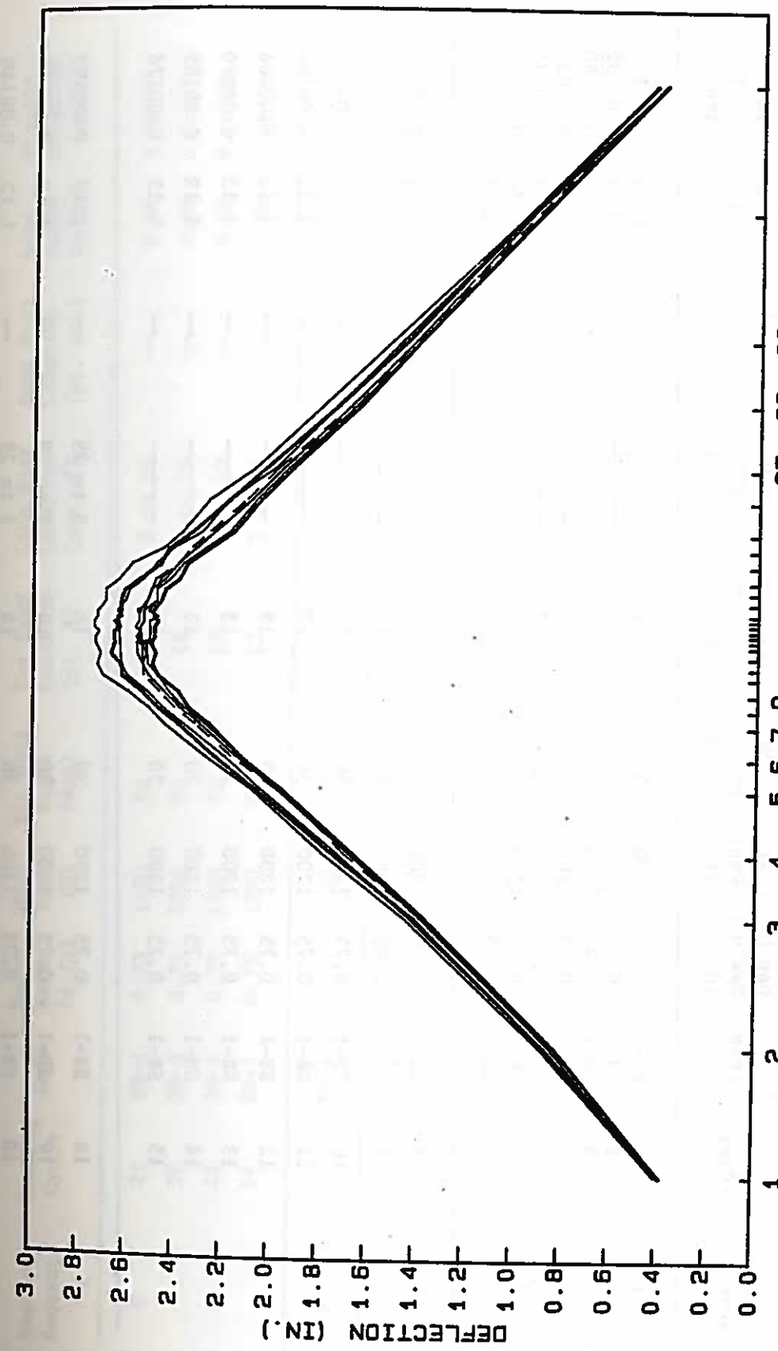

Figure 33. Heat-straightening progression for the damaged girder SB-1 through heating sequence one (7 total heating cycles).

Table 5. Summary of experimental results on the behavior of the test girder SB-1 under the influence of each heating cycle.

Heating Sequence	Heating Cycle	Code	Depth Ratio (d_v/w)	Heat Temp. (F)	Vee Heat Angle (deg)	Vee Heat Location (pt. #)	Line Heat Location (pts. #)	Spot Heat Location (pt. no.)	Load Ratio (M/Mp)	Plastic Rotation (rad)
1	1	SB-1	0.75	1200	30	16	-------	---	0.56	0.00176
	2	SB-1	0.75	1200	30	16	-------	---	0.56	0.00035
	3	SB-1	0.75	1200	30	19	-------	---	0.56	0.00160
	4	SB-1	0.75	1200	30	13	-------	---	0.56	0.00035
	5	SB-1	0.75	1200	30	13	-------	---	0.56	0.00035
	6	SB-1	0.75	1200	30	13	-------	---	0.56	0.00070
	7	SB-1	0.75	1200	30	13	-------	---	0.56	0.00035
2	8	SB-1	0.75	1200	30	13	-------	---	1.12	0.00281
	9	SB-1	0.75	1200	30	13	-------	---	1.12	0.00071
	10	SB-1	0.75	1200	30	19	-------	---	1.12	0.00105
	11	SB-1	0.75	1200	30	19	-------	---	1.12	0.00106
	12	SB-1	0.75	1200	30	19	-------	---	1.12	0.00106
	13	SB-1	0.75	1200	30	13	-------	---	1.12	0.00070
	14	SB-1	0.75	1200	30	13	-------	---	1.12	0.00105
	15	SB-1	0.75	1200	30	15	-------	---	1.12	0.00176
3	16	SB-1	0.75	1200	30	14	3 to 29	---	1.12	0.00493
	17	SB-1	0.75	1200	30	14	3 to 29	---	1.12	0.00352
	18	SB-1	0.75	1200	30	14	3 to 29	---	1.12	0.00140
	19	SB-1	0.75	1200	30	14	3 to 29	---	1.12	0.00280
	20	SB-1	0.75	1200	30	14	3 to 29	---	1.12	0.00280

Table 5. (Continued)

Heating Sequence	Heating Cycle	Code	Depth Ratio (d_v/w)	Heat Temp. (F)	Vee Heat Angle (deg)	Vee Heat Location (pt. #)	Line Heat Location (pts. #)	Spot Heat Location (pt. no.)	Load Ratio (M/Mp)	Plastic Rotation (rad)
4	21	SB-1	0.75	1200	30	14	3 to 29	---	0.56	0.00175
	22	SB-1	0.75	1200	30	14	3 to 29	---	0.56	0.00070
	23	SB-1	0.75	1200	30	13	3 to 29	---	0.56	0.00106
	24	SB-1	0.75	1200	30	12	3 to 29	---	0.56	0.00175
3	25	SB-1	0.75	1200	30	19	3 to 29	---	1.12	0.00351
5	26	SB-1	0.75	1200	30	19	3 to 29	---	0.00	-0.00141
	27	SB-1	0.75	1200	30	10	3 to 29	---	0.00	0.00105
3	28	SB-1	0.75	1200	30	10	3 to 29	---	1.12	0.00492
	29	SB-1	0.75	1200	30	19	3 to 29	---	1.12	0.00282
6	30	SB-1	0.75	1200	30	8 & 21	3-8 & 21-29	---	1.12	0.00212
	31	SB-1	0.75	1200	30	8 & 21	3-8 & 21-29	---	1.12	0.00320
7	32	SB-1	0.75	1200	30	---	-------	16	----	-0.00492
	33	SB-1	0.75	1200	30	---	-------	16	----	0.00070
8	34	SB-1	0.75	1200	30	16	3-8 & 21-29	---	1.12	0.00141
	35	SB-1	0.75	1200	30	16	3-8 & 21-29	---	1.12	0.00141
	36	SB-1	0.75	1200	30	16	3-8 & 21-29	---	1.12	0.00105

Table 6. Average Plastic Rotation Angle per Vee Obtained from Each Heating Sequence

Beam	Heating Sequence	Number of Cycles	Average Plastic Rotation (rad)	Standard Deviation	Average Plastic Rotation Excluding First Heat (rad)	Standard Deviation
SB-1	1	7	0.00078	0.00063	0.00042	0.00016
	2	8	0.00128	0.00070	0.00106	0.00035
	3	8	0.00334	0.00118	0.00311	0.00106
	4	4	0.00132	0.00052	-------	-------
	5	1	0.00105	-------	-------	-------
	6	2	0.00133	0.00038	-------	-------
	7		-------	-------	-------	-------
	8	3	0.00129	0.00021	-------	-------
SB-2	9	26	0.00131	0.00033	-------	-------
SB-3	10	13	0.00280	0.00208	0.00250	0.00137

experimental measurements of residual stress patterns and how they change with different heating sequences.

The second heating sequence was identical to the first, except that the restraining force was doubled to produce a load ratio of 112 percent. Eight cycles were applied to the damaged girder (heating cycles 8-15). Figure 34 shows the movement obtained in the bottom flange after the completion of each of the first 15 heating cycles. Again, the maximum amount of movement occurred after the application of the eighth heating cycle, which is the first heat applied in this sequence. The maximum plastic rotation angle obtained in this heating sequence was 0.00281 radians. Tables 5 and 6 summarize the measured results of this sequence.

As in the first sequence, movements were relatively small, and only a slight rate of increase occurred after the application of the second heating pattern. Since the web had yielded about its weak axis along a longitudinal line, it was concluded that the stresses acting on the yield line provided an additional restraint in the bottom flange of the girder. However, this additional restraint was acting in the wrong direction and resisted the action of the external jacking forces, thus reducing the thermal contraction of the member. In the third heating sequence, a line heat was used along the entire length of the yield zone in the web, in addition to applying the vee heat and the 112 percent auxiliary jacking force. As will be shown, the line heat by itself does not cause any straightening effect. However, it reduces the yield stress along the line so that the resistance to web straightening would be less when the vee heat is applied to the lower flange. In effect, the web yield line was straightened by hot mechanical straightening, with the flange applying the mechanical force as it was heat-straightened. This technique is frequently used by practitioners. Figure 35 shows a photograph of the actual application of this heating sequence. Two people and two single-orifice torches were required to perform this heating sequence. The line heat was applied to the convex crest of the web, starting from points 3 and 29 moving toward the middle in a direction parallel to the top flange. Each person started heating from one end of the yield line, moving progressively toward the middle of the girder. Just before getting to the middle portion, one of the

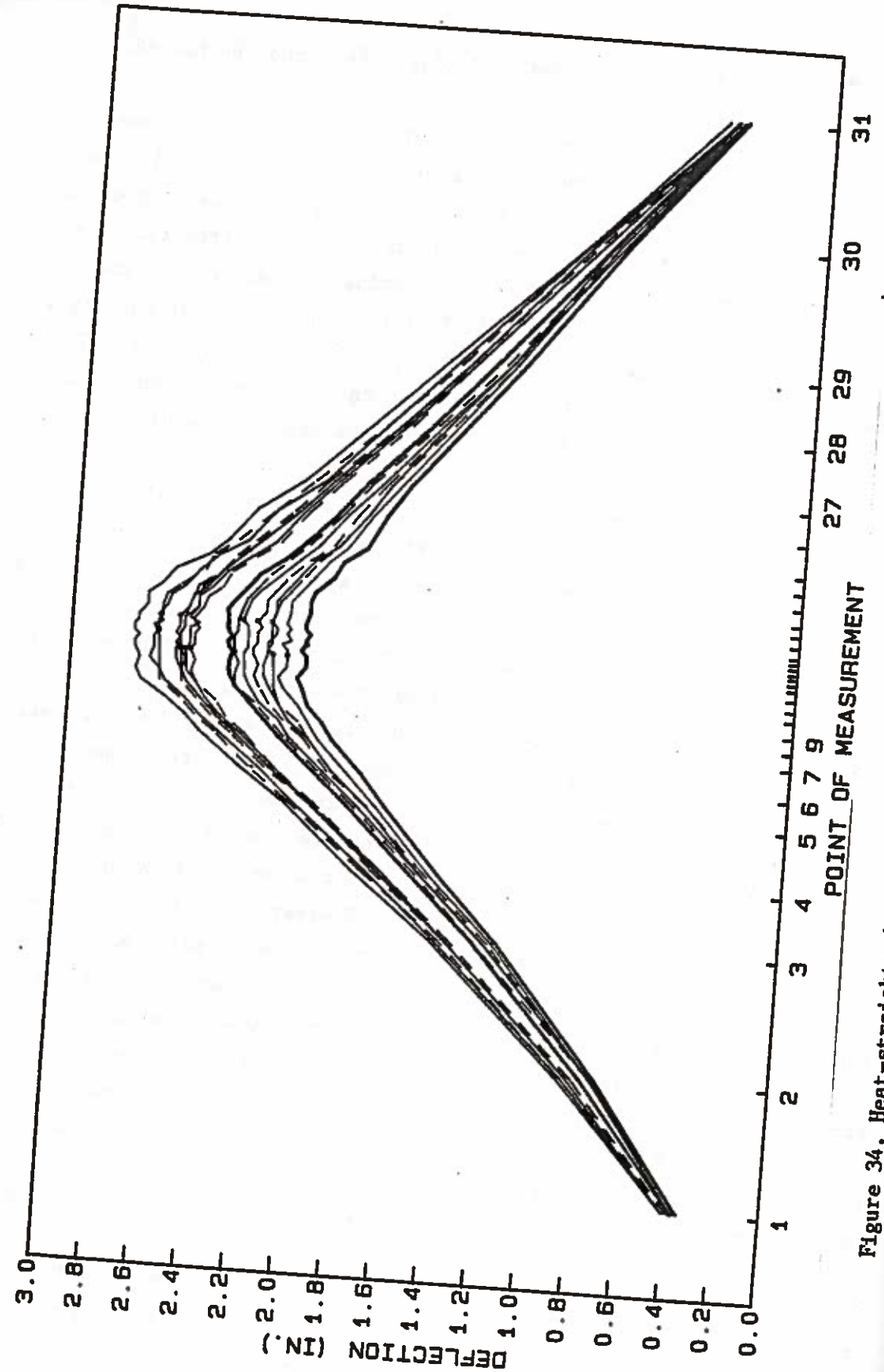

Figure 34. Heat-straightening progression for the damaged girder SB-1 through heating sequence two (15 tatal heating cycles).

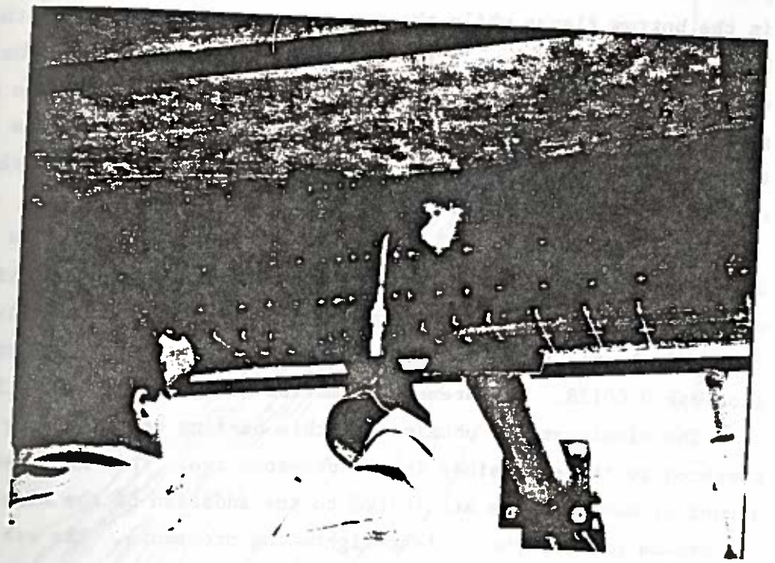

Figure 35. Line Heat in Progress

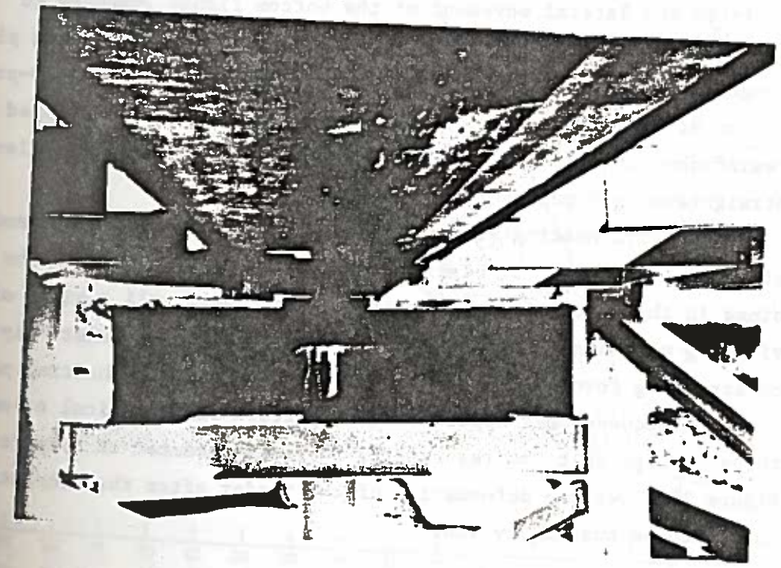

Figure 36. Curvature of the Test Girder SB-1 after the Application of Seventeen Heating Cycles.

practitioners stopped heating the web and started heating the vee area in the bottom flange while the other practitioner continued the line heat. This procedure allowed both practitioners to finish the heating cycle simultaneously. The heated areas in the middle portion of the girder, both in the web and in the flange, were thus near the same temperature. Figure 36 provides a view of the girder after the application of one of these heating cycles.

Figure 37 shows the displacements obtained in the bottom flange during the third heating sequence. The maximum plastic rotation angle obtained in this heating sequence was 0.00493 radians. The average angle of plastic rotation was 0.00309 radians, and the standard deviation was 0.00128. Measurement summaries are given in Tables 5 and 6.

The displacements obtained in this heating sequence were very large compared to those obtained in the previous two. This increase in the amount of movement was attributed to the addition of the line heat in the web as part of the heat-straightening procedure. The web yield line, which resulted during the damage inducement process, produced additional internal constraints against straightening of the bottom flange. These constraints were acting opposite to the jacking force and resisted the lateral movement of the bottom flange, tending to straighten the beam. Heating of the yield line helped form a plastic hinge line with a reduced yield level to decrease the counter-productive action of the resistance. In essence, the web not only offered less resistance but also was slightly straightened as the bottom flanged straightened and pulled the web along.

The third heating sequence produced the most consistent and effective movement. By heating both the web yield line and the plastic hinge in the bottom flange during the same cycle, all regions of initial yielding were heated simultaneously. In addition, a relatively high constraining force was used. To further evaluate the heating patterns, a fourth sequence was applied. This pattern was identical to sequence three, except that the restraining force was reduced to 56 percent. Figure 38 shows the deformation of the girder after the completion of one of these heating cycles.

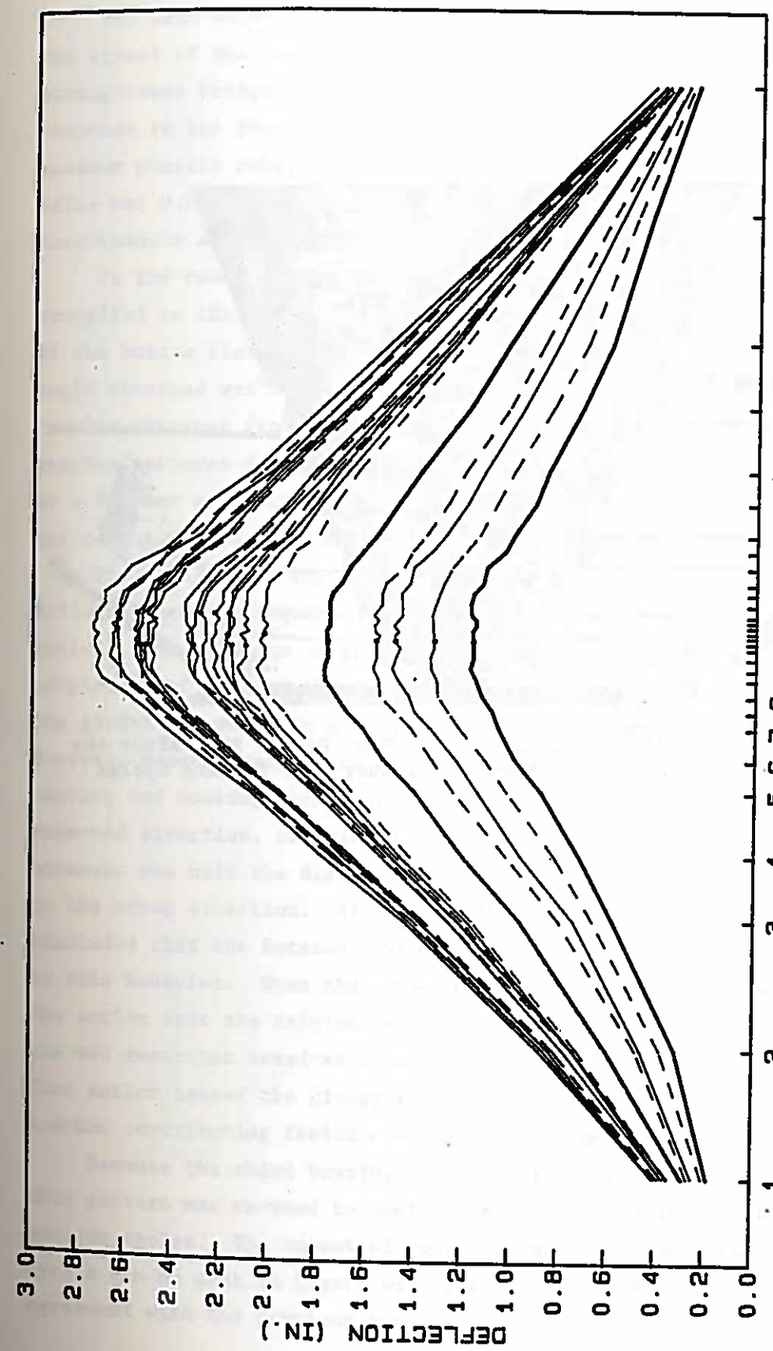

Figure 37. Heat-straightening progression for the damaged girder SB-1 through heating sequence three (20 tatal heating cycles).

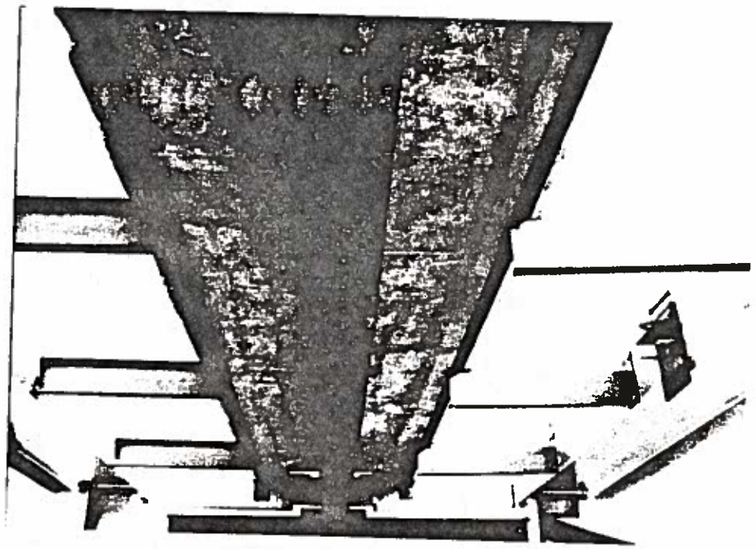

Figure 38. Curvature of the Test Girder SB-1 after the Application of Twenty-Four Heating Cycles

The main objective of applying this heating sequence was to study the effect of the restraining force on the behavior of the heat-straightened bridge girder. The movement of the bottom flange in response to the fourth heating sequence can be seen in Figure 39. The maximum plastic rotation obtained was 0.00175 radians, while its average value was 0.00132 radians, with a standard deviation of 0.00052. Measurements are summarized in Tables 5 and 6.

In the twenty-fifth heating cycle, heating sequence three was reapplied to the girder. The last curve in Figure 40 shows the movement of the bottom flange due to this heating cycle. The plastic rotation angle obtained was 0.00351 radians, which is in agreement with the results obtained from heating cycles 17 to 21. Thus, intermixing heating patterns did not decrease the effectiveness of pattern three. As a further evaluation of the restraining force, heating sequence three was repeated with the load ratio reduced to zero.

Figure 41 shows the displacements obtained during this fifth different heating sequence, in addition to all the subsequent heating cycles. Measurements of the movements of the bottom flange upon the completion of the twenty-sixth heating and cooling cycle revealed that the girder had moved in a direction opposite to the vee heat direction. However, measurements taken after the completion of the twenty-seventh heating and cooling cycle show that the girder had moved back in the expected direction, coinciding with the direction of the vee heat. That movement was half the distance that the girder had previously displaced in the wrong direction. After a review of both heating cycles, it was concluded that the internal redundancy of the web might have contributed to this behavior. When the external jacking force, which was opposing the action that the deformed web had on the bottom flange, was removed, the web restraint acted as a jacking force in the opposite direction. That action caused the girder to displace in the wrong direction. Another contributing factor could have been residual stresses.

Because the third heating sequence proved to be the most effective, this pattern was re-used to perform the twenty-eighth and twenty-ninth heating cycles. The amount of movement caused by these two heating cycles can be seen in Figure 42. The plastic rotations obtained were in agreement with the previous results obtained using the same heating

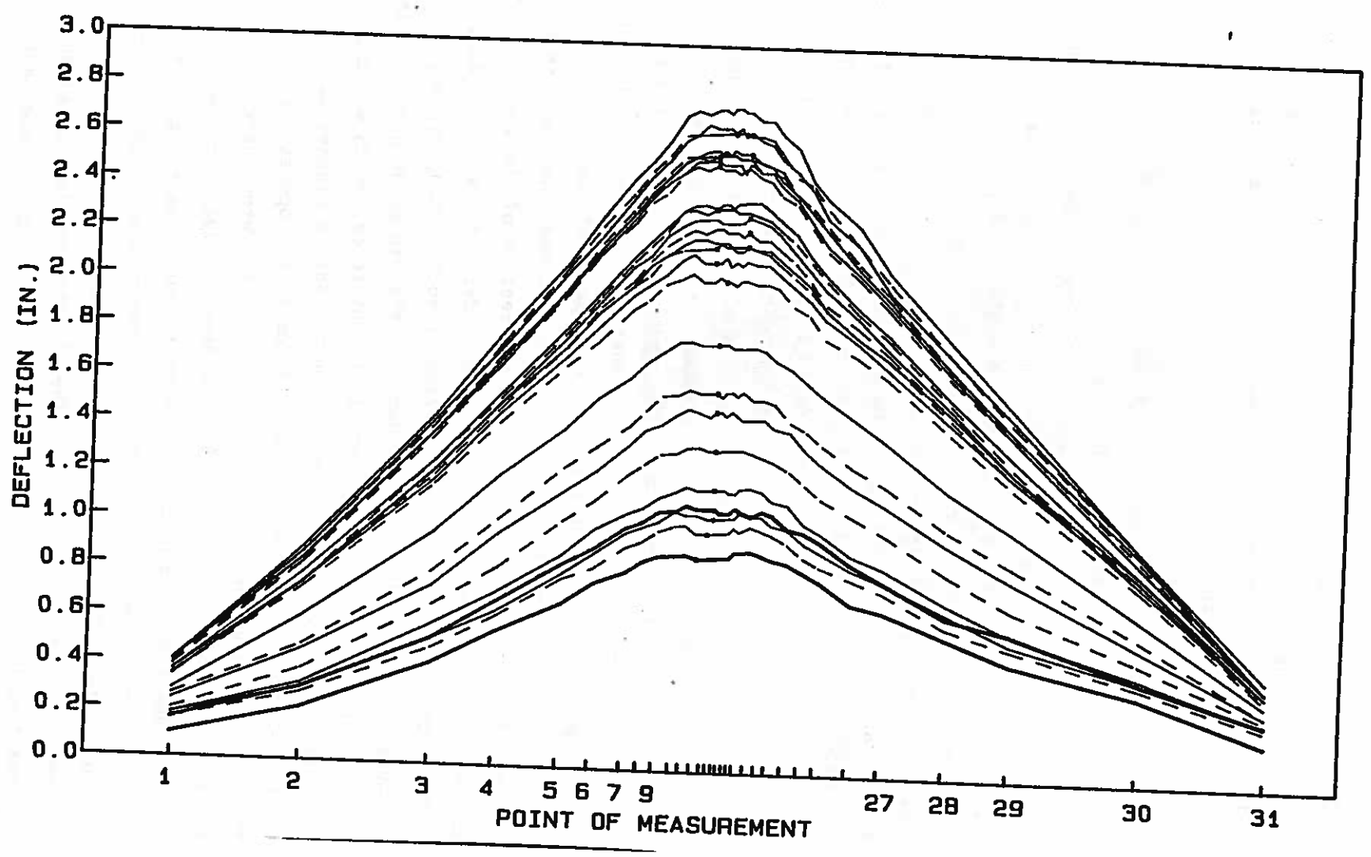

Figure 39. Heat-straightening progression for the damaged girder SB-1 through heating sequence four (24 total heating cycles).

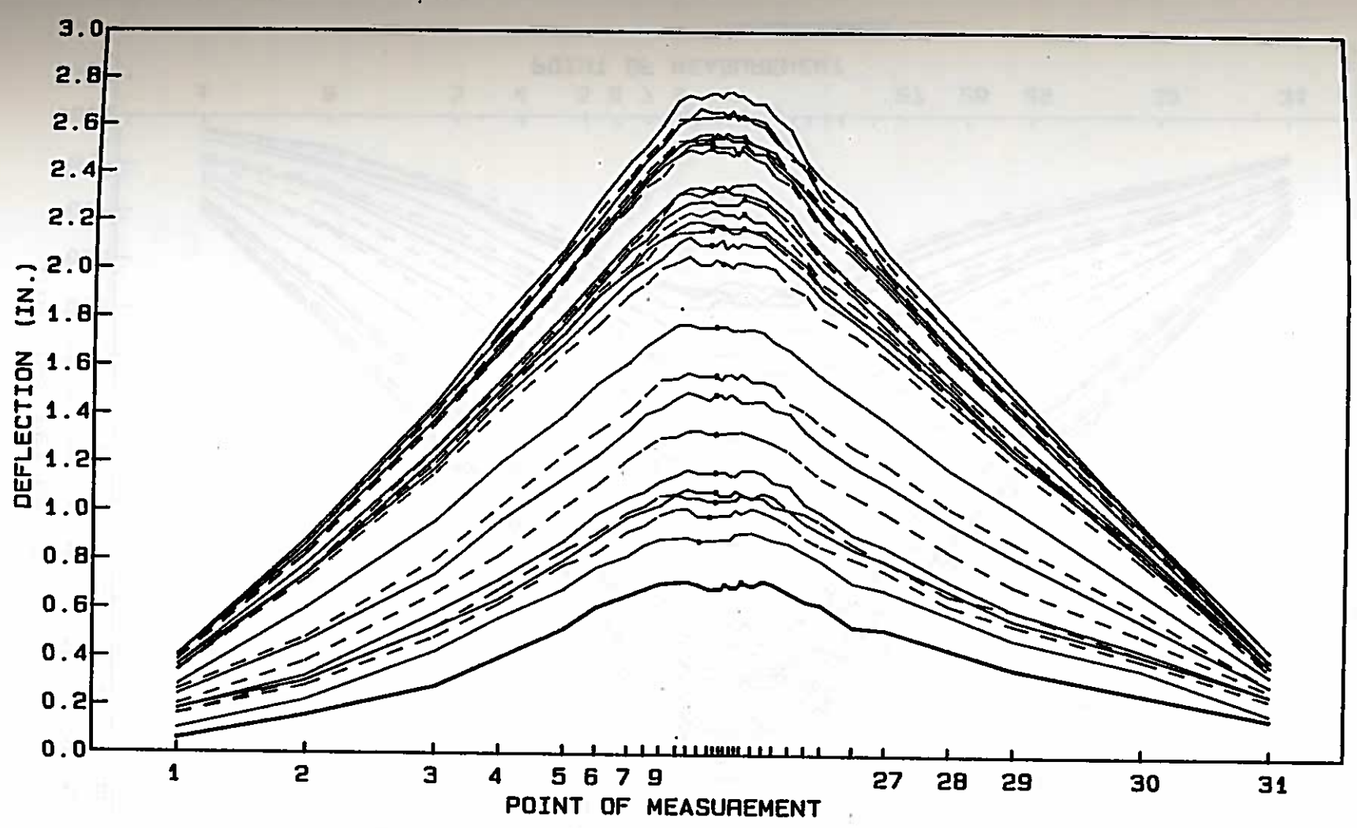

Figure 40. Heat-straightening progression for the damaaged girder SB-1 repeating heating sequence three (25 total heating cycles).

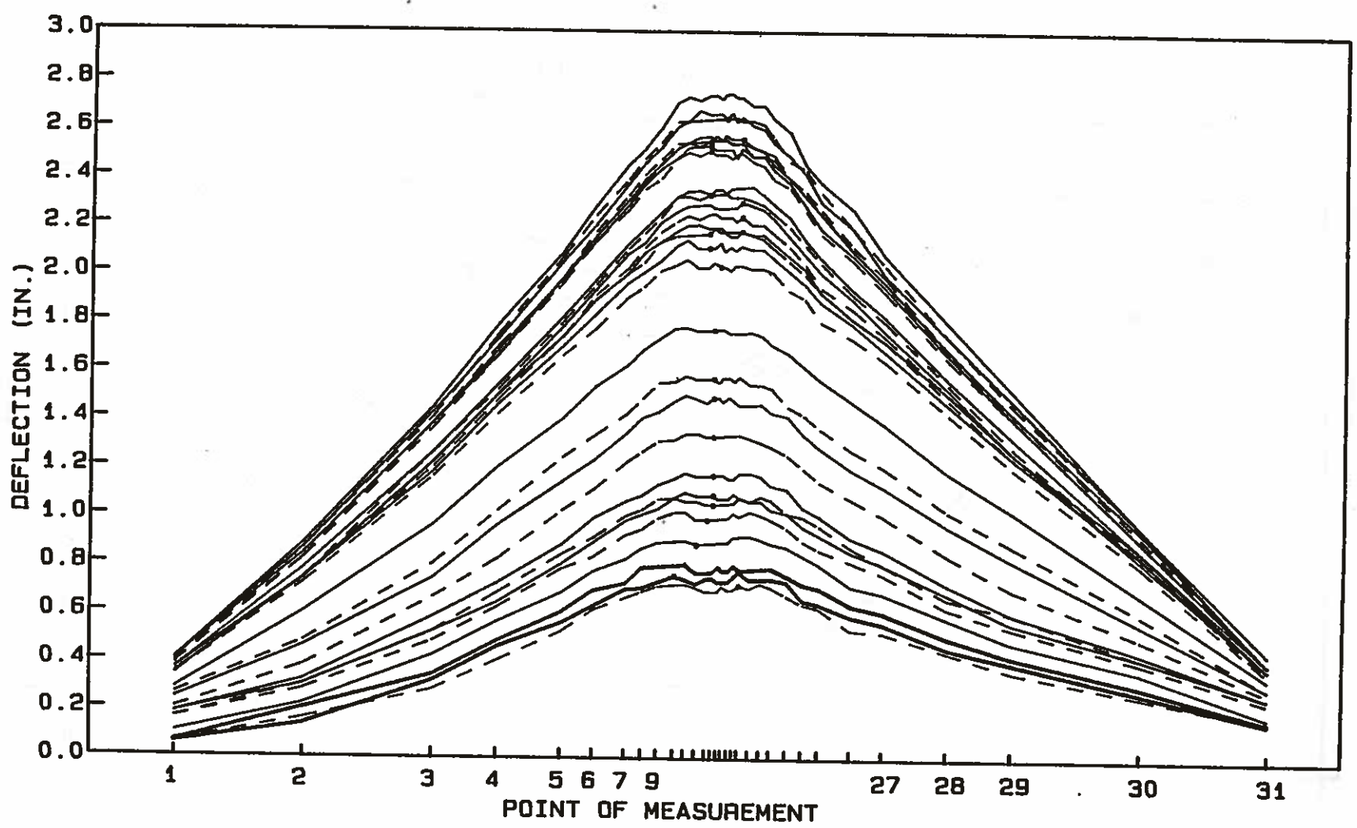

Figure 41. Heat-straightening progression for the damaged girder SB-1 through heating sequence five (27 total heating cycles).

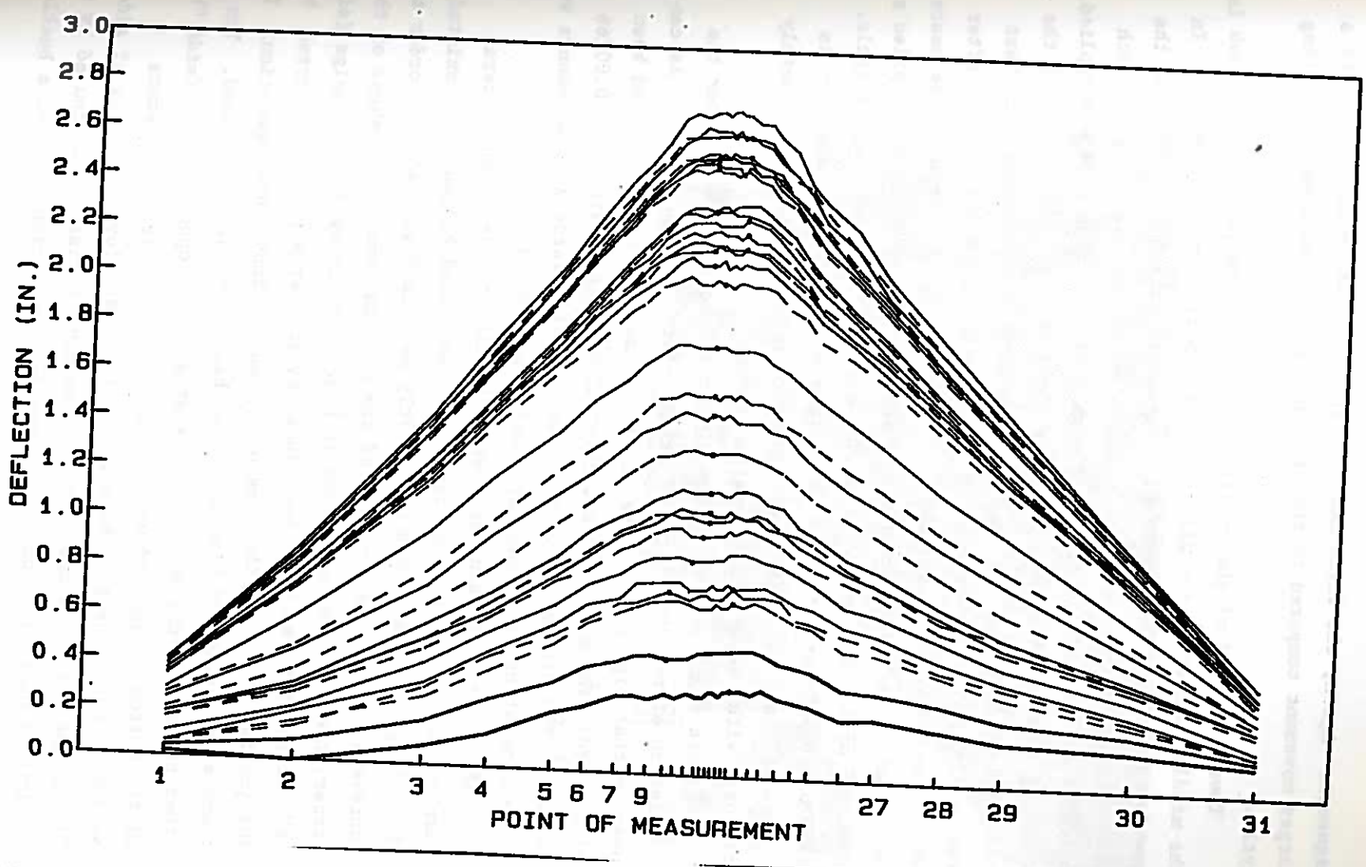

Figure 42. Heat-straightening progression for the damaged girder SB-1 repeating heating sequence three (29 total heating cycles).

sequence. Again, the first heating cycle in this sequence produced a larger movement compared to that produced by the twenty-ninth heating cycle.

Toward the end of the repair work, it was observed that the web in the middle portion of the girder has been perfectly straightened. In heating sequence six, to prevent an overstraightening of the web, the web was not heated in sections where no curvature was present. Each practitioner heated one side of the girder. One line heat was applied, starting from point 3 and continuing through point 8, after which the vee area was heated at point 8. At the same time, another line heat was applied, starting from point 29 and going through point 21, after which another vee area was heated at point 21 also. Thus, 2 vee heats were used in this sequence. A 112 percent jacking force was applied at point 16 of the bottom flange at the beginning of each heating cycle. A view of the girder after the completion of this heating sequence is shown in Figure 43. The figure shows that the girder was completely restored with respect to lateral deformation.

Figure 44 shows the deformation in the bottom flange after the completion of the thirtieth and thirty-first heating cycles. As can be seen in that figure, the lateral displacement of the girder had been eliminated. The average plastic rotation angle obtained was 0.00266 radians. The standard deviation was 0.00076. These last movements were quite consistent with those of heating sequence 3.

After the successful heat-straightening repair of the lateral displacement of the bottom flange, two localized bulges still existed in that flange. These bulges are clearly seen in Figure 45. In order to achieve a complete restoration of the original undeformed shape of the girder, the bulges were removed in heating sequence 7. One bulge (side "d") of the bottom flange was caused by the large pressure exerted by the jacking device at the time of the damage inducement operation. The shape and location of that bulge has been previously described. The other bulge was very small. It existed on the opposite side (side "h") of the bottom flange and was caused by differential temperature variation during heating between the upper and lower surfaces of side "h" of the bottom flange. That temperature variation was caused by the repetitive heating of only the lower surface, which produced a buckle.

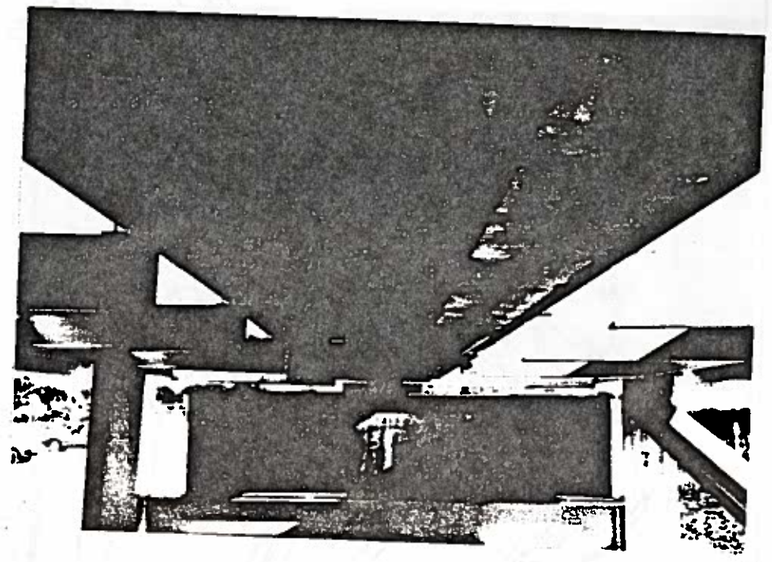

Figure 43.. Curvature of the Test Girder SB-1 after the Application of Thirty-One Heating Cycles

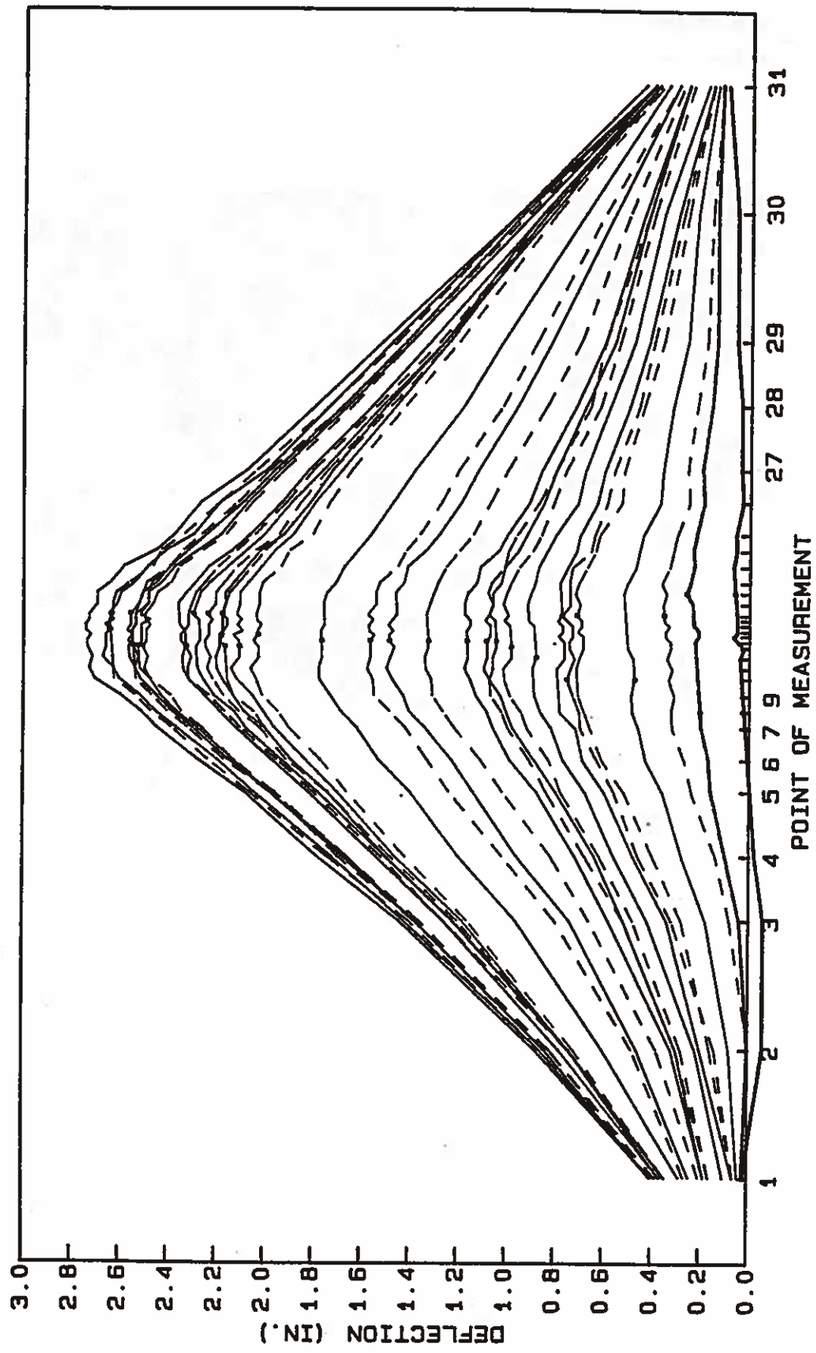

Figure 44. Heat-straightening progression for the damaged girder SB-1 through heating sequence six (31 total heating cycles).

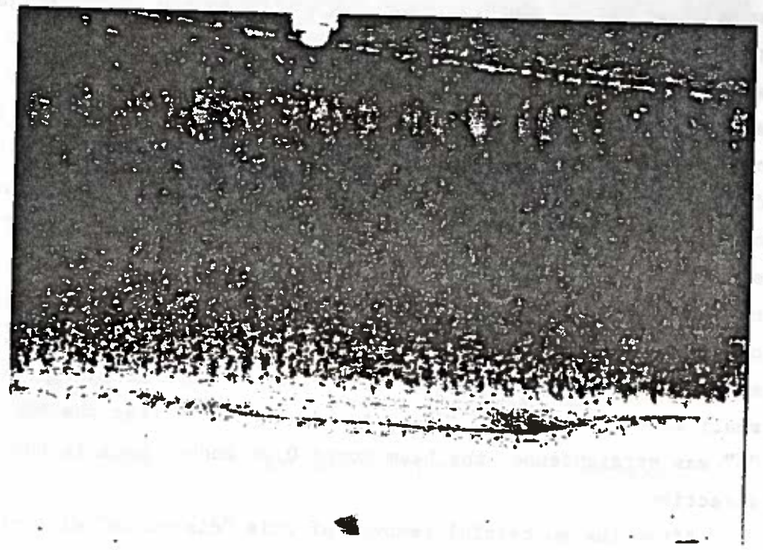

Figure 45. Close-Up View of the "Dish-Like" Distortion in Girder SB-1

Figures 46 and 47 show the bulge removing operation in progress. Both spot heats and circumferential line heats were applied to the "dish-like" bulge. The circumferential line heats were applied to the boundaries of the bulge where yielding had occurred. Then successive spot heats were performed along the entire length of the bulge in order to straighten the flange. The maximum temperature was always limited to about 1200°F. A constant jacking force of about 6,700 pounds was applied to the bulge before any heat was applied. After the completion of the heat, the force was increased to 13,400 pounds or 15,700 pounds, depending on the amount of straightening required. This technique is called hot mechanical straightening. After the completion of straightening of the "dish-like" bulge on side "d," it was noticed that the beam deflected laterally backwards 0.28 inches in a direction opposite to the movements which had been previously recorded. That movement was expected, since the spot heats were acting similarly to small vee heats placed in the wrong location. After the buckle on side "h" was straightened, the beam moved 0.04 inches back in the right direction.

After the successful removal of this "dish-like" distortion during the seventh heating sequence, deflection measurements were again taken along the girder. As can be seen in Figure 48, after cycle 31 the bottom flange had deflected backwards (in a direction opposite to the vee direction) about 0.28 inches. During cycle 32, there was a slight forward movement (Figure 49).

To remove the new lateral deflection of the bottom flange, the final heating sequence was the same procedure as used in heating sequence six. However, since the largest displacement was obtained around point 16, where most of the spot heats were applied, only one vee heat was applied at this point. Again, a 112 percent jacking force was exerted on the bottom flange. The final undeflected shape of the test girder is shown in Figure 50.

The effect of heating cycles 34, 35, and 36 on the behavior of the bottom flange of the girder is plotted in Figure 51. Also shown in Figure 51 is the progressive behavior of the heat-straightened full-scale, composite simulated bridge girder. As can be seen in that figure, the final configuration was less than 0.1 inch from being

Figure 46. Bulge Removal Operation in Progress

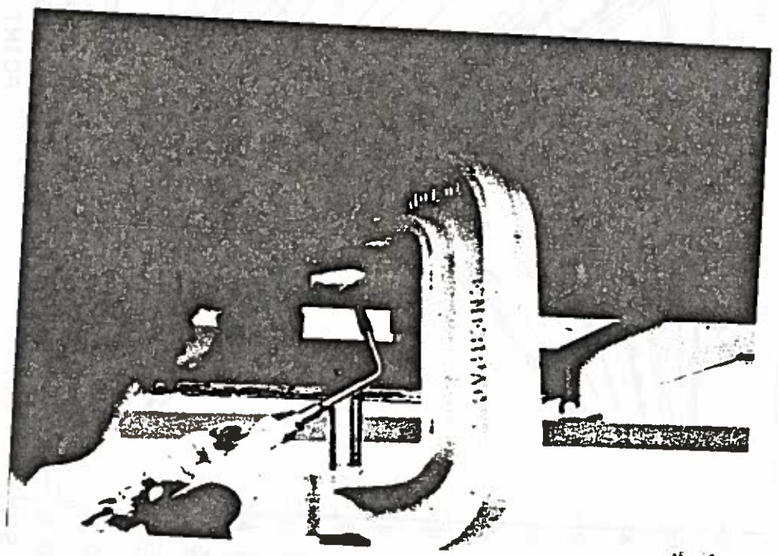

Figure 47. Buckle Removal Operation in Progress

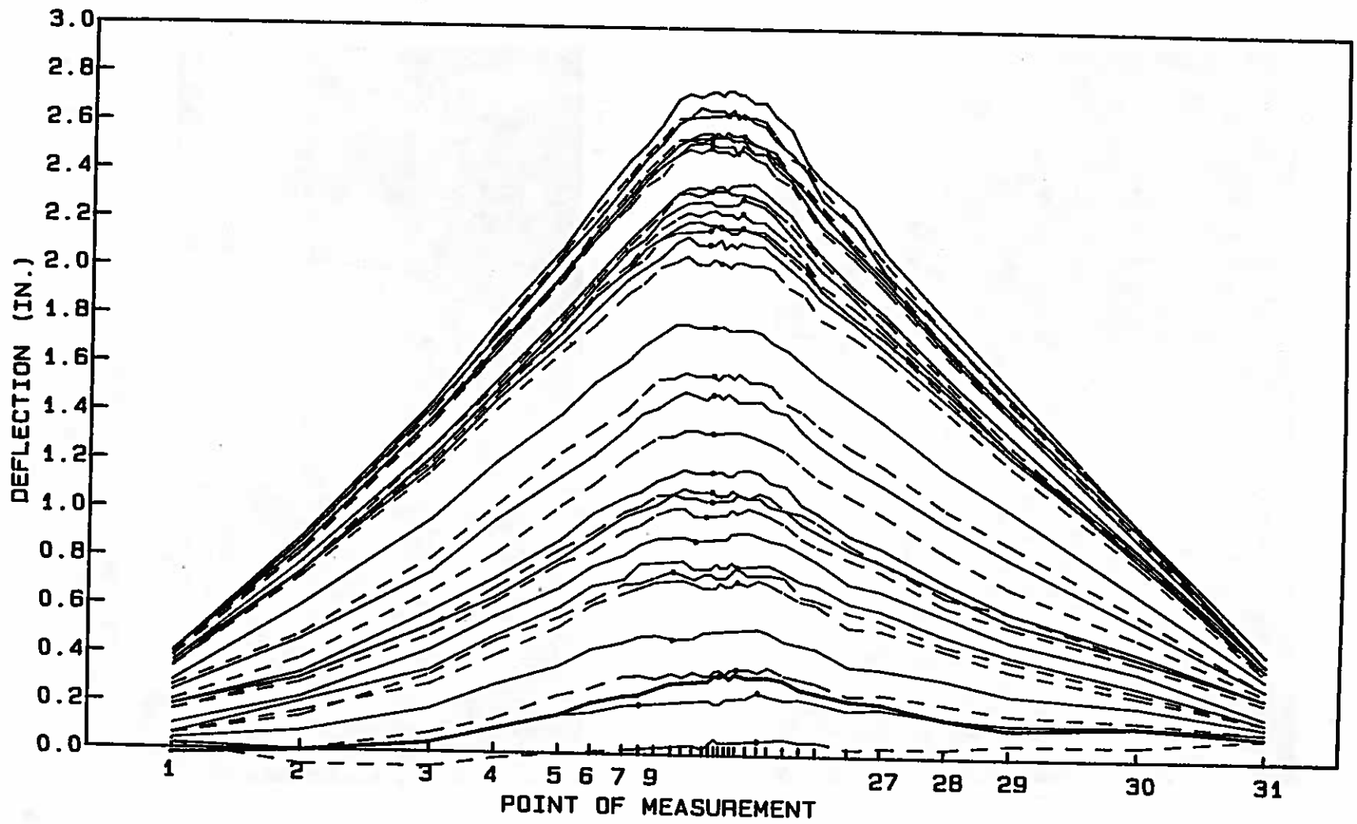

Figure 48. Heat-straightening progression for the damaged girder SB-1 through the thirty-second heating cycle.

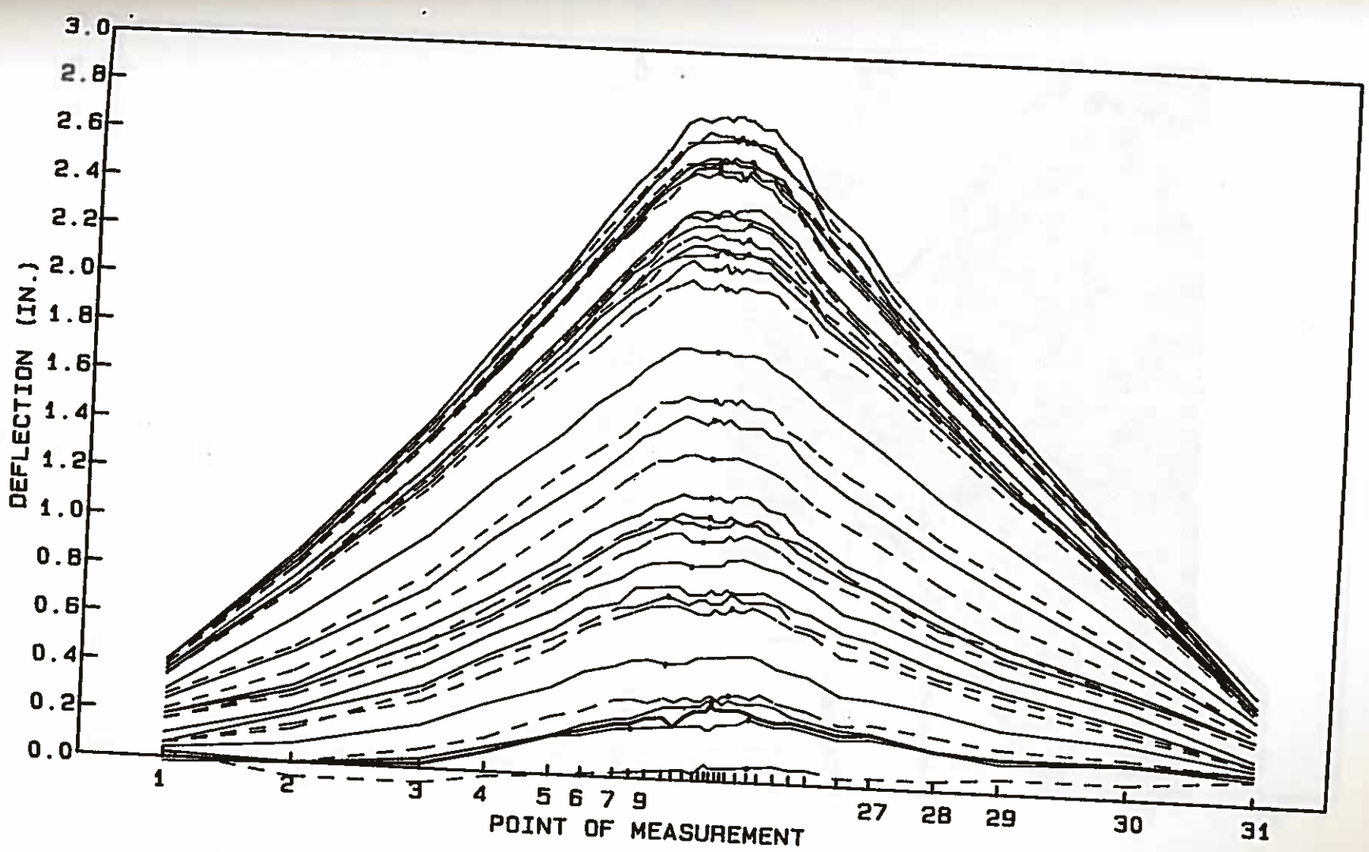

Figure 49. Heat-straightening progression for the damaged girder SB-1 through heating sequence seven (33 total heating cycles).

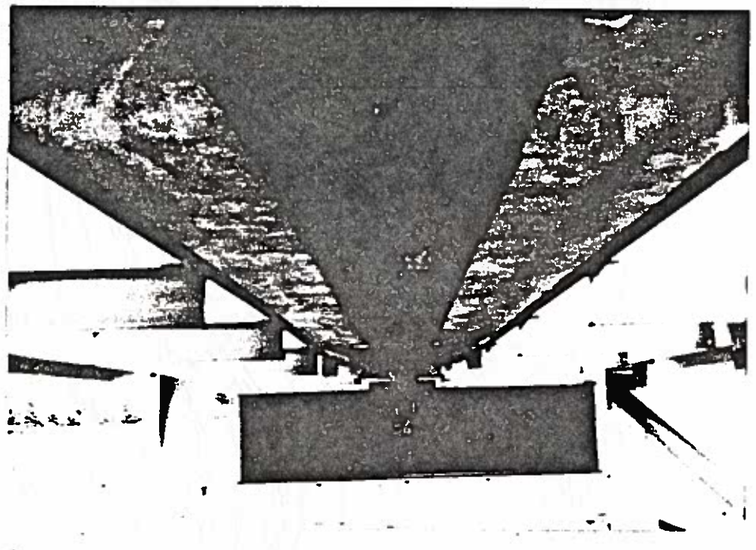

Figure 50. View of the Repaired Test Girder SB-1 after the Completion of the Heat-Straightening Process

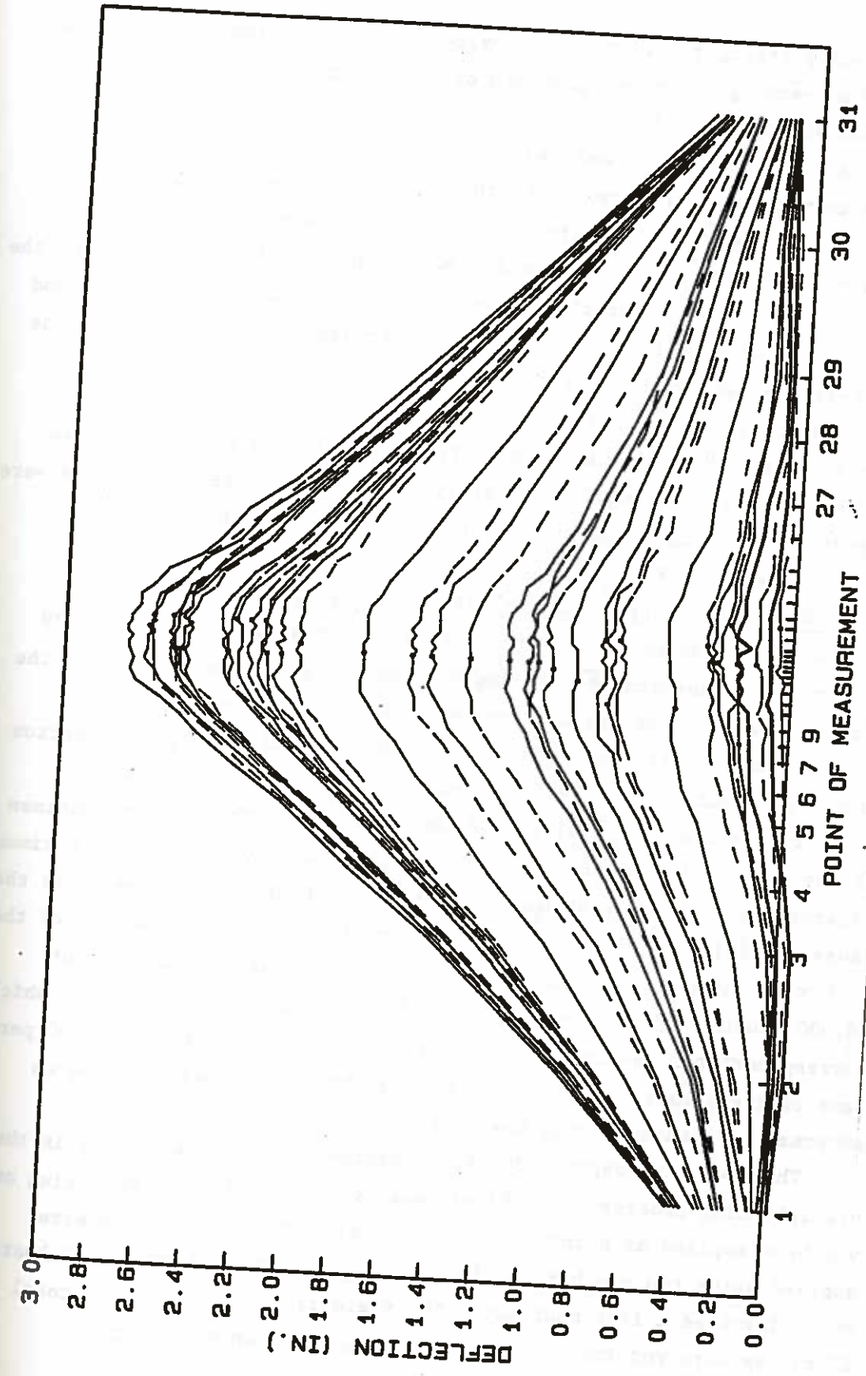

Figure 51. Heat-straightening progression for the damaged girder SB-1 through heating sequence eight (36 total heating cycles).

perfectly straight. Figure 52 provides a cross-sectional view showing the heat-straightening progression on the rotational behavior of the girder about point 16.

A slight curvature existed at the left end of the test girder. That curvature was not caused by the heat-straightening process, but rather was present in the girder before the inducement of damage. Figure 53 shows a cross-sectional view of the rotational behavior of the girder at point 1. When the girder was damaged, the bottom flange and web deflected elastically and assumed a straight position. During the heat-straightening process, those elements tended to return to their original deflected positions. Thus, when the heated portions were straightened, the original bend in the girder became evident. These curvatures were very small and barely seen. Since these curvatures were a part of the original shape of the girder, no attempt was made to heat-straighten that portion.

Case SB-2: Description and Evaluation of the Process

After the completion of this repair process, the same W 10 x 39 girder was re-damaged by exerting a concentrated static force with the jacking device. The maximum load applied was measured to be 32,000 pounds. That force caused a permanent deflection in the bottom flange of about 2.23 inches in magnitude.

After a thorough analysis of the behavior of this girder specimen in response to the damage inducement, it was concluded that the maximum external jacking force should be limited to 36 percent of the force that causes yielding of the member. Based on the structural behavior of the W 10 x 39 girder during damage inducment, the yield force is about 16,000 pounds. Therefore, a jacking force of about 5,200 pounds, which corresponds to 35 percent of the yield force of the girder and 100 percent of the plastic force of the bottom flange only, was used as an external constraint during the heat-straightening process.

Three-quarter-depth, 1200°F, 30-degree vee heats were used in the straightening process. The first heating cycle was performed using one vee heat applied at point 16. However, all subsequent cycles were applied using two vee heats. In addition to the vee heats, each heating cycle involved a line heat along the yield line in the web. A total of 13 cycles were required prior to removing the flange buckles.

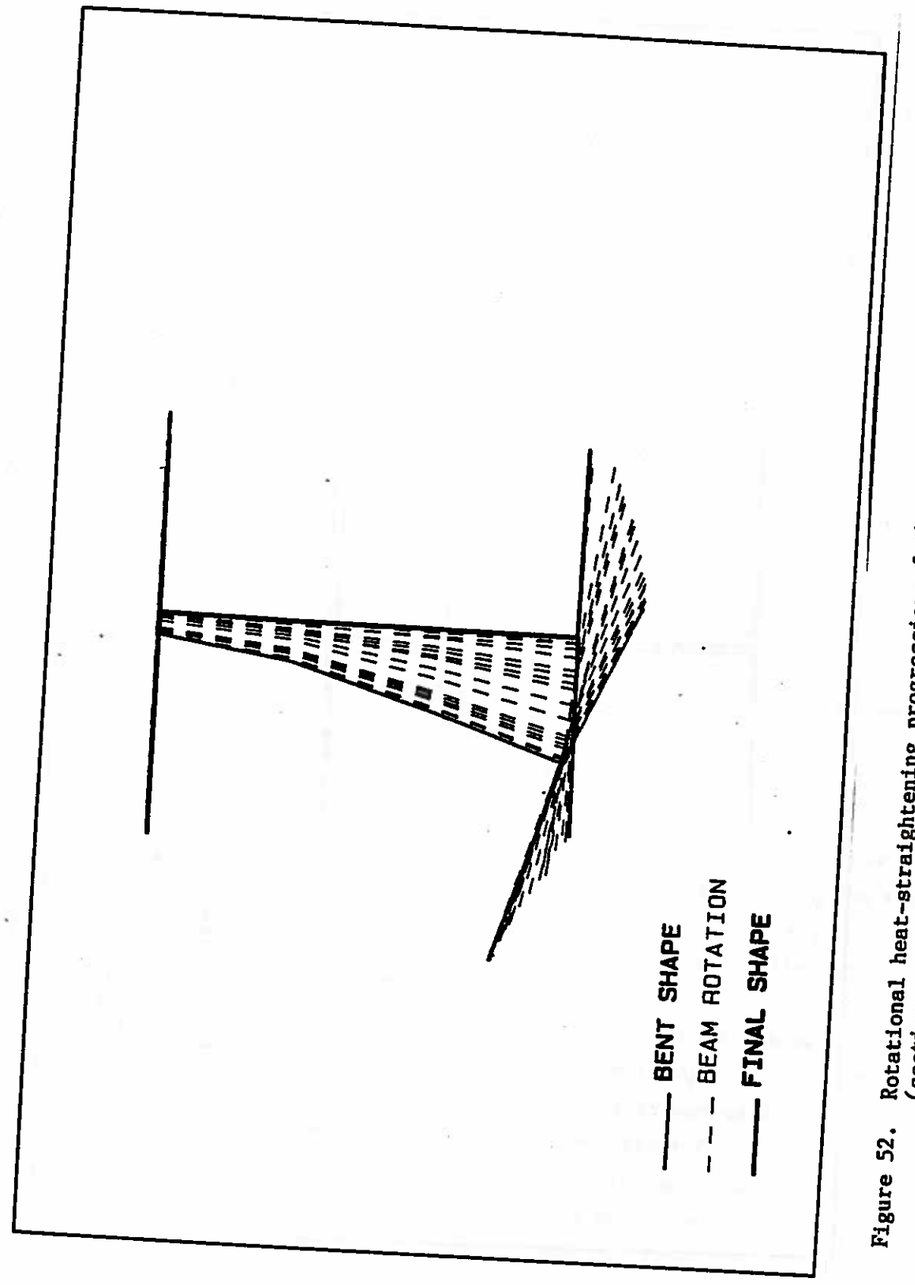

Figure 52. Rotational heat-straightening progressiono f the damaged girder specimen SB-1 (section at point 16).

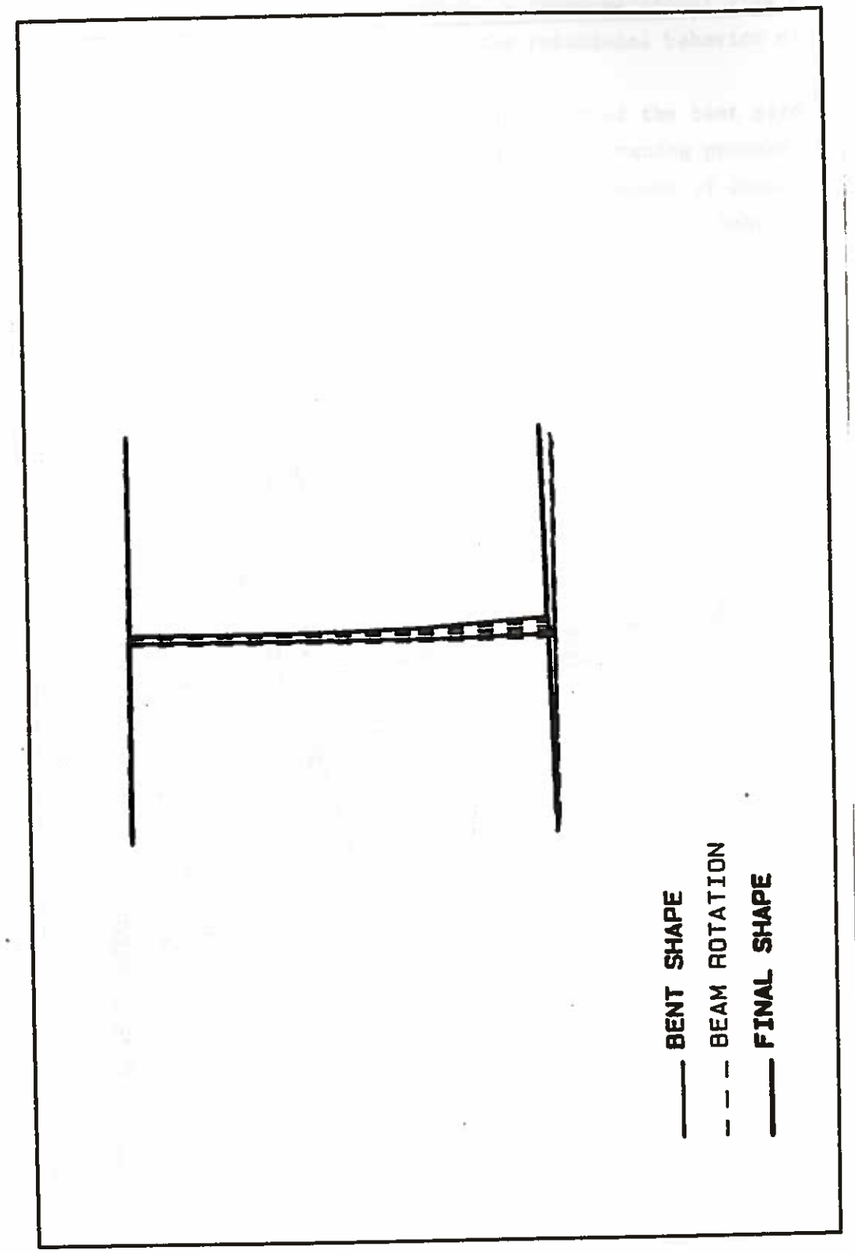

Figure 53. Rotational heat-straightening progression of the damaged girder specimen SB-1 (section at point 1).

Figures 54-56 illustrate the procedure followed during this heat-straightening operation. At the end of the repair process, hot mechanical straightening was used to remove the "dish-like" distortion in the bottom flange. Figure 57 shows a photograph of the repaired girder.

The values of the plastic rotation angles obtained during each heating cycle are shown in Table 7. Figure 58 shows a plot of the progressive effect of heats on the behavior of the girder up to the thirteenth heating cycle. After the application of the thirteenth heating cycle, the lateral displacement of the girder was eliminated. However, the "dish-like" distortion was still present in the bottom flange.

As can be seen in Figure 58, the deformation obtained after the completion of the first heating cycle was greater than that obtained after subsequent heat applications. This phenomenon was also observed during the SB-1 heat-straightening repair of this girder. Although the residual stresses are suspected of being the primary cause of this phenomenon, a residual stress analysis was not conducted during this phase of the project. However, residual stress tests are planned for tests on later heat-straightened girders.

All subsequent heating cycles (cycles 2 to 13) were performed by applying two vee heats to the bottom flange as well as a line heat to the web. The decision to apply 2 vee heats in the same heating cycle was made because the middle portion of the bottom flange between the vee heats was relatively straight. The average plastic rotation angle obtained during those heating cycles was 0.00257 radians, while the standard deviation was 0.00065.

The fourteenth heating cycle was applied in order to remove the "dish-like" distortion which exists in the bottom flange. A plot of the deflections obtained during this heating cycle is presented in Figure 59. The magnitude of this deflection was about 0.18 inches in a direction opposite to the vee direction. The fifteenth heating cycle was applied to remove the slight buckles which developed in the bottom flange during the heating process. Also shown in Figure 59 is the final

Figure 54. Line Heat Applied to the Yield Line of the Web of Girder SB-2

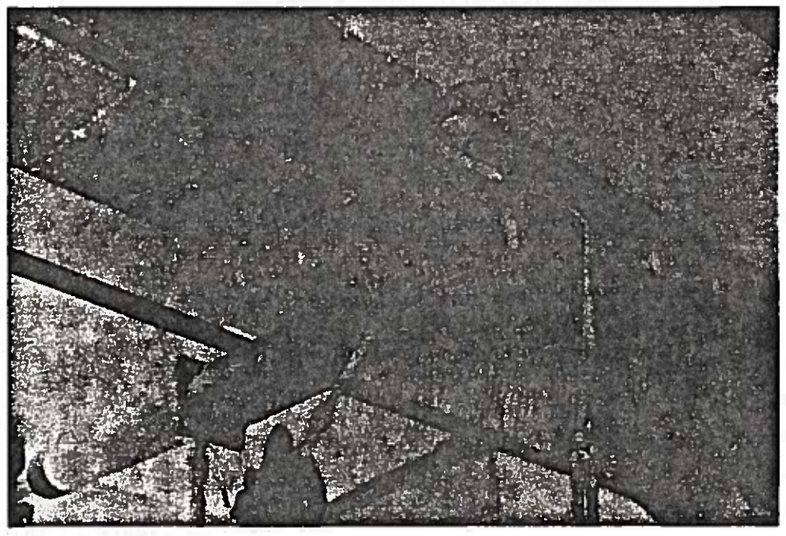

Figure 55. Both Line Heat and Vee Heat Applied Simultaneously.

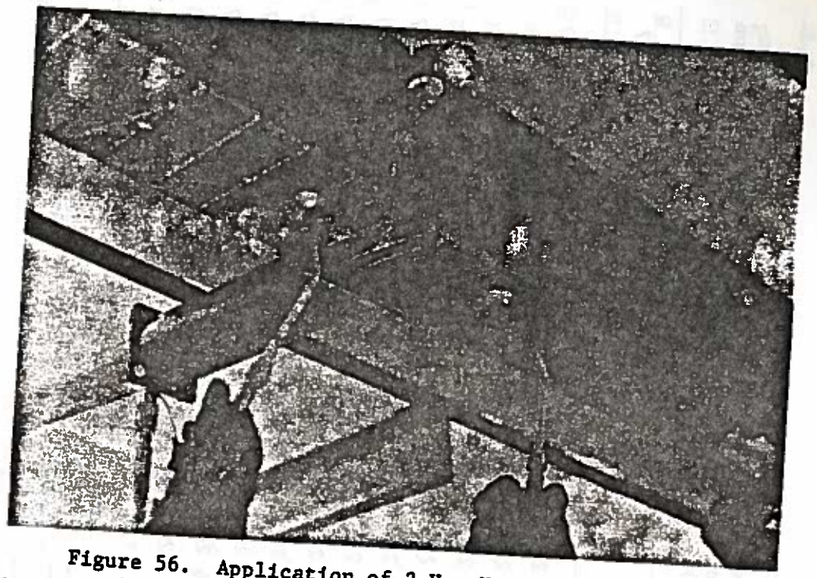

Figure 56. Application of 2 Vee Heats on the Bottom Flange of Girder SB-2

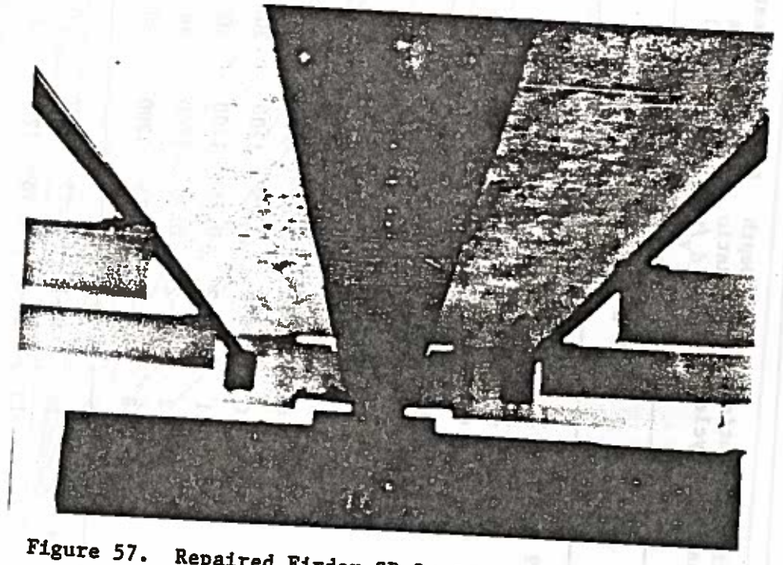

Figure 57. Repaired Firder SB-2 after the Completion of the Heat-Straightening Process

Table 7. Summary of experimental results on the behavior of the test girder SB-2 under the influence of each heating cycle.

Heating Sequence	Heating Cycle	Code	Depth Ratio (d_v/w)	Heat Temp. (F)	Vee Heat Angle (deg)	Vee Heat Location (pt. #)	Line Heat Location (pts. #)	Spot Heat Location (pt. no.)	Load Ratio (M/Mp)	Plastic Rotation (rad)
	1	SB-2	0.75	1200	30	16	3 to 29	--	1.00	0.00617
9	2	SB-2	0.75	1200	30	10 & 22	3 to 29	--	1.00	0.00312
	3	SB-2	0.75	1200	30	10 & 22	3 to 29	--	1.00	0.00138
	4	SB-2	0.75	1200	30	10 & 20	3 to 29	--	1.00	0.00308
	5	SB-2	0.75	1200	30	10 & 20	3 to 29	--	1.00	0.00344
	6	SB-2	0.75	1200	30	10 & 20	3 to 29	--	1.00	0.00137
	7	SB-2	0.75	1200	30	10 & 20	3 to 29	--	1.00	0.00257
	8	SB-2	0.75	1200	30	10 & 20	3 to 29	--	1.00	0.00257
	9	SB-2	0.75	1200	30	10 & 20	3 to 29	--	1.00	0.00257
	10	SB-2	0.75	1200	30	10 & 20	3 to 29	--	1.00	0.00257
	11	SB-2	0.75	1200	30	10 & 20	3 to 29	--	1.00	0.00257
	12	SB-2	0.75	1200	30	10 & 20	3 to 29	--	1.00	0.00208
	13	SB-2	0.75	1200	30	10 & 22	3 to 29	--	1.00	0.00311
7	14	SB-2	0.75	1200	30	--	3 to 29	16	1.00	-0.00308
	15	SB-2	0.75	1200	30	--	3 to 29	16	1.00	0.00034
	16	SB-2	0.75	1200	30	16	3 to 29	--	1.00	0.00206

Figure 58. Heat-straightening progression for the damaged girder SB-2 through the thirteenth heating cycle.

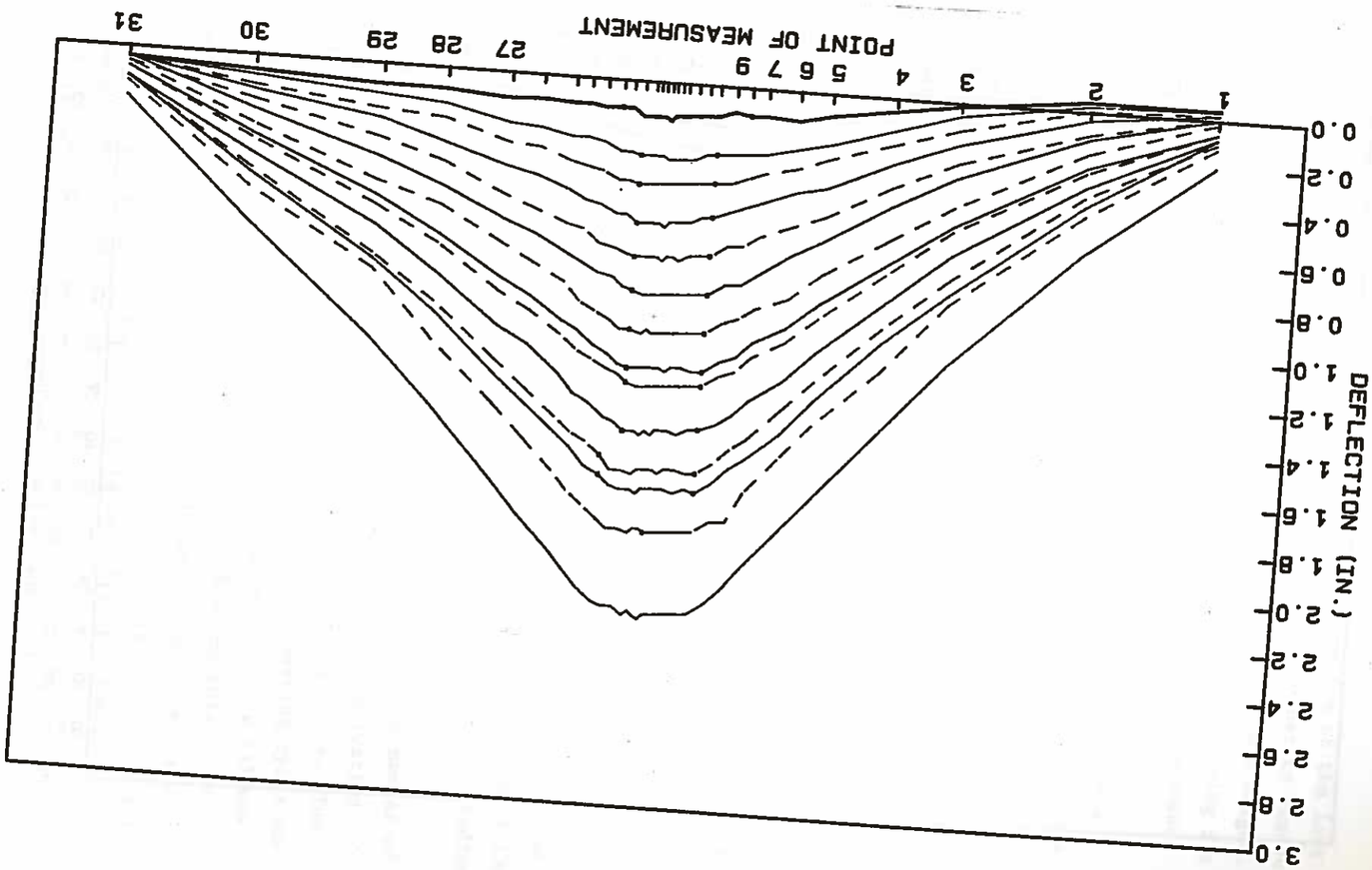

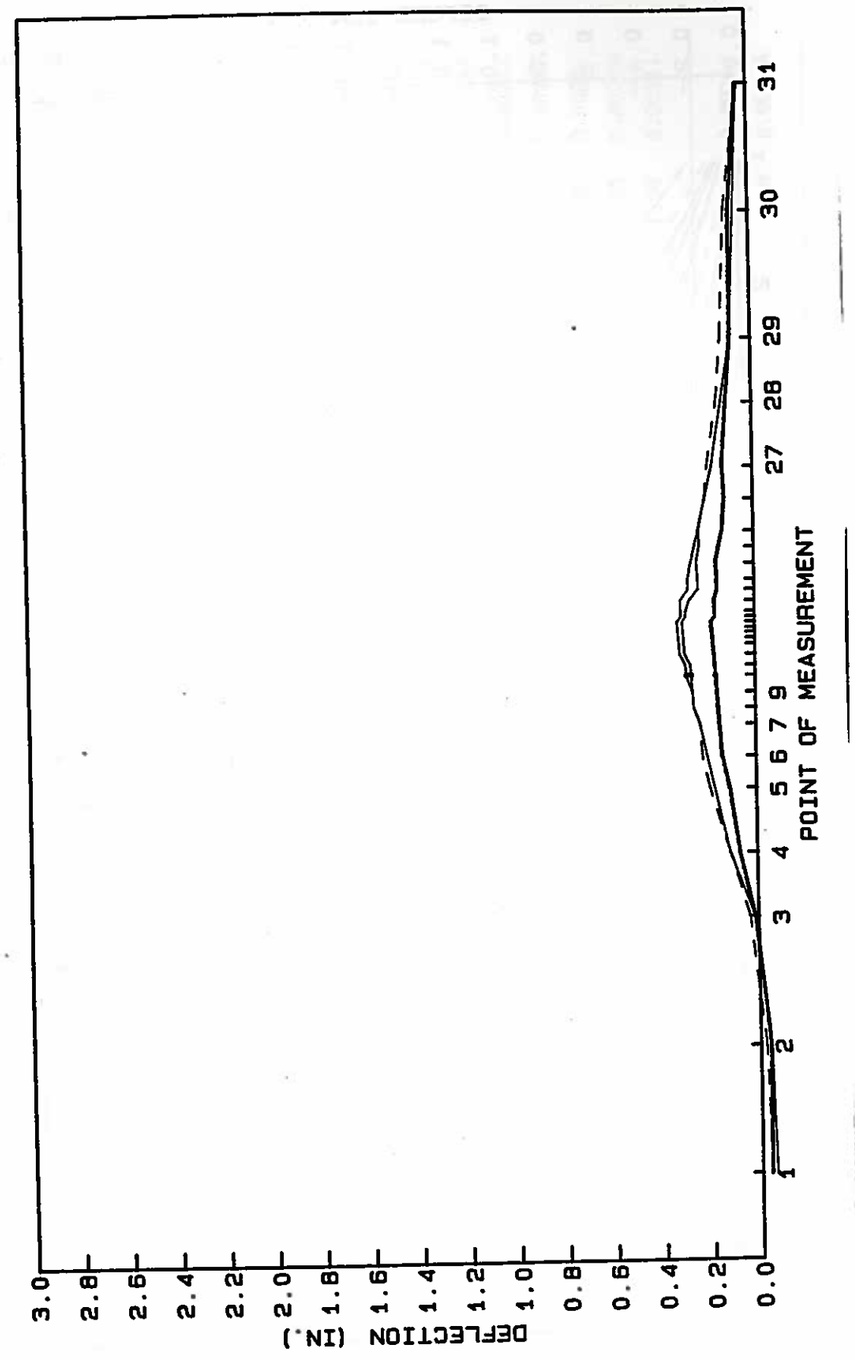

Figure 59. Heat-straightening progression for the damaged girder SB-2 through the sixteenth heating cycle).

straightened shape of the girder after the application of the last heating cycle. That heating cycle was performed in order to remove most of the lateral deflection resulting from the removal of the bulges. Figure 60 provides a cross-sectional view of the girder showing its rotational behavior in response to the heat-straightening process.

Case SB-3: Description and Evaluation of the Process

Because the structural behavior of this girder specimen was unknown, the horizontal component of the jacking force applied as an external constraint was restricted to 2,850 pounds. This force corresponds to one-third of the force that would cause plastic yielding of the bottom flange only. The restriction was utilized in order to ensure that no instabilities would occur during the heating process.

For all heating cycles, 1200°F, three-quarter-depth, 30-degree vee heats were used to straighten the damage. During each heating cycle, a line heat was used along the yield line between points 4 and 17 in order to reduce the yield stresses acting on this line. Thus, a single sequence was used for all heats. Figure 61 provides a picture of the girder after completion of the heat-straightening process.

The straightening process required 28 heating cycles for completion. Figure 62 shows the amount of movement obtained in response to each heating cycle. The values of the plastic rotation angles achieved during each of the 28 heating cycles are shown in Table 8. Again, the maximum plastic rotation angle was obtained after the application of the first heating cycle. That angle was computed to be about 0.01095 radians.

During the course of the heat-straightening process, it was observed that the amount of plastic rotation decreases as the number of vee heats applied at the same location increases. That observation became clear after the application of the twelfth heating cycle. The amount of plastic rotation angle obtained during this heating cycle was 0.00102 radians. However, the following heating cycle (cycle 13) was performed by applying the vee heat to point 10. Heating this virgin location produced a plastic rotation angle of about 0.00308 radians, which is about 3 times as large as the previous plastic rotation angle. A low plastic rotation angle was again obtained after the completion of the sixteenth heating cycle. During this heating cycle, the vee heat was reapplied at point 13. The plastic rotation angle produced was

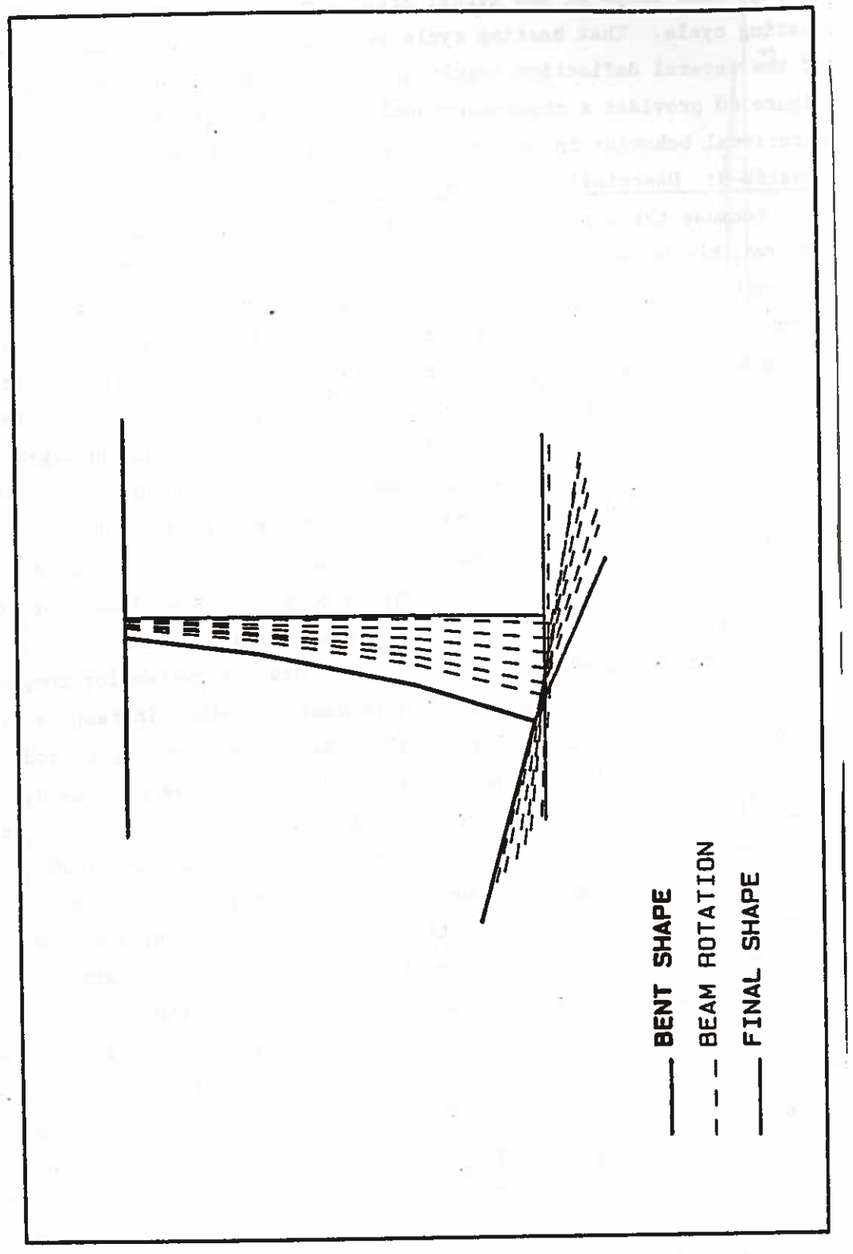

Figure 60. Rotational heat-straightening progression of the damaged girder specimen SB-2 (section at point 16).

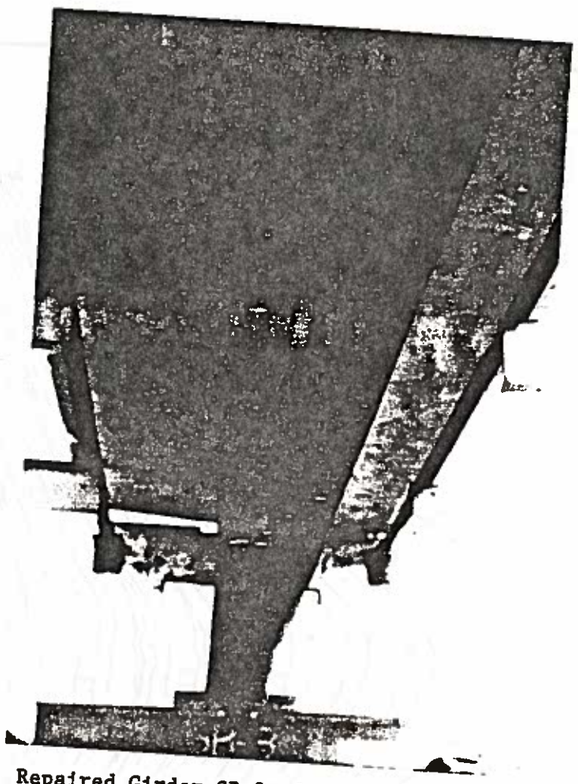

Figure 61. Repaired Girder SB-3 after the Completion of the Heat-Straightening Process

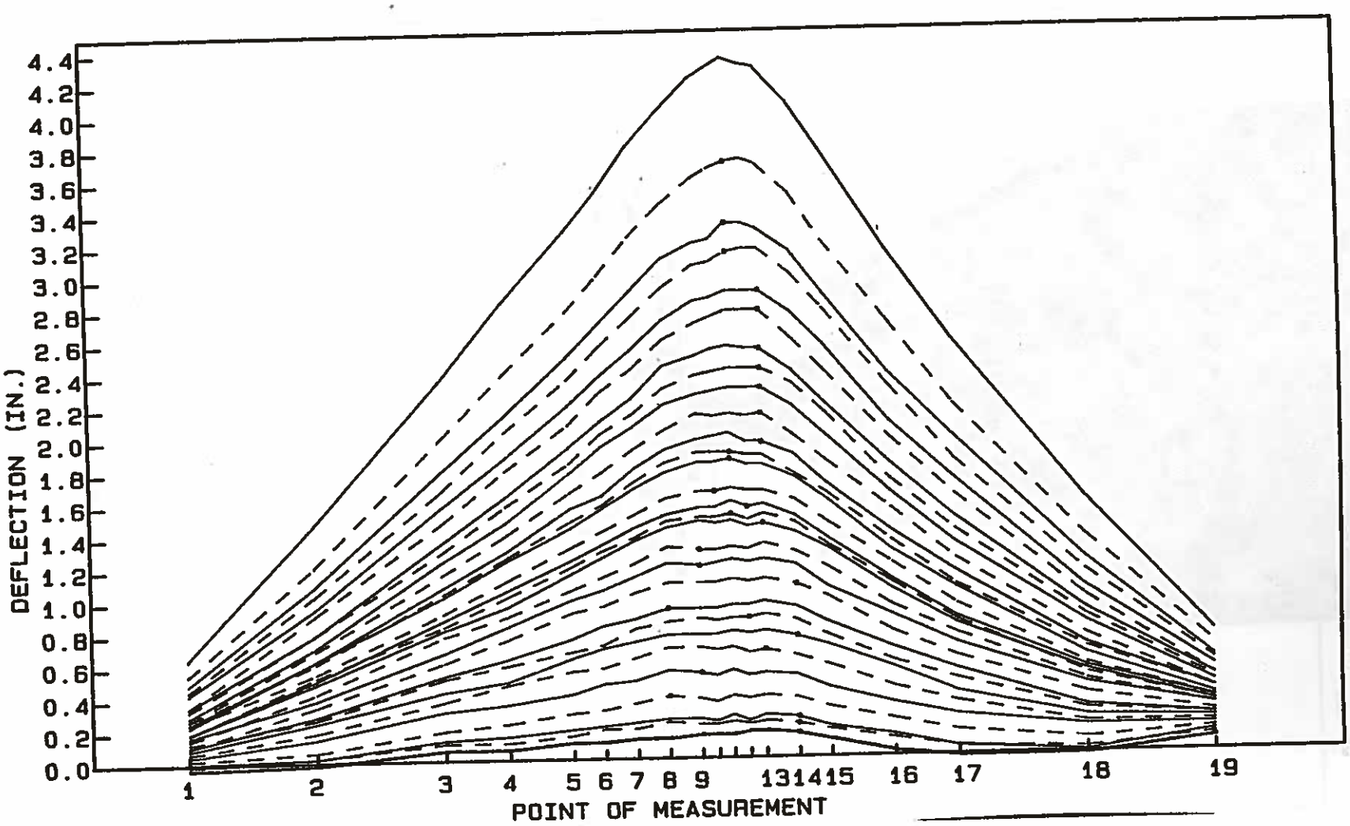

Figure 62. Heat-straightening progression for the damaged girder SB-3 up to the twenty-eighth heating cycle.

Table 8. Summary of experimental results on the behavior of the test girder SB-3 under the influence of each heating cycle.

Heating Sequence	Heating Cycle	Code	Depth Ratio (d_v/w)	Heat Temp. (F)	Vee Heat Angle (deg)	Vee Heat Location (pt. #)	Line Heat Location (pts. #)	Spot Heat Location (pt. no.)	Load Ratio (M/Mp)	Plastic Rotation (rad)
10	1	SB-3	0.75	1200	30	11	4 to 17	---	0.33	0.01095
	2	SB-3	0.75	1200	30	11	4 to 17	---	0.33	0.00752
	3	SB-3	0.75	1200	30	11	4 to 17	---	0.33	0.00308
	4	SB-3	0.75	1200	30	13	4 to 17	---	0.33	0.00448
	5	SB-3	0.75	1200	30	13	4 to 17	---	0.33	0.00279
	6	SB-3	0.75	1200	30	13	4 to 17	---	0.33	0.00412
	7	SB-3	0.75	1200	30	13	4 to 17	---	0.33	0.00240
	8	SB-3	0.75	1200	30	13	4 to 17	---	0.33	0.00244
	9	SB-3	0.75	1200	30	13	4 to 17	---	0.33	0.00309
	10	SB-3	0.75	1200	30	13	4 to 17	---	0.33	0.00310
	11	SB-3	0.75	1200	30	11	4 to 17	---	0.33	0.00205
	12	SB-3	0.75	1200	30	11	4 to 17	---	0.33	0.00103
	13	SB-3	0.75	1200	30	10	4 to 17	---	0.33	0.00308
	14	SB-3	0.75	1200	30	12	4 to 17	---	0.33	0.00171
	15	SB-3	0.75	1200	30	11	4 to 17	---	0.33	0.00137
	16	SB-3	0.75	1200	30	13	4 to 17	---	0.33	0.00103

Table 8. (continued)

Heating Sequence	Heating Cycle	Code	Depth Ratio (d_v/w)	Heat Temp. (F)	Vee Heat Angle (deg)	Vee Heat Location (pt. #)	Line Heat Location (pts. #)	Spot Heat Location (pt. no.)	Load Ratio (M/Mp)	Plastic Rotation (rad)
	17	SB-3	0.75	1200	30	9	4 to 17	--	0.33	0.00308
	18	SB-3	0.75	1200	30	9	4 to 17	--	0.33	0.00171
	19	SB-3	0.75	1200	30	14	4 to 17	--	0.33	0.00209
	20	SB-3	0.75	1200	30	8	4 to 17	--	0.33	0.00275
	21	SB-3	0.75	1200	30	12	4 to 17	--	0.33	0.00138
	22	SB-3	0.75	1200	30	14	4 to 17	--	0.33	0.00174
	23	SB-3	0.75	1200	30	13	4 to 17	--	0.33	0.00209
	24	SB-3	0.75	1200	30	9	4 to 17	--	0.33	0.00274
	25	SB-3	0.75	1200	30	8	4 to 17	--	0.33	0.00274
	26	SB-3	0.75	1200	30	14	4 to 17	--	0.33	0.00209
	27	SB-3	0.75	1200	30	14	4 to 17	--	0.33	0.00070
	28	SB-3	0.75	1200	30	14	4 to 17	--	0.33	0.00105

about 0.00103 radians. Looking back at the second heat-straightening repair of the W 10 x 39 composite girder, it was observed that this phenomenon did not occur there, even though the vee heats were applied to the same point during almost all heating cycles. However, during this heating sequence, two vee heats were applied to the bottom flange per cycle. That distinctive difference between the two heating sequences could be the reason behind the absence of this phenomenon from the behavior of the W 10 x 39 girder. Local residual stresses, which are produced by the vee heats, are suspected to be the main cause of this behavior. A buildup of residual stress would result after several heats. The residual stresses would then tend to restrict the movement of the girder by impeding the previously unrestrained thermal contraction of the heated material during the cooling process.

A slight reverse curvature occurred at the right end of the girder where the hinge support is located. Because this reverse curvature was small in magnitude, heat straightening was not applied to correct this over-straightening. A cross-sectional view of the rotational behavior of the girder at point 11 is shown in Figure 63.

Comparison of Various Heating Sequences

Listed in Table 6 is the average value of the plastic rotation angles per cycle per vee obtained from each heating sequence. These values show the effect of two of the most important factors influencing the behavior of heat-straightened damaged steel girders: the external jacking force and the heating pattern.

For comparison purposes, the average value of the displacement of the bottom flange of the damaged girder under the influence of each of the various heating sequences is plotted in Figure 64. Each curve represents the average of all the heating cycles in a corresponding heating sequence. For cycles with more than one vee heat, the results are divided by the number of vees.

It can be seen from these results that there exists a distinct advantage for applying an auxiliary jacking force to the girder during the heat-straightening process. A comparison between the results obtained from heating sequence 1 to those obtained from heating sequence 2 shows that the plastic rotation increased 64 percent just by doubling the jacking force. Comparing the results obtained using heating

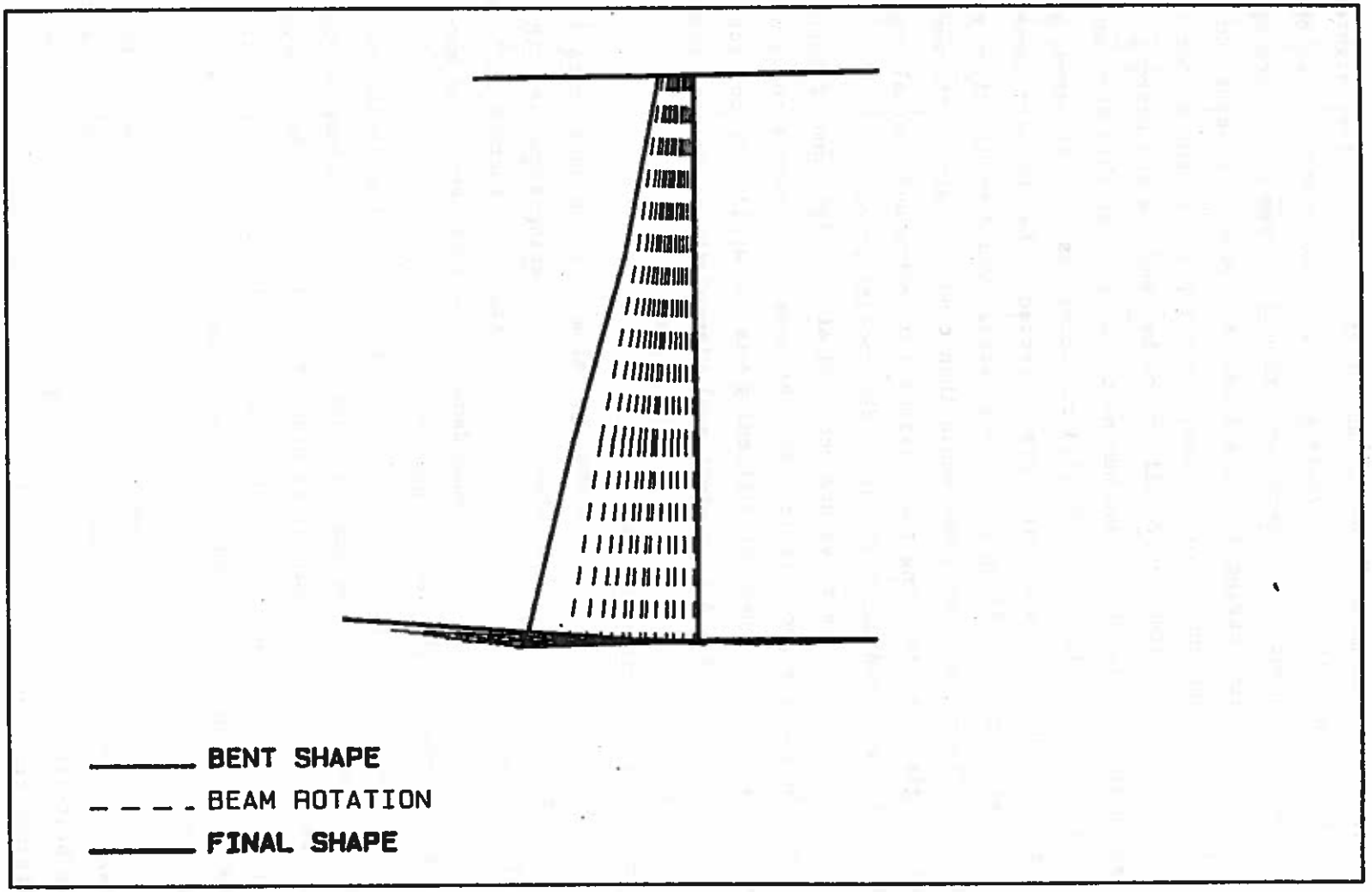

Figure 63. Rotational heat-straightening progression of the damaged girder specimen SB-3 (section at point 11).

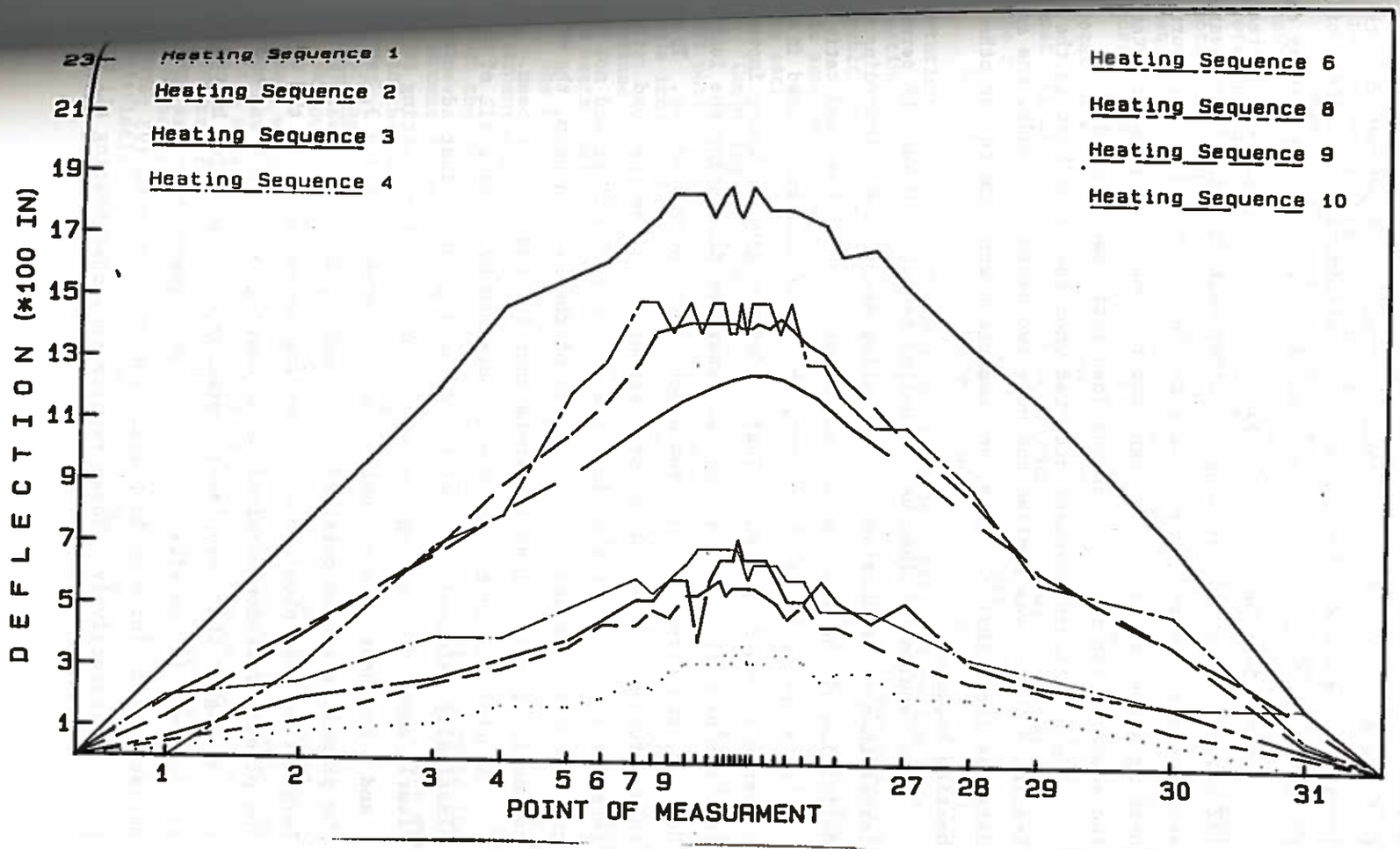

Figure 64. Comparison of the behavior of the test girder under the influence of different sequences of heat-straightening.

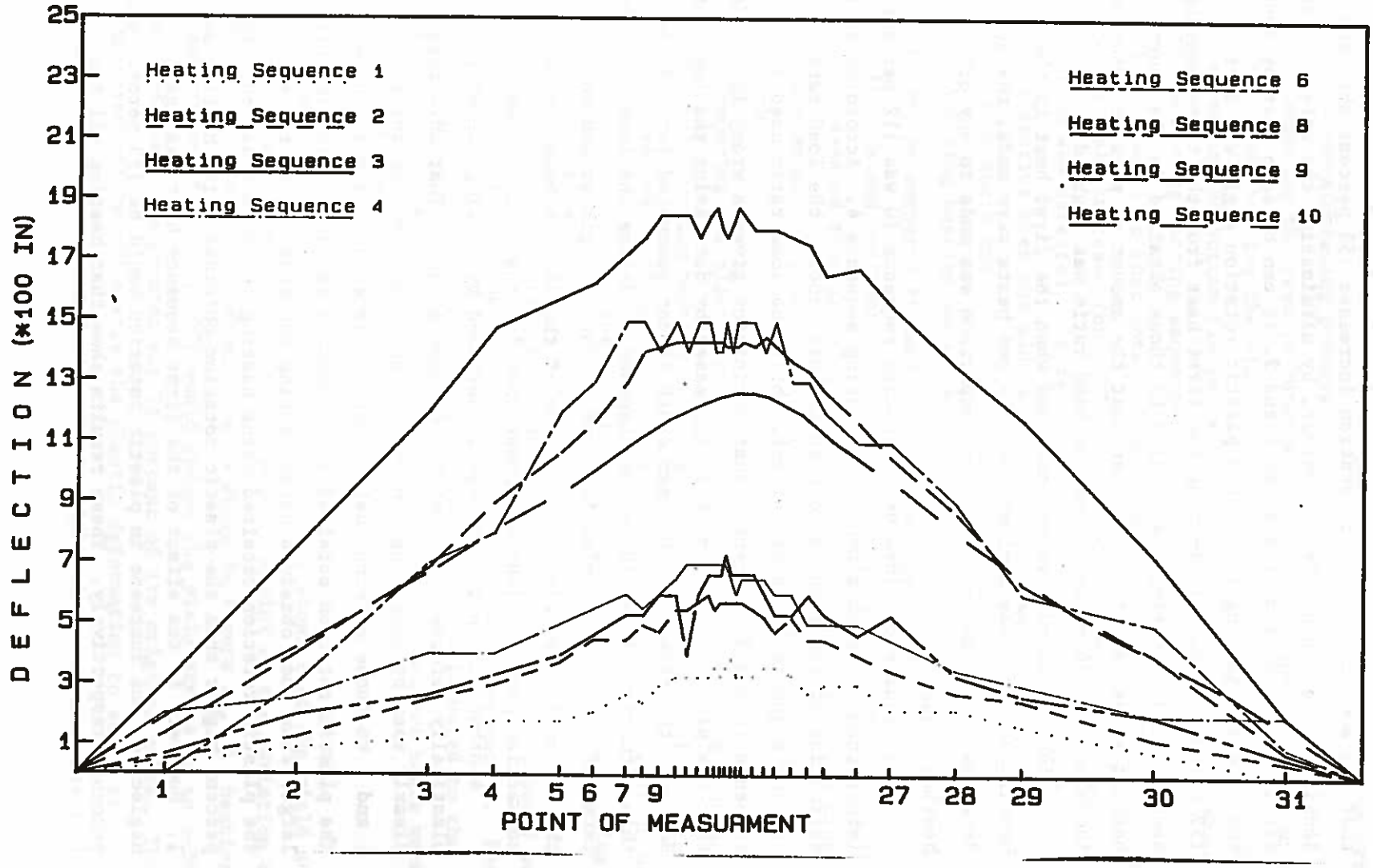

Figure 64. Comparison of the behavior of the test girder under the influence of different sequences of heat-straightening.

sequence 3 to those obtained using heating sequence 4, it can be seen that the amount of plastic rotation increased 153 percent when the jacking force was doubled. However, by eliminating the effect of the first heat in heating sequences 1 and 2, it can be seen that by doubling the external jacking force, the plastic rotation angle was increased by 152 percent. Also, eliminating the first heat from the third heating sequence and comparing the results to those obtained in the fourth heating sequence, it can be seen that the amount of plastic rotation increased by 136 percent when the load ratio was doubled.

Since backward movement occurred when the first heat in the fifth heating sequence was applied and only two heats were made, the available data was inconclusive. Thus, no comparison was made to any other heating sequence.

The results obtained using heating sequence 10 was 112 percent larger than those obtained using heating sequence 4. According to the definition of the load ratio used in this report, the load ratio used in heating sequence 4 was 56 percent, while the load ratio used in heating sequence 10 was 33 percent. That definition gives a wrong impression that the plastic rotation angle increases by decreasing the load ratio. However, the effect of the beam depth is not accounted for. To remedy this situation, it would be advantageous to define the load ratio in terms of the yield or plastic force of the full girder and not that of the bottom flange only. In the case of the 24-inch beam, the web connection provided less stiffness than for the 10-inch beam.

Another distinct advantage is obtained by heating all of the plastically deformed zones of the damaged girder. That advantage can be clearly seen by comparing the results obtained from heating sequences 1 and 2 to those obtained using heating sequences 4 and 3, respectively. The plastic rotation obtained using heating sequence 3 was 161 percent larger than that obtained using heating sequence 2. At the same time, the plastic rotation obtained using heating sequence 4 was only 69 percent higher than the plastic rotation obtained using heating sequence 1. However, if the effect of the first sequence heat was again neglected, the increase in plastic rotation would be 193 percent and 214 percent, respectively. These results show that heating all the

plastically deformed zones of the girder can significantly accelerate the heat-straightening process.

Comparing the results obtained using heating sequences 3 and 8 reveals that heating the middle portion of the web increases the plastic rotation in the bottom flange by 141 percent. Comparing the results obtained using heating sequence 2 (neglecting the effect of the first sequence heat) to that obtained using heating sequence 8 showed that just a small increase (only 22 percent) in the amount of plastic rotation was detected. It can be concluded that the web line heat was most effective when the middle portion of the web was heated. That was the region where the external jacking force was applied.

Applying heating sequence six doubled the amount of plastic rotation as compared to heating sequence eight. Since the effect of heating the end portions of the yield line in the web was small, this result revealed that applying two vee heats in the same cycle produces the same amount of plastic rotation as applying two heating cycles of one vee each.

Comparing the plastic rotation obtained using heating sequence 9 to that obtained using heating sequence 4 reveals that the plastic rotation angle increased by 95 percent. That increase in plastic rotation was obtained by increasing the jacking force by 79 percent and applying two vee heats instead of one.

The plastic rotation angle obtained using heating sequence 9 was 23 percent smaller than that obtained using heating sequence 3. Even though the decrease in plastic rotation could be attributed to the 11 percent decrease in the applied jacking force, two vee heats were used in the heating process instead of one.

Restraining Force Considerations

Various researchers (2, 6, 18, 22) have shown that the yield stress decreases when the temperature increases. A plot of the variation of the yield stress with temperature is shown in Figure 65. A heating temperature of about 1200°F would reduce the yield stress in an A-36 steel member to approximately 36 percent of its original value. This characteristic would enable the plastic deformation to occur at relatively low stresses during the straightening process. Due to this

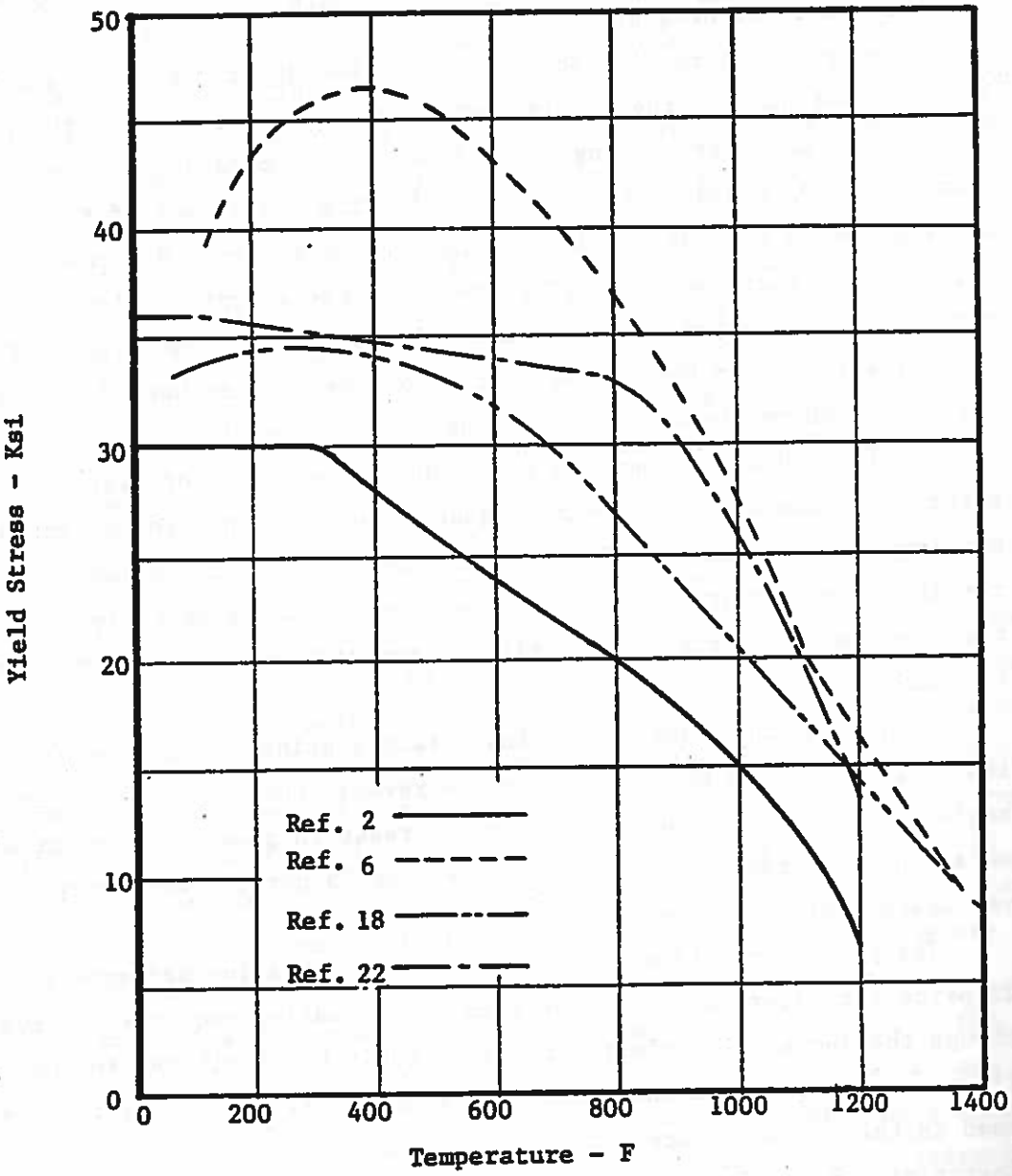

Figure 65. Plot of yield stress vs. temperature.

fact, the presence of the external jacking force could help straighten the web while it is hot due to increased plastic flow.

To evaluate this aspect further, six additional heating cycles were applied to the girder specimen SB-1. In the first two cycles of this series, only a line heat in the web between points 3 and 29 was applied. The rest of the heating cycles encompassed the use of the same line heat, in addition to applying a jacking force of 112 percent to the bottom flange at point 16. No vee heats were used.

The results obtained from the first two heating cycles showed that applying the line heat by itself did not produce any movement in the bottom flange of the girder. The results obtained from the next four heating cycles showed that applying the 112 percent jacking force produced about a 0.04-inch lateral movement per cycle in the flange. The fact that the applied external jacking force was about 36 percent of the measured force that caused initial yield of the girder, combined with the fact that the yield stress is reduced to 36 percent of its original value when the member is heated to 1200°F, resulted in plastic flow that produced deformation of the system. However, this movement was very small compared to the movement obtained using the more effective heating patterns.

A thorough evaluation of the behavior of the W 10 x 39 composite girder during the second heat-straightening repair operation (SB-2) showed that the middle portion of the web did not over-straighten, as was the tendency during the first heat-straightening repair operation (SB-1). The slight reduction in the jacking force probably reduced the plastic flow in the web enough to prevent this problem.

A tentative conclusion at this stage of the research is that by keeping the stress level due to restraining forces in the damaged zones to less than one-third of yield, over-straightening is not likely to occur and structural instabilities will be minimized.

Comparison to Existing Analysis Formulas

For the repair of the damaged composite girder, 1200°F, three quarter depth, 30 degree vee heats were applied to the bottom flange. The camber prediction formula developed originally by R. Holt (16) has been previously derived. Using Equation 6, the predicted plastic rotation obtained from each heating cycle is:

= 2 * 0.00864 * 0.75 * tan(30/2)

= 0.00347 radians.

where,

Sp = 0.00864 from Figure 3 at 1200°F and

d_v/w = 0.75

Moberg (20) presented a modified Holt formula, Equation 7. Using this equation, the predicted plastic rotation from each heating cycle is:

= 2 * 0.00864 * (0.75)2 tan(30/2) thus,

= 0.00260 radians

Table 4 provides a list of the plastic rotation angles obtained from each heating sequence. From this table, it is apparent that both of these formulas overestimate the amount of plastic rotation achieved using both the first and second heating sequences.

The average value of the plastic rotation produced using the third heating sequence was slightly larger than the value obtained using the modified Holt equation and slightly smaller than that predicted by the Holt equation.

Heating sequences 4, 5, 8, and 10 all produced plastic rotation values smaller than those predicted by both the Holt and the modified Holt equations.

Heating sequences 6 and 9 were performed using two vee heats at the same time. Therefore, the amount of plastic rotation per vee heat predicted by both equations should be doubled. Thus, the Holt equation predicts a plastic rotation value of 0.00694 radians, while the modified Holt gives a plastic rotation angle of 0.00520 radians. These values clearly overestimate the plastic rotation obtained in this heating sequence.

The best correlation occurred between these empirical formulas and the results obtained using the third heating sequence. It appears that these formulas best predict the amount of plastic rotation when the line heat is applied to the web and a load ratio of about 112 percent is obtained in the bottom flange.

The large variation in all the other results indicates that the effectiveness of the existing empirical formulas in predicting the exact amount of plastic rotation obtained from each heating cycle is doubtful.

These formulas neglect to take into account many variables, such as the external jacking forces and/or constraints and the internal constraints provided by the plastically yielded zones of the member.

Maximum Allowable Strains

Shanafelt and Horn (28) recommended that for all primary tension members or primary members with tension areas in severe fatigue critical portions, the maximum allowable strains should not exceed 5 percent or more than 15 times the yield point strains. It was also recommended that for primary tension members with no fatigue critical areas, the nominal strain should not be more than 5 percent. If those limits are exceeded, heat-straightening should not be applied to the damaged member unless the straightened elements are fully strengthened by providing additional splice material. The radius of curvature (R) is given by:

$$R = EI/M \quad (8)$$

where,

E = modulus of elasticity

I = moment of inertia

M = applied moment

Using the flexure formula relating moment to stress for a plate element:

$$M = IF/(W/2)$$

where,

F = actual stress in the member

W = width of the member

thus,

$$R = WE/(2F) \quad (9)$$

based on 5% strain, F/E = 0.05 and

$$R = W/0.1 \quad (10)$$

Considering bending of the flange about its strong axis, the width of the bottom flange of the damaged W 10 x 39 girder was 7.985 inches. Thus, the limit on the radius of curvature based on 5 percent allowable strains is about 7 feet. The minimum radius of curvature of the transverse deflection of the bottom flange was 18 feet. Therefore, this radius of curvature is greater than the recommended minimum.

For weak axis bending, the thickness of the flange was 0.53 inches. Thus, the limit based on 5 percent strains is 0.4 feet. A minimum radius of curvature of 0.8 feet had developed in the flange by bending

about its weak axis. Therefore, the recommended minimum radius of curvature was not exceeded.

For weak axis bending of the web, the thickness of the web was 0.315 inches. Thus, the limit based on 5 percent strains is 0.3 ft. The minimum radius of curvature calculated in the web was 0.4 feet, which is greater than the minimum set by Shanafelt and Horn.

Therefore, the maximum curvature in both the web and the flange satisfied the recommended criteria. Heat straightening was applied to the girder specimen without strengthening. After the completion of the heat-straightening repair, the member was checked again and no cracks had developed at any place on the girder.

The second damage induced on the W 10 x 39 composite girder was less severe than the initially straightened damage. Thus, the maximum curvature in both the web and the flange should satisfy the recommended criteria. After the girder was repaired by heat straightening, a thorough check for cracks proved that the member was free of them.

The damage induced on the W 24 x 76 composite girder produced a minimum radius of curvature in the bottom flange of 8 feet in the transverse direction. The minimum radius of curvature recommended for an 8.99-inch-wide flange is about 7.5 feet, which is less than the actual curvature.

The limit for a 0.68-inch-thick flange is 0.6 inches. This limit proved to be far less than the actual radius of curvature in the deflected member. The same was true for the radius of curvature in the web. Thus, the limit on the radius of curvature specified by Shanafelt and Horn was not exceeded, and heat straightening could be used to straighten the damaged member.

Yield Zones

Shanafelt and Horn (28) also suggest that heat straightening should be applied only in the regions which corresponds to the yielding of the material:

$$Ry = WE/(2\ Fy) \qquad (11)$$

where,

Ry = radius of curvature at yield

Fy = yield point stress

Portions of the member where the radius of curvature is less than Ry are elastically deformed. These areas should return to their original undeformed positions when adjacent, plastically deformed portions had been heat-straightened.

The determination of the plastically yielded areas of the deformed girder could be obtained by evaluating Equation 11:

- Web bending about its weak axis, Ry = 11 feet.
- Flange bending about its strong axis, Ry = 268 feet.
- Flange bending about its weak axis, Ry = 18 feet.

In order to determine the yield zones in the bottom flange, the radii of curvature were computed from the laterally measured deflections. Those radii of curvature are shown in the second column of Table 9. A comparison of these values to the radius of curvature at yield revealed that the bottom flange had been plastically deformed as a long, flat plate in bending about its strong axis. That yield zone encompassed portions of the bottom flange which are located between points 8 and 24.

The radii of curvature were also computed to determine the yield zones caused by rotation of the flange about its weak axis. Those radii of curvature are shown in the third column of Table 9. By comparing these values to the yield radius of curvature of the flange for bending about its weak axis, it was observed that the portion of the flange between point 9 and point 22 had completely yielded as a flat plate in bending about its weak axis.

The radii of curvature computed along the width of the bottom flange are shown in column 4 of Table 9. A thorough study of these results revealed that the bottom flange had yielded by bending longitudinally about its weak axis at its junction with the web between points 12 and 20. That yield line, in junction with the yielding of the flange about its weak axis, resulted in a "dish-like" shape.

The values of the radii of curvature are also computed along the weak axis of the web. These values are shown in column 5 of Table 9. Comparing these values to the value of the yield radius of curvature in the web revealed that the web had been plastically deformed as a long, flat plate in bending about its weak axis in a direction parallel to the top flange. The curvature in the web was gradual. The yield line

Table 9. Calculated Radii of Curvature, R, for SB-1.

Measuring Point	Flange Bending About Strong Axis ("h") (ft)	Flange Bending About Weak Axis ("e") (ft)	Flange Bending About Longitudinal Axis (ft)	Web Bending About Weak Axis (ft)
1	---	---	33.0	∞
2	600	-240.0	66.7	37.5
3	600	∞	∞	3.1
4	480	300.0	-66.7	2.3
5	400	300.0	-22.2	---
6	360	37.5	-22.2	---
7	300	75.0	-33.3	---
8	39	37.5	-13.3	---
9	38	-9.4	-66.7	---
10	-19	-6.8	-22.2	1.5
11	-18	-1.6	-22.2	1.4
12	∞	3.3	-3.9	1.4
13	∞	2.7	-3.0	---
14	30	-0.8	-3.7	---
15	∞	0.8	-3.5	---
16	∞	-1.0	-6.1	0.4
17	-38	1.6	-4.4	---
18	-40	-1.6	-4.4	---
19	-38	1.8	-3.3	1.4
20	-40	5.4	5.1	---
21	-40	-1.2	-22.2	---
22	-40	-6.3	-33.3	---
23	-42	-37.5	-66.7	---
24	-45	-37.5	-66.7	---
25	-387	150.0	∞	---
26	-400	75.0	∞	---
27	600	-300.0	∞	1.8
28	∞	∞	-33.3	2.2
29	∞	-218.0	-66.7	4.5
30	∞	480.0	33.3	22.5
31	∞	∞	66.7	37.5

occurred about 2.5 inches below the top flange, starting from midway between points 2 and 3 and extending to midway between points 29 and 30. Figure 23 provides a graphical illustration of all the yield zones in both the web and the bottom flange of the damaged girder.

Table 10 provides a list of the actual radii of curvature present in the W 10 x 39 composite girder after the second damage inducement operation (SB-2). Based on these values, areas which had yielded during the operation were identified. Figure 25 provides a graphical illustration of those results.

Shown in Table 11 are the actual radii of curvature computed to determine all the yield zones in the damaged W 24 x 76 composite girder. Evaluating Equation 11:

- Web bending about its weak axis, Ry = 15 feet.
- Flange bending about its strong axis, Ry = 302 feet.
- Flange bending about its weak axis, Ry = 23 feet.

Dashed areas of Figure 29 identify all the yield zones in the W 24 x 76 composite girder.

Effect of the Jacking Force on the Inelastic Behavior

As mentioned earlier, this report is a part of a broader research project on the use of heat-straightening techniques. The ultimate goal of that project is to develop a microcomputer program that will accurately design a heat-straightening repair procedure for damaged structural steel members. As a first step in that direction, the structural behavior of the damaged system should be defined.

The initial damage induced on the composite girder formed a yield line in the web that encompassed approximately an 11-foot span of the 19.5-foot-long specimen. The ratio of the yield line length to the entire length of the girder was 56 percent. That yield line occurred at 2.25 inches below the top flange. That point was located at the upper quarter point of the clear depth of the web between flanges.

The distance between the point of load application and the yield line was about 6.875 inches. The full plastic moment capacity of the web at first yield is 10.72 k-in/ft. Assuming that the web has plastically yielded along the 11-foot span and varies linearly between the end points of the yield line to a zero value at both ends of the full length, the calculated yield moment capacity of the web would be

Table 10. Calculated Radii of Curvature, R, for SB-2.

Measuring Point	Flange Bending About Strong Axis ("h") (ft)	Flange Bending About Weak Axis ("e") (ft)	Flange Bending About Longitudinal Axis (ft)	Web Bending About Weak Axis (ft)
1	---	---	∞	∞
2	-480	-300	∞	12.5
3	-480	-300	∞	5.4
4	∞	∞	∞	4.2
5	∞	200	-66.6	4.2
6	∞	37.5	-66.6	
7	∞	-50	-33.3	
8	37.5	-12.5	-13.3	2.1
9	37.5	-12.5	-16.6	1.9
10	18.7	12.5	-9.5	
11	∞	9.6	-4.7	
12	∞	2.3	-4.7	2.3
13	∞	16.6	-6.0	
14	∞	∞	-4.4	
15	∞	∞	-4.1	
16	2.0	∞	-3.5	2.5
17	∞	16.6	-3.7	
18	-2.0	2.0	-3.3	
19	5.5	2.0	-5.1	
20	-8.3	0.5	-2.6	2.0
21	16.6	-0.7	-8.3	
22	∞	5.5	-13.3	
23	37.5	-5.3	-33.3	1.7
24	∞	18.7	-33.3	
25	300	150	-33.3	
26	450	150	-66.6	2.7
27	∞	480	-66.6	
28	-600	∞	∞	3.6
29	-480	480	∞	8.5
30	1200	-200	∞	
31	---	---	∞	∞

Table 11. Calculated Radii of Curvature, R, for SB-3.

Measuring Point	Flange Bending About Strong Axis ("h") (ft)	Flange Bending About Weak Axis ("e") (ft)	Flange Bending About Longitudinal Axis (ft)	Web Bending About Weak Axis (ft)
1	---	---	-84.4	118
2	-800	300	-42.2	39.3
3	-1200	-480	∞	19.6
4	315	300	-28.1	14.7
5	315	300	-84.4	13.9
6	-75	-75	84.4	13.9
7	50	∞	84.4	13.9
8	150	-300	∞	12.4
9	37.5	100	-16.9	11.8
10	∞	-9	42.2	11.8
11	8.0	12	∞	10.7
12	-37.5	-5	28.1	11.2
13	18.8	21	-84.4	11.8
14	37.5	37	-84.4	12.4
15	120	-120	∞	13.1
16	-200	∞	∞	12.4
17	-315	-800	-84.4	14.7
18	-343	-800	-42.2	21.4
19	---	---	∞	236

approximately 163 k-in. Dividing this value by the distance to the point of load application, it can be seen that an applied force of 23.7 kips would cause yielding in the web.

The calculated plastic moment capacity of the flange is 304 k-in. Assuming that the flange would fail when a plastic hinge is formed at the point of load application, the applied external force that would cause failure of the flange only was 5.2 kips.

A combination of both of these mechanisms would form the assumed failure mechanism of the girder. Thus, an applied external jacking force of 28.9 kips would reach the plastic moment capacity of the girder. These calculations compared favorably with the 28.0 kips measured in the field during the initial damage inducement process.

After the girder was completely repaired, it was re-damaged in an attempt to better understand the structural behavior of the girder specimen. The lateral deflection of the bottom flange was measured while loads were gradually applied. Those deflection measurements were taken at the point of load application, point 16. Figure 66 shows the experimental load-deflection behavior of the girder in comparison to the theoretical load-deflection behavior of the bottom flange only. An analysis of these results revealed that the girder specimen started to yield at an applied load of approximately 16,000 pounds. The plastic moment capacity of the girder was achieved with an applied force of about 21,000 pounds. For SB-2, the damage induced on the composite girder formed a yield line in the web that encompassed approximately a 7.5-foot span of the 19.5-foot-long specimen. The ratio of the yield line length to the entire length of the girder was 39 percent. That yield line occurred at 3.5 inches below the top flange. The ratio of this distance to the depth of the web between flanges was 38 percent. The distance between the point of load application and the yield line was about 5.625 inches. The moment capacity of the web at first yield is 10.72 k-in/ft. Assuming that the web has plastically yielded along the 7.5-foot span and varies linearly between the end points of the yield line to a zero value at both ends of the full length, the calculated yield moment capacity of the web would be approximately 142 k-in. Dividing this value by the distance to the point of load

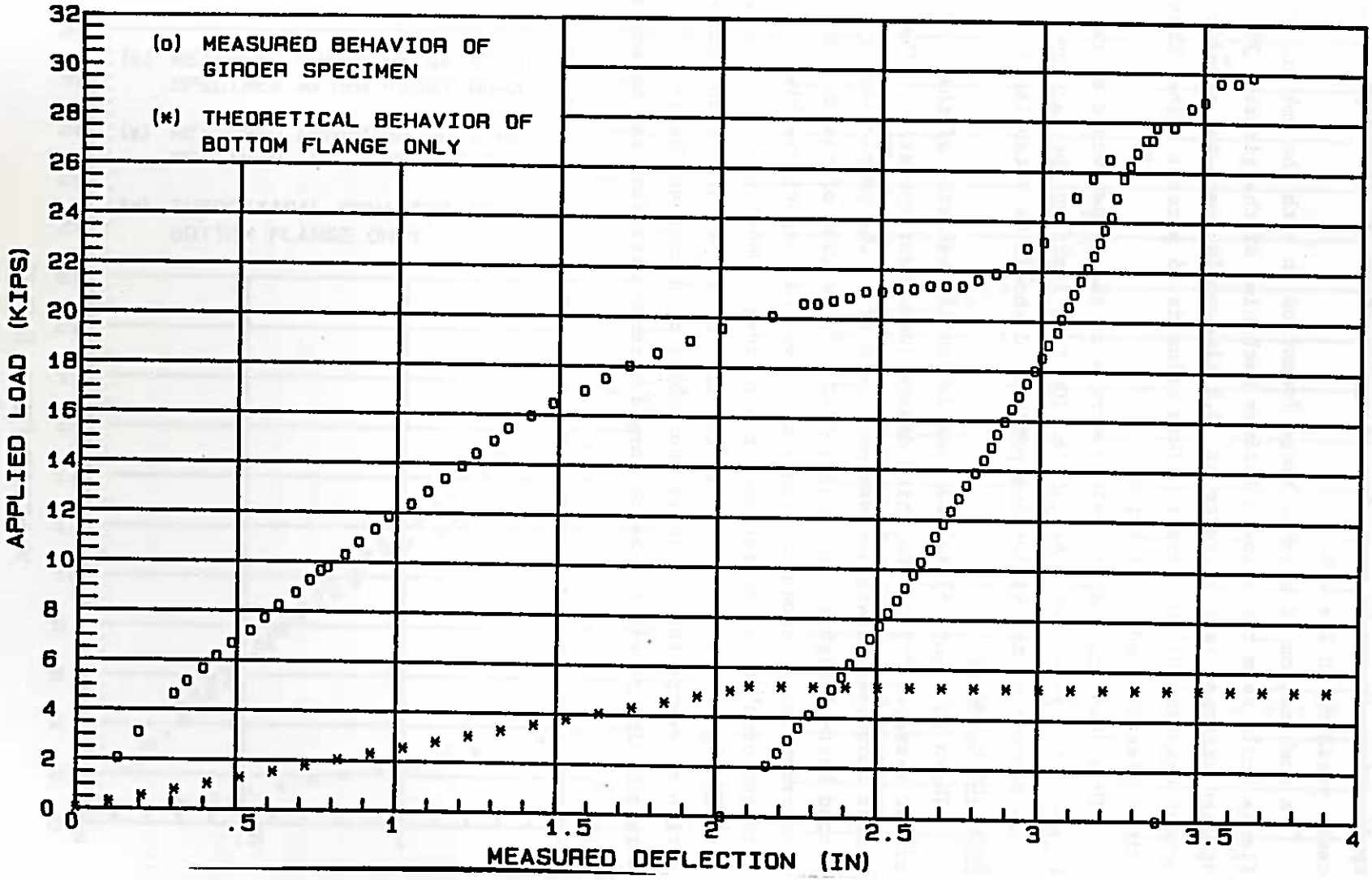

Figure 66. Load-deflection behavior of a composite W 10 X 39 girder specimen laterally loaded to simulate impact.

application, it can be seen that an applied force of 25.3 kips would cause yielding in the web.

A combination of plastic hinge formation in both the web and the flange would form the assumed failure mechanism of the girder. Thus, an applied external jacking force of 30.5 kips would reach the plastic moment capacity of the girder. This value is 45 percent higher than the actual plastic load of 21 kips.

Thus, knowing that the yield stress of the girder would be reduced by about 64 percent when heated to 1200°F, a limit on the jacking force of 36 percent of the yield line point load should be established.

Repetitive Damage

Shown in Figure 67 is the load-deflection behavior of the W 10 x 39 girder measured during the third damage inducement operation. The third damage inducement operation was performed after the completion of the second heat-straightening repair, SB-2. Comparison of the two load-deflection curves shown in Figure 67 shows that repetitive heat straightening had no effect on the structural behavior of the W 10 x 39 composite girder specimen. This comparison is the first such documentation to verify that at least two cycles of damage and heat-straightening repair can be performed without degrading the material.

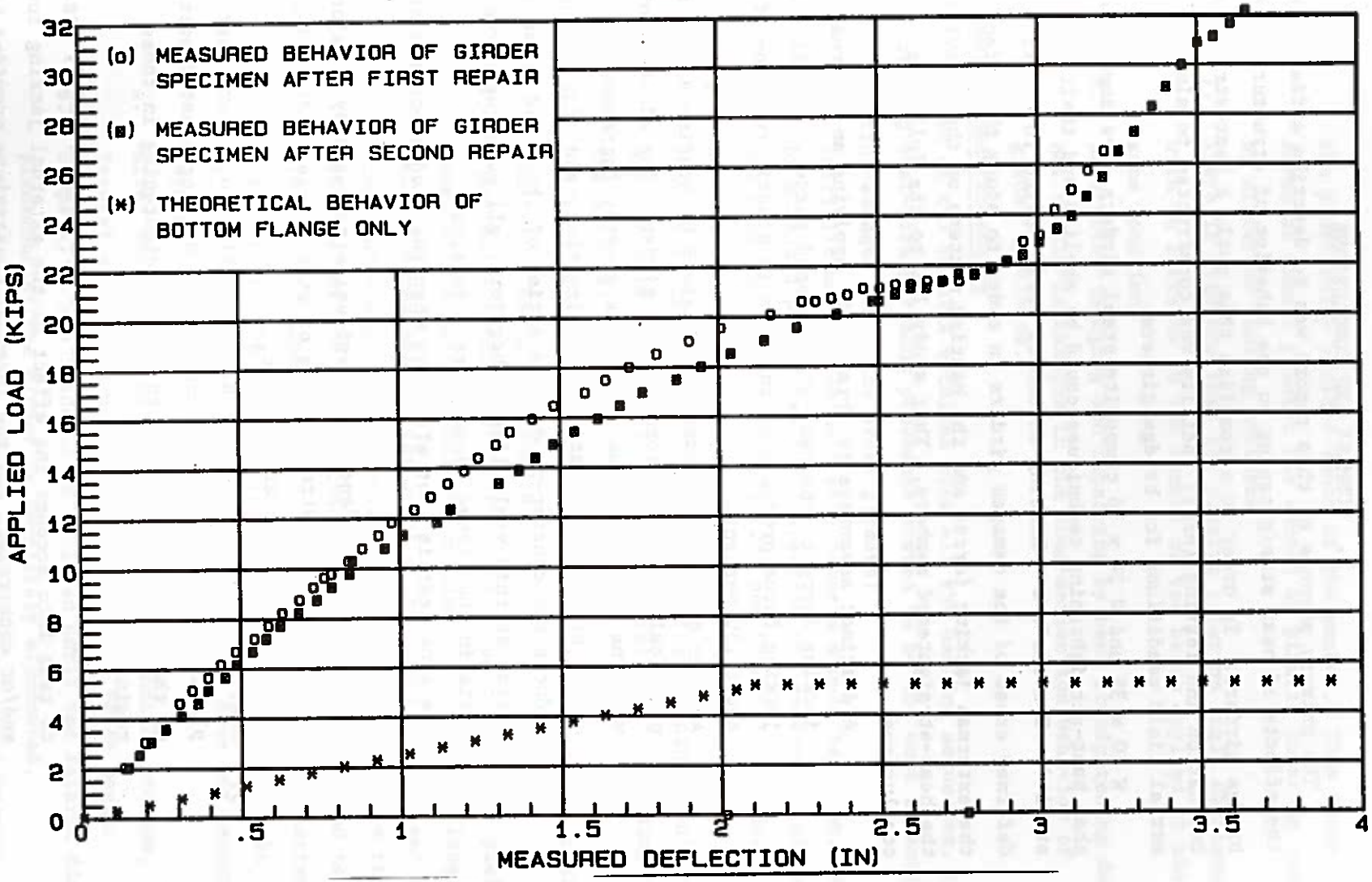

Figure 67. Load-deflection behavior of a composite W 10 X 39 girder specimen laterally loaded to simulate impact.

5. SUMMARY AND CONCLUSIONS

The primary purpose of this report was to describe a field study of the effects of heat straightening on the behavior of structural steel bridge girders. In order to accomplish this goal, a Heat-straightening Evaluation And Testing (HEAT) facility was constructed to simulate actual field conditions for bridge girders.

W 10 x 39 and W 24 x 76 composite steel girders were damaged so that heat-straightening techniques could be applied and their effects studied. Ten different heating sequences were applied to plastically deformed areas of the damaged girders in order to study the effect of the external jacking forces and the heating pattern on the behavior of the heat-straightened members. That study led to the following conclusions:

1. A distinct advantage is obtained by applying an external jacking force to the heat-straightened girder. Doubling the jacking force produces an increase in plastic rotation of about 150 percent.
2. Another distinct advantage is obtained by heating all of the plastically deformed zones in the girder. The addition of the web line heat along the yield line greatly increases the amount of plastic rotation. Heating the yield line in the web reduces the counter-productive action of the yield stresses acting at this yield line. Therefore, all subsequent vee heats in the flange become more effective.
3. The line heat is most effective when the middle portion of the web is heated.
4. There is some evidence that residual stresses play a major role in the heat straightening of wide flange girders where large deformations are present.
5. Heat straightening should only be applied to regions where plastic deformation has taken place. Heating elastic portions of the girder could cause an over-straightening in those regions.
6. Existing analysis formulas, such as Equations 6 and 7, neglect to take into account the effect of the external jacking forces and/or constraints and the internal constraints provided by

the plastically yielded zones of the member. Thus these formulas cannot predict the amount of plastic rotation caused by different heating patterns.

7. There is evidence that the plastic rotation angle decreases with an increase in the number of vee heats applied at the same location.
8. Repetitive damaging and repairing by heat straightening does not result in changes in the load-deflection behavior of girder specimens.

Recommended Procedures

Based on the results obtained from all the heating sequences, the following heat-straightening procedure proved to be the most effective in repairing damaged composite steel girders:

1. Initial damage assessment measurements should be taken. A set of standard procedures for inspection and assessment of damage has been presented by Moberg (20) and Shanafelt and Horn (28).
2. All the plastically yielded zones in the girder should be identified using Equation 11. Heat straightening should be applied only to the regions which correspond to yielding of the material.
3. The point of maximum curvature in the damaged flange should be identified using Equation 10.
4. A maximum external jacking force of 36 percent of the yield force of the girder should be applied to the bottom flange as well as a vee heat at the point of maximum curvature and a line heat along the entire length of the yield line in the web. The maximum heating temperature should be limited to 1200°F. The depth of the vee heat should be three-quarters of the depth of the flange. The angle of the vee should be selected so that the width of the vee base does not exceed 4 inches.
5. After the completion of the heating and cooling process, lateral deflection measurements are to be taken again.
6. Steps 3, 4, and 5 should be followed until the lateral displacement of the girder is completely eliminated.
7. Bulges should be removed by hot mechanical straightening.

6. REFERENCES

1. Manual of Steel Construction, 8th ed, American Institute of Steel Construction.
2. "Flame Shortening Eyebars to Equalize Stresses," Bulletin No. 460, American Railway Engineering Association.
3. Avent, R. R., "Use of Heat Straightening Techniques for Repair of Damaged Steel Structural Elements in Bridges," Interim Report, Vol. 1, La. HPR Study No. 85-3St, Report No. FHWA/LA-86/193, Louisiana Transportation Research Center, Baton Rouge,1986.
4. Avent, R. R., and Boudreaux, R. J., "Heat-Straightening Effects on the Behavior of Plates and Rolled Shapes," Volume 2, 1987.
5. Avent, R. R., "Heat-Straightening of Steel: Fact and Fable," Volume 3, 1987.
6. Blodgett, O. W., "Distortion . . . How Metal Properties Affect It," Welding Engineer, February 1972, pp. 40-46.
7. Brockenbrough, R. L., and Ives, K. D., "Experimental Stresses and Strains from Heat Curving," Journal of the Structural Division, ASCE, Vol. 96, No. ST7, Proc. Paper 7400, July 1970, pp. 1305-1331.
8. Brockenbrough, R. L., "Theoretical Stresses and Strains from Heat Curving," Journal of the Structural Division, ASCE, Vol. 96, No. ST7, Proc. Paper 7410, July, 1970, pp. 1421-1444.
9. Ditman, Oleg, "Determination of Thermal Shrinkage in Structural Steel," M.S. Thesis, University of Washington, 1961.
10. "How Fire Destroyed and Fire Repaired Air Force Hangers," Engineering-News Record, June 18, 1959, pp. 50-53.
11. Fadous, George M., "Heat-Straightening Effects on the Behavior of a Full-Scale Simulated Bridge Girder," M.S. Thesis, Louisiana State University, 1987.
12. "Flame Buckled this Steel . . . And Flame Straightened It," Part 1, Welding Engineer, February 1959, pp. 40-43.
13. Harrison, H. L., "A Study of the Holt Method of Heat (Contraction) Straightening," M.S. Thesis, University of Washington, 1950.
14. Holt, Joseph E., "Flame Straightening: A Friend in Need," Welding Engineer, Vol. 40, No. 10, October 1955, pp. 44-46, Vol. 40, No. 12, December 1955, pp. 30-31.

15. Holt, Joseph E., "Contraction as a Friend in Need," Typed and Copyrighted, 1938.
16. Holt, Richard E., "Primary Concepts in Flame Bending," Welding Engineer, Vol. 56, No. 6, June 1971, pp. 416-424.
17. Holt, Richard E., "Flame Straightening Basics," Welding Engineer, Vol. 50, No. 9, September 1965, pp. 49-53.
18. Horton, David L., "Heat Curved Mild Steel Wide Flange Sections: An Experimental and Theoretical Analysis," M.S. Thesis, University of Washington, 1973.
19. "Kinks Go Up in Flames," Engineering News Record, April 9, 1981, p. 17.
20. Moberg, K. L., "Damage Assessment And Contraction Straightening of Steel Structures," M.S. Thesis, University of Washington, 1979.
21. Newman, Ernest M., "Repair of Fire Damaged Structural Steel," Military Engineer, No. 344, November-December 1959, pp. 448-450.
22. Nichols, J. I., and Weerth, D. E., "Investigation of Triangular Heats Applied to Mild Steel Plates," Engineering Journal, AISC, October 1972, pp. 137-141.
23. "Oxyacetylene Torches Straighten Fire-Warped Steel," Welding Engineer, March 1959, pp. 31-34.
24. Roeder, C. W., "Use of Thermal Stresses for Seismic Damage Repair," Final Report, NSF Grant CEE-8205260, University of Washington, Seattle, 1985.
25. Roeder, C. W., "Experimental Study of Heat Induced Deformation," Journal of Structural Engineering, ASCE, Vol. 112, No. 10, October 1986, pp. 2247-2262.
26. Rothman, R. L., "Flame Straighten Quenched and Tempered Steels in Ship Construction," Ship Structures Committee, Report No. 247, 1973.
27. Rothman, R. L., and Monroe, R. E., "Effect of Temperature and Strain Upon Ship Steels," Ship Structures Committee, Report No. 235, 1973.
28. Shanafelt, G. O., and Horn, W. B., "Guidelines for Evaluation and Repair of Damaged Steel Bridge Members," NCHRP Report No. 271, Transportation Research Board, National Research Council, Washington, June 1984.